



POLITECNICO
DI TORINO



EPFL

MASTER OF SCIENCE IN NANOTECHNOLOGIES FOR ICTs

**Electrochemical fingerprinting of liquids using
cross-sensitive polymers arrays and
machine learning**

Master thesis

Author:
Gianmarco Gabrieli

Supervisors:
Dr. Matteo Cocuzza
Dr. Carlo Ricciardi

External Supervisor:
Dr. Patrick Ruch

IBM **Research** | Zurich

Declaration of Authorship

I, Gianmarco GABRIELI, declare that this thesis titled “*Electrochemical fingerprinting of liquids using cross-sensitive polymers arrays and machine learning*” and the work presented in it are my own. I confirm that:

- this work was done wholly or mainly while in candidature for a research degree at this University;
- where any part of this thesis has previously been submitted for a degree or any other qualification at this University or any other institution, this has been clearly stated;
- where I have consulted the published work of others, this is always clearly attributed;
- where I have quoted from the work of others, the source is always given. With the exception of such quotations, this thesis is entirely my own work;
- I have acknowledged all main sources of help;
- where the thesis is based on work done by myself jointly with others, I have made clear exactly what was done by others and what I have contributed myself.

Signed: _____

Date: _____

To Federico and Giorgia
I hope science and progress will shine your future

*A Federico e Giorgia
Spero che scienza e progresso illuminino il vostro futuro*

Abstract

Electronic tongues have been involved in the revolution of the traditional chemical sensing of liquids. The concepts of sensitivity and selectivity have started to assume different meanings, adapting to a new approach to the fingerprinting of complex liquid solutions. Electrochemical transducers are the most widely exploited read-out mechanisms for arrays of sensors that transform a chemical information into an electrical one, more manageable and easier to interpret. With respect to the voltammetric and amperometric techniques, that require dealing with moderate voltage and current values, potentiometry demonstrates to be the most suitable sensing method, compatible with the miniaturization and portability objectives of those types of devices. Open circuit voltage measurements allow to record potential signals coming from different electrodes of the array, which are functionalized with specific active materials. The present work provides an insight into the development of a portable potentiometric sensor for the analysis of complex multi-components liquid media. In particular, conductive polymers such as Polyaniline, PAPBA and Polypyrrole are presented, studied and characterized. Properties of polymeric coatings can be tuned by properly modifying the electropolymerization conditions in terms of reagents' nature and concentration, deposition technique and control of the doping process. It is shown the possible integration on the same array of the films expressing the most reliable responses, in order to build a cross-sensitive system. Each polymer, being characterized by a certain sensitivity towards multiple ionic species, would respond in a different way. The analysis of the voltage traces is performed taking into account the simultaneous variation expressed by the integrated sensors, providing qualitative responses for the identification and classification of different solutions. Machine learning algorithms produce results related to the capability of the system to interpret correctly the acquired data for the recognition process. Such analytical procedures require training and calibration of the electronic tongue prior to the actual implementation. A reasonable and balanced data set, consisting of enough observations, can be created by automating the tests operations through a microfluidic system, that comprises multiple components to allow the sensor to be in contact with the correct test solution for a specific amount of time. Multiple additional approaches have been proposed to enhance the miniaturization of the device, which has been employed for the classification of different mineral water brands. After the collection of the potentiometric responses, a certain pre-processing allows to extract meaningful features from the signals, which are related to the dynamic interaction of the polymers with the minerals. This operation allows to achieve a dimensional reduction of the variables' space to be considered. Classification results validate the electronic tongue capabilities and close the feedback loop that connects the multidisciplinary aspects that lay behind the present work.

Le lingue elettroniche hanno rivestito un ruolo fondamentale nella rivoluzione dei metodi tradizionali per l'analisi chimica di liquidi. I concetti di sensitività e selettività hanno iniziato ad assumere connotazioni differenti, adattandosi al nuovo approccio nel riconoscimento di soluzioni liquide complesse. I trasduttori elettrochimici sono i più evoluti sistemi integrati in matrici di sensori che trasformano segnali chimici in elettrici, più accessibili e facili da interpretare. Rispetto alle tecniche voltammetriche e amperometriche, che richiedono il coinvolgimento di valori moderati di tensione e corrente, la potenziometria risulta essere il metodo più appropriato, compatibile con gli obiettivi di miniaturizzazione e portabilità di tali dispositivi. Misure di tensione a circuito aperto permettono l'analisi di segnali provenienti da elettrodi diversi della matrice, che vengono funzionalizzati con materiali attivi specifici. Questo elaborato fornisce una comprensione approfondita dello sviluppo di un sensore potenziometrico portatile per l'analisi di liquidi complessi multicomponente. In particolare, i polimeri conduttivi come Polianilina, PAPBA e Polipirrolo vengono presentati, studiati e caratterizzati. Le proprietà dei rivestimenti polimerici possono essere modulate modificando accuratamente le condizioni di elettropolimerizzazione in termini di concentrazione e natura dei reagenti, tecnica di deposizione e controllo del processo di drogaggio. Viene descritta la possibile integrazione sulla stessa matrice di films che dimostrano essere più affidabili per la costruzione di un sistema cross-sensitivo. Ciascun polimero, essendo caratterizzato da una certa sensitività verso molteplici specie ioniche, risponde in maniera differente. L'analisi dei segnali in tensione viene effettuata considerando l'evoluzione simultanea espressa dai sensori integrati, fornendo risultati qualitativi per l'identificazione e classificazione di soluzioni differenti. Gli algoritmi di machine learning producono dei risultati relativi alla capacità del sistema di interpretare correttamente i dati acquisiti per il processo di riconoscimento. Tali procedure analitiche richiedono l'allenamento e la calibrazione della lingua elettronica prima ancora della reale implementazione. Un insieme di dati ragionevole e bilanciato, contenente un numero sufficiente di osservazioni, può essere creato automatizzando le operazioni di test attraverso un sistema microfluidico comprendente diversi componenti, per permettere al sensore di essere in contatto con la soluzione di test corretta per un periodo di tempo ben definito. Molti approcci differenti sono stati proposti per l'attuazione della miniaturizzazione del dispositivo, che è stato impiegato per la classificazione di acque minerali differenti. A seguito della raccolta dei dati, un loro pre-trattamento permette l'estrapolazione di caratteristiche significative dei segnali, che sono legati all'interazione dinamica dei polimeri con i minerali, in modo tale da fornire una riduzione delle dimensioni dello spazio delle variabili da considerare. I risultati della classificazione validano le capacità della lingua elettronica e chiudono il meccanismo di feedback che connette gli aspetti interdisciplinari che caratterizzano il presente elaborato.

Acknowledgements

I would first like to thank my supervisor at ZRL IBM Research, Dr. Patrick Ruch, for his immense support throughout all the master thesis period. He gave me the chance to get in touch with a professional environment, being a great source of inspiration to me. I will never forget all the time spent together and all the passion for research he transmitted to me. I would also like to thank Dr. Bruno Michel and the Smart System Integration Group for the wonderful working experience they let me to live. My gratitude goes also to all the Hypertaste team, that made possible a live demonstration of the project and helped me for the development of the thesis. I am extremely grateful to Dr. Rui Hu, that introduced me to the machine learning world, for the intense work we have done together. Of course, I need to thank also my office mates for their help, support and time we spent enjoying the breaks at work. Many thanks also to Dr. Matteo Cocuzza and Dr. Carlo Ricciardi, my supervisors at Politecnico di Torino.

I would like also to thank all of those that supported me during these academic years:

My mother and my father, for having taught me everything, for having always believed in me and for the strength and courage they gave me to take on new challenges. My sister Lorena and my brother Antonio, who did everything for me. I am infinitely grateful for their love, especially in difficult times.

Beatrice, who made me smile more than whatever mark and gave me pleasures that go beyond any *laude*. Her unconditional love in these years has been the key for my happiness and has brought me back to reality in every situation.

Ilaria and Luca for their kindness and for the serenity they transmitted to me.

My "*fratelli forever*", friends forever without I cannot help myself. "*Gli amici miei*" and "*Tracanarelli*" that made special every come back at home and with whom I shared infinite laughs and amusement.

Ross, Flavia, Vinci, Mària, Tino and Sara, my Turin's family that lived with me unforgettable experiences and years.

Marcello, that helped me to overcome obstacles and shared with me a thousands of joys and worries.

Gianmario and Alberto that faced the last two "*crazy*" years with me, among movings, exams, fear, pizza and crepes.

The first floor of *Collegio Einaudi* and all of those that I met or I lived with, for their help in making me who I am.

Vorrei innanzitutto ringraziare il mio supervisor ad IBM Research, il Dr. Patrick Ruch, per il suo immenso sostegno durante tutto il periodo di tesi. Non dimenticherò mai tutti i momenti passati assieme e la passione che mi ha trasmesso per la ricerca. Vorrei inoltre ringraziare il Dr. Bruno Michel e il gruppo Smart System Integration per la fantastica esperienza lavorativa che mi hanno fatto vivere. La mia gratitudine va anche al team di Hypertaste, che ha reso possibile una dimostrazione dal vivo del progetto e che mi ha aiutato per lo sviluppo della tesi. Sono inoltre grato alla Dr.ssa Rui Hu, che mi ha introdotto al mondo del machine learning, per il lavoro intenso che abbiamo fatto insieme. Naturalmente, devo ringraziare i miei compagni di ufficio per il loro aiuto, supporto e tempo passato a divertirci durante le nostre pause. Molte grazie anche al Dr. Matteo Cocuzza e al Dr. Carlo Ricciardi, i miei relatori del Politecnico di Torino.

Vorrei poi ringraziare tutti coloro che in questi anni di studio mi sono stati accanto e mi hanno continuamente sostenuto:

Mamma e papà per avermi insegnato tutto, per aver sempre creduto in me e per avermi dato la forza e il coraggio di affrontare nuove sfide. Mia sorella Lorena e mio fratello Antonio, che hanno fatto di tutto per me. Sono infinitamente grato per il loro affetto, soprattutto nei momenti di difficoltà.

Beatrice, che mi ha regalato più sorrisi di qualsiasi trenta e gioie che vanno al di là di ogni possibile lode. Il suo amore incondizionato in questi anni è stato la chiave per la mia felicità e mi ha riportato alla realtà in ogni situazione.

Ilaria e Luca per la loro dolcezza e per la serenità che mi hanno trasmesso.

I miei "fratelli forever", amici da sempre di cui non potrei fare a meno. "Gli amici miei" e i "Tracanarelli" che hanno reso speciale ogni ritorno a casa e con cui ho condiviso infinite risate e divertimenti.

Ross, Flavia, Vinci, Mária, Tino e Sara, la mia famiglia torinese con cui ho vissuto esperienze ed anni indimenticabili.

Marcello, senza il quale non avrei potuto superare molti ostacoli e con cui ho condiviso mille gioie e preoccupazioni.

Gianmario e Alberto che hanno affrontato gli ultimi due anni "pazzeschi" con me, tra traslochi, esami, paure, pizze e crepes.

Il primo piano del Collegio Einaudi e tutti coloro che ho incontrato e con cui ho vissuto, per aver contribuito a rendermi ciò che sono.

Table of contents

1	Introduction	1
1.1	Electronic tongue: a tool driving the future of chemical analysis of liquids	1
1.2	Potentiometric cross-sensitive arrays	4
2	Materials and Methods	5
2.1	Electrochemical Methods	5
2.1.1	Potentiometric measurements	5
2.1.2	Cyclic Voltammetry	6
2.1.3	Electropolymerization	11
2.2	Conductive Polymers	12
3	Electrodeposition, study and characterization of CPs	15
3.1	Introduction	15
3.2	Polyaniline’s electropolymerization and tunable properties	15
3.2.1	Growth process	17
3.2.2	Effects of electropolymerization conditions	20
3.2.3	Potentiostatic electropolymerization characteristics	25
3.2.4	Doping of PANI films	28
3.3	PAPBA: a new multifunctional polymer	30
3.3.1	Impact of deposition parameters	31
3.4	Study of polypyrrole growth and stability	36
3.4.1	Integration of anionic species in the polymer matrix	37
3.5	Characterization of electrodeposited polymers	40
3.5.1	Profilometric analysis	40
3.5.2	SEM characterization: film morphology	45
3.5.3	Raman spectra of electrodeposited polymers	47
4	Microfluidic system for automated testing of liquids	50
4.1	Microfluidic components integration	50
4.1.1	Flow sensors	50
4.1.2	Micromixers	53
4.1.3	Additional components	53

4.1.4	Pressure-controlled flow	53
4.2	Complete experimental setup and calibration	55
4.2.1	Volumes estimations of the microfluidic connections	56
4.2.2	System validation and limitations	58
4.3	Fully automated tests	59
5	Cross-sensitive arrays fabrication and characterization	62
5.1	Sensors design	62
5.2	Limitations of multiple polymers integration	64
5.2.1	Effect of PANI/PAPBA deposition on PPy electropolymerization	65
5.2.2	Effect of PPy deposition on PANI/PAPBA electropolymerization	67
5.3	Electrochemical characterization of polymeric films deposited on the arrays	68
5.3.1	Cyclic voltammetric studies	69
5.3.2	Potentiometric sensitivity	70
5.4	Towards a miniaturized portable "Electronic tongue"	74
5.4.1	Dynamic signals' components	75
5.4.2	Differential cross-sensitive signals	77
6	Machine Learning and device implementation	80
6.1	Processing of a sensor array response	80
6.2	Intelligence transfer: Electronic tongue training	81
6.3	Reduction of high-dimensional features spaces	82
6.3.1	Down-sampling and polynomial interpolations	83
6.3.2	Assisted features selection	84
6.4	Mineral waters showcase	87
6.4.1	Classification results	89
7	Conclusions	93
7.1	Future challenges	93
	Bibliography	95

List of figures

1.1	Workflow representation of an electronic tongue system	2
1.2	Comparison of the analytical procedures between traditional chemical sensors and electronic tongues	3
2.1	Saturated Calomel Electrode (SCE) structure	7
2.2	Three electrodes setup for CV and electropolymerization	8
2.3	Cyclic Voltammograms conventions	9
2.4	Cyclic voltammetry traces formation	9
2.5	(a) Homogeneous polishing movement and (b) diamond and alumina slurries treatment on Pt electrode.	13
2.6	The structure of polyacetylene and its conjugated double bonds.	13
3.1	Switch of Polyaniline oxidation states.	16
3.2	Doping of emeraldine base to achieve a conductive PANI state.	17
3.3	CV electrodeposition of PANI on Pt rod.	19
3.4	(a) Shift of the scan window effect and (b) Impact of precursors' concentration on PANI growth rate.	20
3.5	Effect of electrolyte's concentration on CV electrodeposited PANI on Pt electrode.	21
3.6	(a) Potentiodynamic deposition of PANI on Pt rod with <i>HCl</i> -based solution. (b) Comparison of charge involved in electropolymerization depending on the electrolyte's concentration.	22
3.7	Potentiometric response of (a) Cl^- doped and (b) SO_4^{2-} doped PANI in different concentrations of $MgSO_4$	23
3.8	CV electrodeposition at different scan rates.	24
3.9	(a) Potentiodynamic deposition of PANI on Au/ENIG and (b) comparison with deposition on Pt.	25
3.10	Potentiostatic deposition of PANI on Pt varying reagents' concentrations.	26
3.11	Current measured during the potentiostatic deposition of PANI on Au/ENIG.	27
3.12	Extraction of first growing phase during a potentiostatic deposition on AU/ENIG.	28

3.13	CVs recorded at different scan rates in 1M H_2SO_4 solution for a potentiodynamic deposited PANI.	29
3.14	Quadratic interpolation of the current peaks trend obtained by varying the square root of the CVs scan rate.	30
3.15	Potentiodynamic (a) and potentiostatic (b) PANI after doping/undoping with H_2SO_4	30
3.16	Poly-3-aminophenylboronic acid (PAPBA) chain.	31
3.17	Evolution of a PAPBA deposition without Cl^- incorporation	32
3.18	Current and total charge measured during PAPBA electropolymerization (50 mM APBA and 200 mM NaCl) with and without Nafion. . .	33
3.19	Potentiometric response of PAPBA films deposited with (a) and without (b) Nafion for different concentrations of $MgSO_4$	34
3.20	Spike in the OCV measurements for Nafion-incorporated PAPBA. . .	34
3.21	Current and total charge measured during PAPBA electropolymerization (50 mM APBA and 200 mM NaCl) with different supporting electrolytes.	35
3.22	Potentiometric response of HCl - and H_2SO_4 -based PAPBA films for different concentrations of KCl	36
3.23	Potentiostatic deposition of Polypyrrole with $CaCl_2$ and $K_4Fe(CN)_6$. . .	37
3.24	CVs plot and total exchanged charge of a potentiodynamic deposition of Polypyrrole with $K_4Fe(CN)_6$ on Pt.	39
3.25	Comparison of the potentiostatic and potentiodynamic deposition of PPy on Pt and Au/ENIG.	39
3.26	Surface profile recorded for different PANI films deposited with CV technique.	40
3.27	Linear dependence extraction of the relation between exchanged charge and polymer thickness.	41
3.28	Skewness dependence on surface profile.	42
3.29	Height distributions depending on Kurtosis.	43
3.30	Surface profiles of PPy, PANI and PAPBA.	44
3.31	SEM characterization of Polypyrrole deposited with CA ((a) and (b)) and CV ((c) and (d)) methods	45
3.32	SEM characterization of Polyaniline deposited with CA ((a) and (b)) and CV (c) technique.	46
3.33	Raman spectra of PANI deposited with different techniques and after ageing.	47
3.34	Raman spectra of PAPBA thin films.	48
3.35	Raman spectra of PPy deposited with different salts.	49
4.1	Working principle of a differential thermal flow sensor.	51
4.2	Working principle of a coriolis flow sensor.	52
4.3	Pneumatic pressurization of a flask.	54

4.4	Complete experimental set-up for liquids handling. <i>Credits: Patrick Ruch.</i>	55
4.5	Estimation of volumes through integration of flow rates.	57
4.6	Validation of mixing capabilities.	58
4.7	Representation of the test cell filling	61
5.1	A four electrodes ($\varnothing 2mm$) array and contacts for voltage read-out.	62
5.2	Effect of the oxygen plasma surface treatment on the first deposition cycle of PANI.	64
5.3	Sensor array based on Au/ENIG electrodes.	64
5.4	(a) Brightfield and (b) darkfield optical images of one of the electrodes' edge after the electrodeposition of PAPBA on another electrode.	66
5.5	CV in $0.1M$ KCl of an array's electrode before and after electropolymerization of PANI on another one.	66
5.6	Electrode surface before (a) and after (b) the electrochemical cleaning following the ePPy electropolymerization on another array's electrode.	67
5.7	PAPBA film contaminated by residuals of PPy electropolymerization on another electrode.	68
5.8	Complete array of four polymers: PPy-CA, PANI-CV, PANI-CA and PPy-CV.	68
5.9	CVs of a PPy($CaCl_2$) film recorded in $0.1M$ KCl at 50 mV/s.	70
5.10	PPy-CA interaction with a $0.1M$ KCl and a $0.1M$ Na_2SO_4 solution (four CVs cycles at 50 mV/s).	70
5.11	CVs at 50 mV/s in $0.1M$ KCl solution of PPy-CA ($Fe(CN)_6^{4-}$), PANI-CV and PAPBA films.	71
5.12	Sensitivity slopes in KCl for PPy films deposited with different techniques (CA and CV).	72
5.13	Sensitivity slopes in $MgSO_4$ for PANI-CV, PAPBA and PPy-CA films.	73
5.14	PANI-CV potentiometric response for a sequence of KCl concentrations interspersed with $0.1M$ KCl	75
5.15	(a) Equilibrium potential and (b) potential variations from $0.1M$ KCl reference signal.	76
5.16	Equivalent sensitivity for couples of polymers deposited on an Au/ENIG array: (a) PPy-CA vs PPy-CV , (b) PANI-CA vs PPy-CA , (c) PANI-CA vs PPy-CV . Tests for KCl , $MgSO_4$, Na_2SO_4 and Na_2CO_3	78
5.17	Dynamic evolution of differential voltages for different salts tests.	79
6.1	Down-sampling on a fast signal transition.	83
6.2	Third order polynomial interpolation and coefficients correlation for two tests performed on the same liquid (0.05M KCl).	84
6.3	Polynomial fits of different orders.	85
6.4	Extraction of features from signal (a) and derivative (b) traces.	86

6.5	Electronic tongue device for mineral waters classification (a) and water brands (b).	87
6.6	Differential voltages traces recorded by dipping the sensor in different mineral water brands and <i>0.01M KCl</i> reference solution.	88
6.7	Scatter plot of 72 water tests for two features.	89
6.8	Principal component analysis for 72 water tests after feature extraction.	90
6.9	Confusion matrices obtained with Random forest (a) and LDA (b) classifiers for 72 water tests with cross-validation.	91

List of tables

3.1	Roughness analysis for seven potentiodynamically (CV) deposited PANI films.	43
3.2	Roughness analysis of different polymeric films.	44
5.1	Sensitivity slopes of differential voltages in Figure 5.16.	78
6.1	Classification accuracies dependency on test time and voltage signals involved.	91

Chapter 1

Introduction

1.1 Electronic tongue: a tool driving the future of chemical analysis of liquids

The development of devices capable of recognizing multiple components through an array of sensors dates back to the '90s, when they were applied to the analysis of spoilage of food products and to the detection of ions and heavy metals. Since then, the number of efforts in the study and fabrication of those systems has been steadily increasing, involving a wider range of applications.

The most accepted definition states:

“The electronic tongue is an analytical instrument comprising an array of nonspecific, low-selective, chemical sensors with high stability and cross-sensitivity to different species in solution and an appropriate method of PARC and/or multivariate calibration for data processing” [1].

Thus, the fundamental trait of the electronic tongues is the possibility to respond reproducibly to a number of different analytes which are dispersed in a solution. In this sense, those systems resemble to mimic the biological ones, where thousands of compounds, which can have very similar structures, could be recognized with detection limits in the range of 1 to several hundred ppb [2]. Indeed, gustatory and olfactory receptors generate complex data patterns that can be rapidly processed by the human brain to produce a response, which is the sensation of taste. This astonishing characteristic of biological systems has been generally exploited in many applications where human expert panels demonstrated to be more accurate than artificial instruments. Nevertheless, mimicking human taste and create some specialized devices results to be more effective in those situations that involve scaling of industrial processes (saving time and financial expenses) as well as poisonous samples (repetitive tasting of drugs and pharmaceuticals). Figure 1.1 contains a schematic representation of the working principle of an electronic tongue [3]. Each sample produce signals of a certain nature which are gathered by the array. Artificial

intelligence analyses all the collected data and provide different results in terms of discrimination, identification and/or quantification.

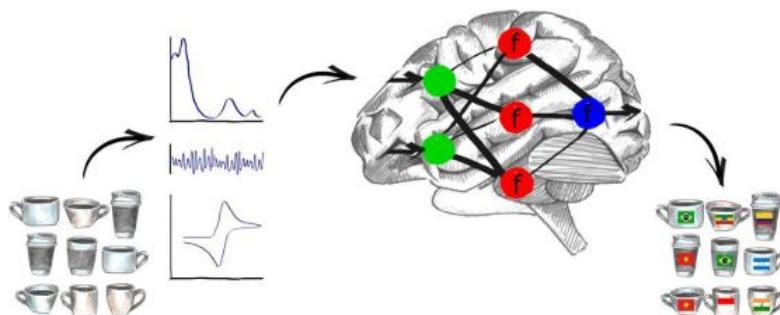


Figure 1.1. Workflow representation of an electronic tongue system

The multifunctional array comprises sensors that can be of different types such as electrochemical (potentiometric, amperometric, voltammetric, impedimetric, conductometric), gravimetric, optical (absorbance, luminescence, reflectance,...) [4], etc. For this reason, sensing materials that have been chosen for the integration in the arrays could vary accordingly to each application. Multitrasduction principles can be applied for the creation of hybrid electronic tongues in order to take advantage of the multiple sensing principles. It is obvious that fingerprinting of liquids and analysis would become more complex and, consequently, more accurate. As regards to the biosensors field, although they represent an extreme case of specificity, many undergo reaction with other substances in the same solution, so that arrays could provide a sort of cross-selectivity. Advances in *BioElectronic Tongue* has been possible through the advent of materials such as Molecularly Imprinted Polymers (MIP). In this case, sensing material deposition occurs in the presence of the targeted molecule, which are removed immediately after synthesis. As a consequence the resulting polymers are able to rebind them in the so formed cavities forming a cross-reactive array [5]. Interestingly, materials properties are properly tuned to show low selectivity and remarkable cross-sensitivity towards as many components as possible. Indeed, the fabrication of an array for multivariate analysis would require a tremendous amount of selective sensors with enough stability, preventing from the device miniaturization. Instead, by integrating a well-defined number of different cross-sensitive elements, the analysis of a multicomponent media would be more efficient producing a *spectrum-like* response. In fact, since each sensor responds in some way to each analyte, the result of the sample analysis is hidden in the evolution of all the extracted signals at the same time. Hence, machine learning approaches and mathematical procedures are oriented towards the pattern recognition (PARC) and multivariate analysis. The most frequently used methods are the partial least-squares regression (PLS), principal component analysis (PCA) and artificial neural networks (ANNs). Qualitative

and quantitative analysis of complex solutions strictly require a training process (calibration) of the electronic tongue in order to apply the above mentioned procedures (Figure 1.2). However, a common goal for all the data processing algorithms is to avoid redundant information that could increase the number of misclassification rather than improving precision, stability and better separation of different classes [6].

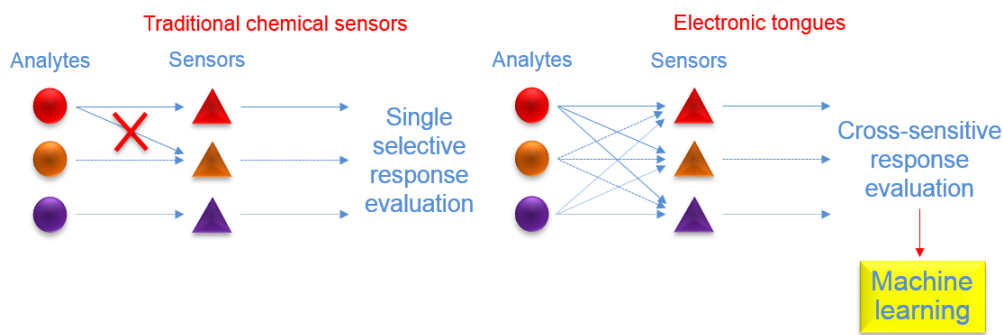


Figure 1.2. Comparison of the analytical procedures between traditional chemical sensors and electronic tongues

In principle, electronic tongues could be characterized by the same parameters of discrete sensors such as selectivity, detection limits etc. Nevertheless, they inevitably possess a different connotation when considering a complex device comprising an array of sensors. First of all, detection limits and selectivity of an electronic tongue depend on the composition of the sensor array as well as on the properties of the sensing material. Thus, the same complex solution under test would display different characteristics for different versions of the electronic tongue. Moreover, such parameters can be derived only after the multivariate analysis and data processing with a strong influence of the adopted calculation method [7]. Instead, other dedicated experimental methods and specific empirical procedures could be used for the determination of the cross-sensitivity of the sensor array. *Vlasov et al.* reported a method based on three different parameters: the average slope of the sensor response for different analytes, the reproducibility and the nonselectivity factors [8].

Nowadays, assessing flavours and detecting compounds, responsible for taste perception in multicomponent mixtures, is the main task driving the applications of electronic tongue. For this reason, it is becoming a versatile tool for food analysis (recognition and origin tracing, evaluation of food quality and freshness, process monitoring, etc.), water analysis, pharmaceuticals industry, biomedical research and safety (national and environmental). Most of the commercial devices rely on more accurate analysis that can be carried out in a laboratory environment. Recently, low-cost portable sensors are being developed since they are believed to have the biggest chance to achieve commercial success. Their main advantage derives from the possibility to serve as perfect screening devices, which can provide preliminary information at lower costs with respect to the sophisticated equipment counterpart.

1.2 Potentiometric cross-sensitive arrays

Electrochemical methods are the simplest and most common transduction mechanisms which have been involved in many research studies for the creation of electronic tongues devices. Chemical interactions can be rapidly converted into electrical signals that, being easily collected and manageable, fit perfectly the requirements for the extensive data processing. The measured signals are capable of providing multiple information coming also from their dynamic components, which are believed to be strictly linked to kinetic reactions and to impact positively the device response [9]. Potentiometry and voltammetry have proven to be the most suitable techniques for electrochemical measurements. Even though it could provide more information regarding the kinetic of a reaction, the voltammetric approach presents some limitations since it requires the interaction of redox-active species. Moreover, it involves the flow of a current between the electrodes resulting in more complex data and more sophisticated integration in miniaturized portable sensors. On the contrary, potentiometric methods do not require dealing with direct application of voltages and current but, rather, it measure an equilibrium condition which results in the collection of Open Circuit Voltages (OCV).

The first arrays based on potentiometric sensors was made of multiple Ion Selective Electrodes (ISEs). Functionalized membranes allowed to collect data from each sensor, that was related to the presence of a specific component in solution. Thus, each electrode, integrated in this *multi-selective* array, could give a response based on the Nikolsky-Eisenmann equation:

$$E = E^0 + \frac{RT}{z_i F} \ln \left[a_i + \sum_j K_{ij} (a_j)^{\frac{z_i}{z_j}} \right] \quad (1.1)$$

where a_i and a_j are the activity of the primary and interfering ion, respectively; K_{ij} is the selectivity coefficient; E^0 is the standard potential; E is the potential difference for the electrochemical cell composed of the ion-selective and reference electrode; z_i and z_j are charge numbers of the primary and interfering ion, respectively, and R is the universal gas constant, T is the absolute temperature and F the Faraday constant. Equation 1.1 takes into account the fact that there exist an ion of interest to be detected (*primary ion*) and a variable number of *interfering ions* for each sensor. Thus, quantitative investigation of a complex liquid would require the knowledge of more and more selectivity coefficients and a limited number of interferences for an accurate analysis. Hence, low-selective sensor arrays revolutionize the conventional electrochemical sensors, replacing the importance of the *selectivity* parameter with the *sensitivity* one and overcoming the limits imposed by the former in the study of multicomponent media. Application of **cross-sensitive** sensor arrays along with **modern mathematical procedures** for signals processing (involving PARC and multivariate analysis) seem driving the future of chemical sensors providing precise qualitative and quantitative information of complex liquids.

Chapter 2

Materials and Methods

2.1 Electrochemical Methods

The fundamental process in electrochemical reactions is the transfer of electrons between an electrode surface and the molecules in the interfacial region, either in solution or immobilized at the electrode surface. The kinetic of such processes can be highly affected by the electrodes surfaces properties and the presence of deposited material. For this reason, microstructure, roughness and blocking of active sites by adsorbed materials need an accurate investigation. The most studied systems by means of electrochemical approaches are Chemically Modified Electrodes (CMEs), for which an evaluation of the relationship of heterogeneous electron transfer and chemical reactivity of electrode surface, the electrostatic phenomena and electron as well as ionic transport in polymers, are necessary. Those analysis are at the basis of the design of electrochemical devices for applications in chemical sensing, energy conversion and storage, molecular electronics, electrochromic displays and electro-organic synthesis. In the following sections, the main electrochemical methods employed for the study and development of an electronic tongue will be introduced. The working principle of potentiometric sensors will be explained as well as the most important techniques aimed at the fabrication and characterization of the sensor array, such as Cyclic Voltammetry and Electropolymerization.

2.1.1 Potentiometric measurements

The interaction between a modified electrode surface and an electrolyte solution can be evaluated through a potentiometric measurement. Potentiometry allows to measure the potential of an electrochemical cell under static conditions, i.e. when the electrochemical cell net current is equal to zero. Thus, whenever an electrode gets in contact with a solution, transfer and movement of charges cause an electrochemical response which is highly dependent on the nature of the electrode surface, with its functionalization, and on the electrolyte composition. Potentiometry represents

the simplest powerful method that can be used in electrochemical sensors for both qualitative and quantitative analysis. Indeed, the first quantitative potentiometric applications appeared soon after the formulation of the Nernst equation (2.1), which relates the electrochemical cell potential to the concentration of electroactive species.

$$E = E_0 + \frac{RT}{nF} \ln(Q_r) \quad (2.1)$$

where E_0 is the standard cell potential, R , T and F have their usual meanings, z is the number of electrons transferred in the cell reaction and Q_r is the reaction quotient of the cell reaction. Q depends on the concentrations of oxidized and reduced forms of the relevant species in solution. As a consequence, depending on the number of ionic charges that interacts with the electrode surface or with the membrane deposited on it, the cell potential would be modified in different ways. Electroactivity of the multiple species can be manifested through mass transfer driven by specific phenomena such as diffusion and migration. The former is associated to the natural response to a depletion or accumulation of species that build up a gradient of concentration. The latter, instead, represents the movement triggered by electrostatic forces that favour certain interactions. Generally, in potentiometry a two-electrodes system is employed:

- the **Working Electrode (WE)** is the one to which it is attributed the variation of E_{cell} due to a change in the analyte's concentration;
- the **Reference Electrode (RE)** ideally provides a stable and known potential.

In all the experiments described in the next chapters, the working electrode potential is always measured against the one of a saturated calomel electrode (SCE). As shown in Figure 2.1, in such electrode the concentration of Cl^- is determined by the solubility of KCl and, for this reason, its potential is maintained fixed, even when some of the solution is lost to evaporation [10]. Potentiometric experiments are performed connecting the two electrodes to a potentiometer. The cell potential corresponds to the open circuit voltage (OCV) that will be measured to evaluate the response of the sensor, which is the evolution of the signal coming from an active material deposited on the working electrode. Potentiometry has been widely exploited for quantitative analysis performed with CMEs and particularly with Ion Selective Electrodes (ISEs). Nevertheless, recording the potential shift of multiple electrodes seems the most promising and simplest way to deal with a sensor arrays for multivariate analysis.

2.1.2 Cyclic Voltammetry

One of the most versatile electrochemical methods is cyclic voltammetry. Such technique is primarily used in all of those investigations which involve charge transfer such as characterization, synthesis and analysis of a wide range of materials. It has

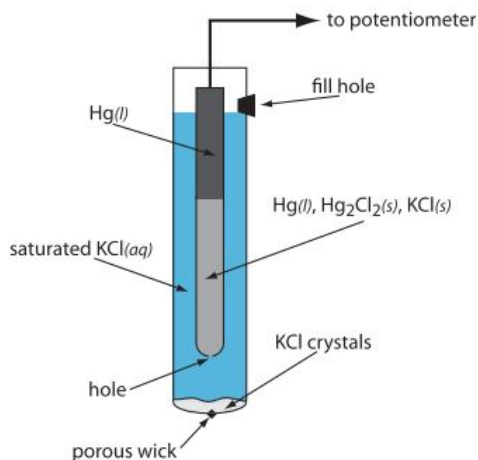


Figure 2.1. Saturated Calomel Electrode (SCE) structure

been shown that it can operate satisfactorily with a large variety of compounds including inorganic, organic, polymer, films and semiconductors. As analytical tool, it has been employed in many scientific areas due to its versatility and flexibility. Generally speaking, Voltammetry has always played a role as complementary method in research, development and application labs. Thanks to its simplicity, sensitivity, speed and low costs, it is considered a prominent technique among many others. It can provide deep insights into the relationship of structure, potential and characteristic activities, monitoring the electrochemical behavior of a great variety of substances [11]. Historically, this branch of electrochemistry was developed starting from the discovery of polarography in 1922. Basically, it refers to the measurement of a current which is originating from the application of a certain potential in a well-defined system comprising multiple electrodes. The aim of the voltammetric methods is thus to track the electroactive species that come from the bulk solution and approaches the electrode surface. With respect to the spectroscopic techniques which evaluate more complex chemical responses, voltammetry allows measurement of speed of the electron transfer process and can give an estimation of the amount of charges which are involved. As a consequence, it may be possible to perform both quantitative and qualitative analysis for the determination of a variety of dissolved inorganic and organic species.

Three electrodes systems

With respect to potentiometry that employs only two electrodes, voltammetric measurements necessarily involve a three electrodes system comprising a Working Electrode (WE), a Reference Electrode (RE) and a Counter Electrode (CE) allowing the accurate application of potential functions and the measurement of the corresponding currents through a Potentiostat (Figure 2.2).

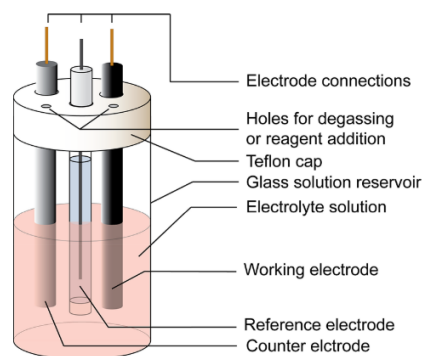


Figure 2.2. Three electrodes setup for CV and electropolymerization

Depending on the applied potential function that is provided to drive the reaction, it is possible to distinguish between different techniques: Linear Sweep Voltammetry (LSV), Square Wave Voltammetry (SWV), Anodic Stripping Voltammetry (ASV), Normal Pulse Polarography (NPP), Differential Pulse Voltammetry (DPV) and Cyclic Voltammetry (CV). CV is the most widely used technique for acquiring qualitative information about electrochemical reactions. Due to its rapid response for the evaluation of the thermodynamics of redox processes, chemical reactions and adsorption processes, it is often the first approach in electroanalytical studies. The required equipment consists of a potentiostat connected to three electrodes which are immersed in a solution. The instrument applies and maintains the potential between the working and the reference electrode while measuring at the same time the current given by the flow of charges between the working and the counter electrodes.

Cyclic Voltammograms

Voltammograms or cyclic voltammograms display the measured current versus the applied potential during the CV. The corresponding traces are obtained by sweeping the potential between two fixed values repeatedly and with a well-defined speed, called sweep rate. Thus, the excitation signal is a linear potential scan with triangular waveform between the two switching potentials. Two conventions are commonly used to report the CV data depending on the way in which the x-axis is shown (Figure 5.10)

The traces contain an arrow indicating the direction in which the potential was scanned and defines the forward and backward sweeping. When the potential is swept towards the negative switching value, the cathodic trace is recorded while the opposite direction produces the anodic plot. The current measured during this process is often normalized to the electrode surface area and referred to as the current density. A peak in the measured current is seen at a potential that is characteristic of any electrode reaction taking place. The peak width and height for a particular process may depend on the sweep rate, electrolyte concentration and the electrode

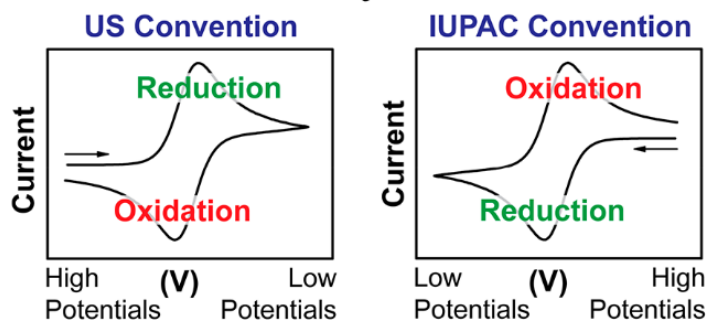


Figure 2.3. Cyclic Voltammograms conventions

material. By applying the Nernst equation to a one electrode reduction system, the activity coefficients are usually referred as the concentrations of the oxidized and reduced forms and the standard potential E_0 is called *formal potential*, which is related to the experimental conditions. Thus, it is possible to predict how a system would respond to a change of the applied potential or of the concentration of species. During a CV, the potential is continuously swept between two values resulting in a variation of the concentration of the species at the electrode interface and in the solution (Figure 2.4).

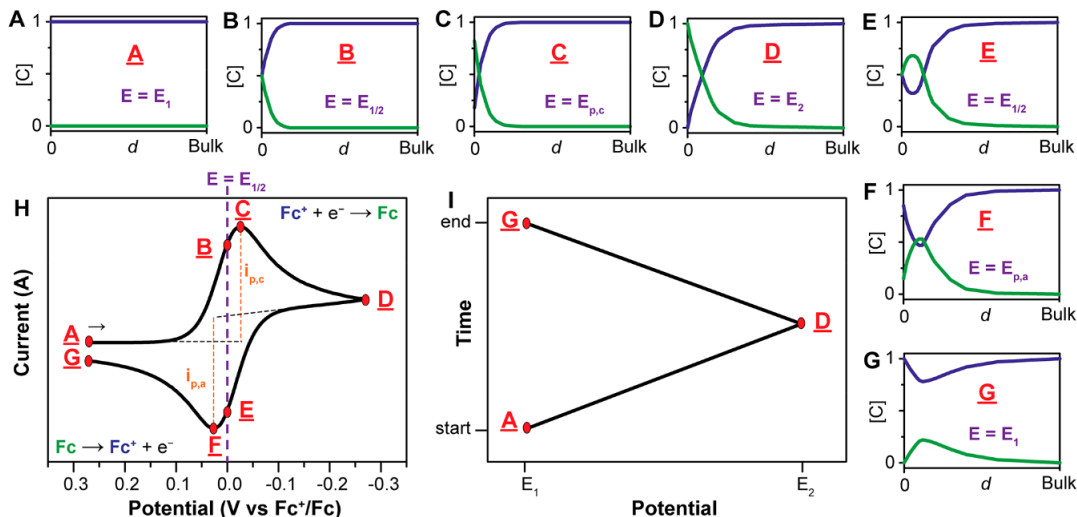


Figure 2.4. Cyclic voltammetry traces formation

When a solution containing oxidized species ($[Ox]$) is scanned to negative potentials (A to B), reduction takes place leading to a local increase of the amount of reduced species ($[Red]$) at the electrode and a consequent depletion of the oxidized elements. If the applied potential matches the formal potential, the equilibrium described by the Nernst equation requires that $[Ox]$ and $[Red]$ reach the same value.

The more the potential is scanned cathodically, the more a depletion in the oxidized species leads to an increase of the reduced ones. When a peak of the cathodic current is achieved, the reactions are dictated by the diffusion of [Ox] from the solution that are instantaneously reduced. Consequently, the increasing amount of [Red] form the so called *diffusion layer*, whose growth starts to slow down the mass transport of [Ox]. Thus, the measured current experiences a decrease if scanning to more negative potentials (D). The ratio of the concentrations of oxidized and reduced species reaches its minimum when applying the negative switching potential, satisfying the Nernst equation.

When the potential is swept back towards positive values the reduced species are oxidized back and when E equals again the formal potential, the two concentrations at the electrode surface are the same. When sweeping towards more positive values the anodic peak is achieved before the current values slightly decrease reaching the minimum value when approaching the positive switching potential. The visualization of the cyclic voltammogram allows the determination of the formal potential, which is defined as the halfway between the potentials applied to reach the anodic and cathodic current peaks. Additional information could be extracted related to the kinetics of the reaction as well as to the reversibility of the processes. Indeed, the Nernstian equilibrium is achieved much faster in the case of low electron transfer barrier which characterizes reversible reactions. Since the redox system remains in equilibrium throughout the potential scan and the species concentrations always satisfy the Nernst equation, the peak potential separation ($E_{pa}-E_{pc}$) is always equal to $57/n$ mV, where n is the number of electrons involved in the reaction. In the case of high electron transfer barriers, instead, the peak-to-peak separation is much higher due to stronger negative and positive potentials needed to allow the reactions. Thus, chemical reactions are coupled to redox processes and adsorption of either reactants or products occur. In a typical voltammogram, there can be several peaks. From the sweep-rate dependence of the peak amplitudes, widths and potentials of the peaks observed in the voltammogram, it is possible to investigate the role of adsorption, diffusion, and coupled homogeneous chemical reaction mechanisms [12].

The speed at which the potential is varied is defined by the scan rate control parameter. To faster scan rates correspond a decrease in the size of the diffusion layer, leading to higher currents measurements. For electrochemically reversible electron transfer processes involving freely diffusing redox species, the Randles-Sevcik (equation 2.2) describes how the peak current i_p [A] increases linearly with the square root of the scan rate ν [$V \cdot s^{-1}$], n is the number of electrons transferred in the redox event, A [cm^2] is the electrode surface area (usually treated as the geometric surface area), D_0 [$cm^2 \cdot s^{-1}$] is the diffusion coefficient of the oxidized analyte and C^0 [$mol \cdot cm^{-3}$] is the bulk concentration of the analyte.

$$i_p = 0.446nFAC^0 \left(\frac{nF\nu D_0}{RT} \right)^{1/2} \quad (2.2)$$

In addition to verifying that the analyte is freely diffusing, the Randles-Sevcik equation may also be used to calculate diffusion coefficients. Whenever an analyte is absorbed to the electrode surface the experimental current value may vary with respect to the one calculated through equation 2.2. For this reason, it is essential to assess whether an analyte remains homogeneous in solution prior to analyzing its reactivity. Indeed, for an electrode-absorbed species, equation 2.3 can be used to approximate the current response:

$$ip = \frac{n^2 F^2}{4RT} \nu A \Gamma^* \quad (2.3)$$

where Γ^* is the surface coverage [$mol \cdot cm^{-2}$]. Considering an analyte that is believed a freely diffusing species, the deviation from the square root dependence on the scan rate could be interpreted either as (a) an electrochemical *quasi-reversibility* or (b) that the electron transfer may be occurring through *surface-absorbed species* and equation 2.3 could be applied. The peak-to-peak separation shift with scan rate is an indication of the *quasi-reversibility* of the process while *surface absorbed-species* may be characterized by no variation of the peak-to-peak separation.

2.1.3 Electropolymerization

One of the main techniques that is used to grow polymer coatings is electropolymerization. The main advantage of this electrochemical method is the possibility to deposit directly the material on the electrode surface, facilitating its control. By adjusting multiple parameters of the electrochemical experiment, it is possible to locally create polymer films and to modulate their thickness and conductivity. For this reason, chemical polymerization is only used when large quantity of polymer with less control is required. Generally, electrochemical polymerization consists of three different steps:

1. the monomer is oxidized at the anode, leading to the soluble oligomers' formation in the diffusion layer;
2. oligomers are deposited through nucleation and growth processes;
3. the chain is propagated through solid state polymerization.

Even though all the electropolymerization experiments follow the previous three steps, in many cases there could be multiple modifications, thus preventing the establishment of a more general model for such mechanisms. However, it is known that the first step is responsible for the formation of the reactive cationic radicals by applying a well-defined potential to the working electrode. The second step is believed

to be the most important to define the way in which the polymer grows, depending on the different experimental conditions. It has always been of great interest the study of the kinetics of the nucleation and growth process during the electrochemical synthesis in order to perfectly control the density, crystallinity, morphology and all the other main properties of the desired polymer. The most accepted approach to describe those processes is the so called **metal deposition theory**. According to such theory, there exist essentially two basic nucleation phenomena: instantaneous and progressive. The former implies that there is a constant number of nuclei that are forming instantaneously at the beginning of the polymerization, without any additional contribution coming from new nuclei. The latter, instead, takes into account the continuous generation of new nuclei for the formation of the final film. To both the theories it is possible to associate three types of growth: one- (1D), two- (2D), and three- (3D) dimensional processes. 1D growth happens in only one direction, e.g. perpendicular to the electrode surface. In the 2D growth, nuclei preferably grow parallel to the electrode surface, while the 3D growth is characterized by similar rates for both directions of growth of the polymer.

Numerous parameters are involved in the electrochemical synthesis of conductive polymers such as: nature of the doping anion (affecting morphology), order of the polymer rate growth, nature and the composition of the solvent, electrode material (depending on its surface energy controls the ease of the desired polymer deposition), temperature of the electrochemical polymerization etc. Since the electropolymerization is triggered at the working electrode surface, it is of fundamental importance that it is extremely clean with a flat surface area exposed. Electrode *pretreating* prior to electropolymerization includes mechanical polishing, sonication in ultrapure water to remove particles residuals and CV scans in simple electrolyte over a wide potential window to remove any adsorbed species. Mechanical polishing is the first procedure to be applied when a new active material has to be deposited. Pre-treatment of the electrodes surfaces prior to the electropolymerization on Platinum rod, discussed in the next sections, has been performed by figure-eight motions on different polishing pads (Figure 2.5). Diamond powder allows a coarse surface treatment and it is followed by a fine polishing through an alumina slurry.

2.2 Conductive Polymers

The extensive use of conductive polymers (CPs) provides many advantages from the point of view of the chemical diversity, low density, flexibility, corrosion resistance, easy-to-control shape and morphology, and tunable conductivity over their existing inorganic counterparts [13]. Atomic orbitals characterized by sp³-hybridization are engaged in covalent bonds in conventional non conducting organic polymers such as polyethylene. Since the mobility of the corresponding σ – *bonding* valence electrons is fairly low, they do not contribute to the electrical conductivity of the polymer.

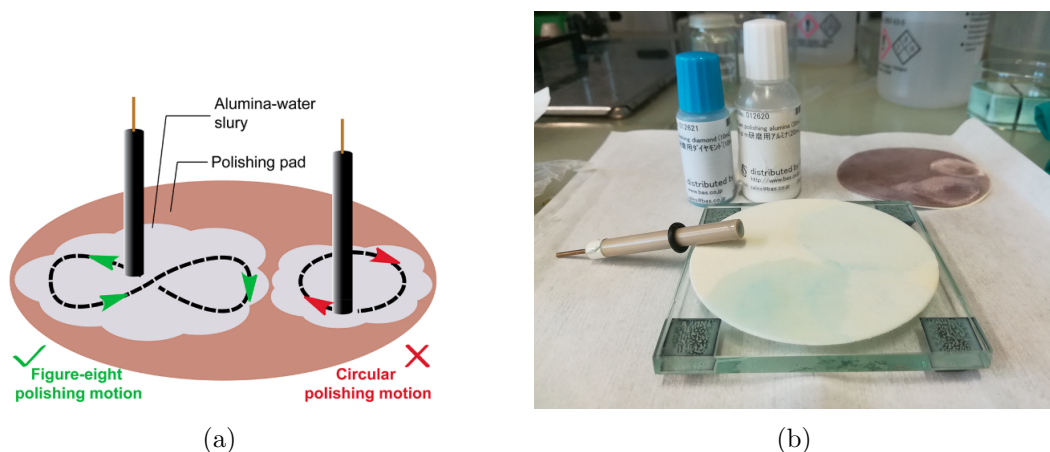


Figure 2.5. (a) Homogeneous polishing movement and (b) diamond and alumina slurries treatment on Pt electrode.

The situation is completely different in Electro Conductive Polymers (ECPs) where contiguous sp^2 hybridized carbon atom centers constitute the backbone of the polymers [14] (Figure 2.6).

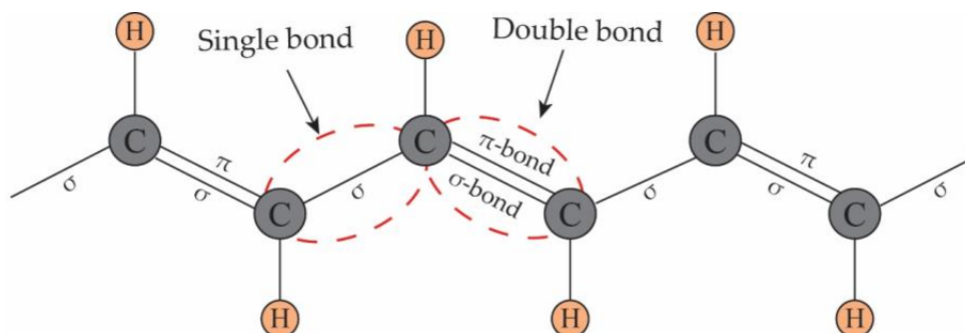


Figure 2.6. The structure of polyacetylene and its conjugated double bonds.

In this case valence electrons occupy the p_z atomic orbital which is placed orthogonally to the other three bonds. Those electrons are the ones involved in the formation of conjugated π molecular orbitals and are highly delocalized. If the polymer backbone is doped by oxidation or reduction processes, it can be positively or negatively charged due to the removal or injection of those valence electrons respectively. Thus, similarly to all the other semiconductors, a one-dimensional electronic band is formed and the mobility of the electrons in the band is highly affected by the polymer doping level. As a consequence, the properties of such materials cover a wide range of applications including electronics, optoelectronics, sensors, and energy devices. CPs possess excellent characteristics such as mild synthesis and processing conditions and, thanks to their tunability, they are characterized by a remarkable

multifunctionality. Recent nanotechnologies advances in the fabrication of versatile CPs nanomaterials, allow an accurate control of the doping level and of the swelling/de-swelling polymer processes, so that they have been introduced in the micro and nano actuators world. For the purpose of the electronic tongue fabrication described in the present work, three different conductive polymers have been studied and synthesized: *Polyaniline* (PANI), *Poly-aminophenyl-boronic-acid* (PAPBA) and *Polypyrrole* (PPy).

Chapter 3

Electrodeposition, study and characterization of CPs

3.1 Introduction

Conductive polymers introduced in the previous chapter have been deposited on different electrodes through electropolymerization. The Platinum rod electrode has been mainly employed for recipes tests and investigation. Optimization of the deposition of all the materials has been carried out on both *Pt* and *Au* with different surface areas. Polymers characterization is presented at the end of the chapter to evaluate the main characteristics of the synthesized films.

3.2 Polyaniline's electropolymerization and tunable properties

Polyaniline films have been of great interest among all the studied conductive polymers due to their unique properties. In particular, it has been demonstrated that such polymeric coatings exhibit some electrical and optical activity as well as environmental stability and redox reversibility. Moreover, due to the low cost of the corresponding monomer, there have been studies on both theoretical and practical aspects related to their application in sensors, electrochemical devices, rechargeable power sources and many others [15]. One of the most interesting peculiarities of Polyaniline is that it exists in multiple forms, depending on the degree of oxidation achieved during the electropolymerization. Leucoemeraldine (eg. leucoemeraldine base) corresponds to the fully reduced form, emeraldine (eg. emeraldine base) is half-oxidized while pernigraniline (eg. pernigraniline base) is the fully oxidized form. The conductivity of Polyaniline film is actually enhanced when properly doping or protonating the emeraldine base through chemical and electrochemical reactions,

allowing mutual conversions in the different forms. The transitions between the oxidized states are characterized by changes in the conductivity and in the color of the films, so that it is possible to easily recognize the level of oxidation that has been achieved. The Polyaniline form, that is commonly employed as conductive polymer in multiple applications, is the green emeraldine one which is characterized by the highest conductivity. In figure 3.1, it is shown an example on how to change the oxidation state of the polymeric chain in order to create different coatings characterized by specific conductivity levels. When reducing the green emeraldine salt to leucoemeraldine or oxidizing it to perningraniline, a steep decrease in the conductivity can be noticed.

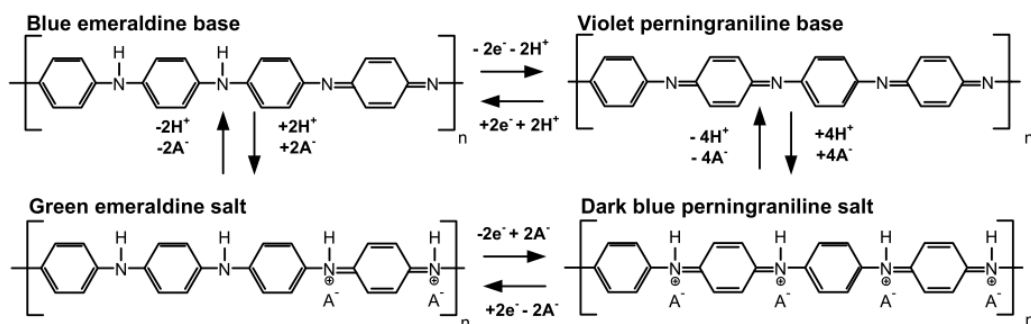


Figure 3.1. Switch of Polyaniline oxidation states.

During the electrochemical polymerization, anilinium radical cations are formed by aniline oxidation on the electrode and it has been demonstrated that the chemical reaction that leads to the formation of the polymer coating is auto-catalytic [16]. However, the nature of the polymerized process depends on multiple factors such as the electrode material, the electrolyte solution, the dopant ions and the pH of the electrolyte. In particular, strong acidic aqueous electrolytes are required for the formation of a conductive Polyaniline forms, while higher pH values generally are involved in the deposition of short conjugation oligomeric chains. A crucial role during the electrodeposition is played by the doping ions, mainly derived from the electrolyte solution, that strongly affect the morphology, the conductivity, the rate of the Polyaniline growth and the degradation process. The first electropolymerization step is the anodic oxidation of aniline monomers to create the aniline cation radicals, which are strictly linked to the entire reaction rate. When two anilinium radicals couple and expel two protons, a rearomatization allows the formation of a dimer. Dimers can be further oxidized and react with other components leading to the formation of oligomers and, eventually, to the polymeric chain. Doping ions are finally linked to satisfy the neutrality requirements and determine most of the film properties. Unlike most of the other conductive polymers, the radical cations are formed at the nitrogen atoms of the polymeric chains. Moreover, since such atoms are also involved in the conjugated double bonds, the electrical conductivity is affected

by both the oxidation and protonation (doping) degree. Indeed, the emeraldine base half-oxidized form is composed by the same amount of amine (-NH-) and imine (=NH-) sites. When the latter are protonated, a well-defined structure containing delocalized bonds with the doping ions can be formed, eventually giving rise to a high conductivity behavior of the chain. The other oxidized states of Polyaniline are not characterized by such peculiarity due to either overoxidation (perningraniline) that prevents bonds and charges delocalization, or full-reduction (leucoemeraldine) that is characterized by undoped imine sites (Figure 3.2).

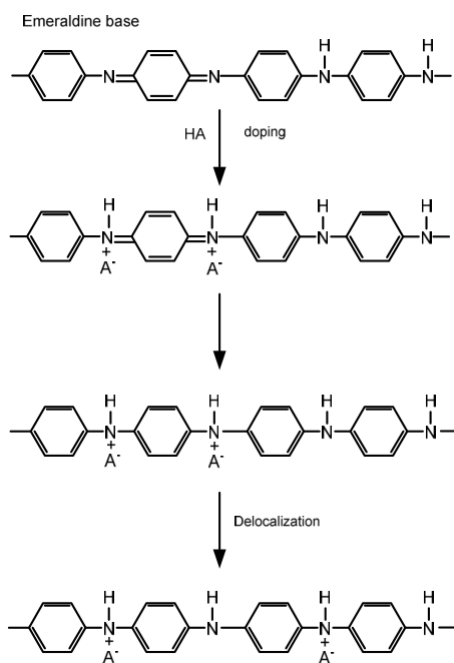


Figure 3.2. Doping of emeraldine base to achieve a conductive PANI state.

In general, the undoped emeraldine form has a conductivity in the order of 10^{-2} [$S \cdot cm^{-1}$] while doping can increase such value up to 10^3 [$S \cdot cm^{-1}$]. Morphology, temperature and moisture amount also affect significantly the conductive behavior of these polymer coatings.

3.2.1 Growth process

It has been demonstrated that Polyaniline films could be grown both on bare electrodes and on pre-treated surfaces, leading to the formation of PANI with different electrochemical properties. In case of specific modifications performed on the electrode surfaces to enhance the formation of the polymer, different electropolymerization conditions could be applied with respect to bare electrode surfaces. In particular, it has been shown in previous works [17] that electrosynthesis on engineered substrates could be achieved with a moderate concentration of the acidic electrolyte

solution and with low concentration of monomer precursors. In the present work, electrodeposition has been performed mainly on inert metallic substrates such as Platinum and Gold, employing both potentiodynamic and potentiostatic methods. For this reason, pre-treatment of the surfaces was not a strict requirement for the formation of the polymer coatings. However, since the same Pt rod has been repeatedly used for the study of multiple electropolymerization recipes, it has been polished with diamond and alumina powders prior to each deposition. In the previous sections, it has been already mentioned that Polyaniline growth can be easily achieved when using acidic electrolyte solutions due to the chemical processes involved during the formation of the films. One of the most used acid for this purpose is the sulfuric one, due to the well-defined electrochemical activity of the corresponding synthesized coatings. Many previous works report that the CV potential window to be used for the potentiodynamic creation of the film is from -0.2V to 1.0V in order to allow the characteristic oxidation and reduction peaks formation. The upper constraint of such range is usually limited and, in some cases, can be slightly reduced in order to avoid the overoxidation of the films, and consequently their fast degradation. The minimum scan rate that is usually applied for this conductive polymer is about 50 mV/sec , while the number of cycles can be modulated depending on the reactivity of the substrate and on the desired film thickness. Indeed, the cyclic voltammograms of an electropolymerization experiment contains some well-defined peaks, whose increasing intensity indicates that additional material is being deposited at each iteration of the potential sweep. It is known that the electrooxidation of aniline causing the polymerization follows a two-electron transfer process, described by the following equation 3.1:

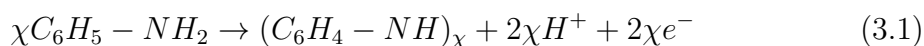


Figure 3.3 shows the cyclic voltammograms of the 15 cycles with a scan rate of 50 mV/s in the potential range -0.2 to 1.0 V at Pt-rod electrode in $0.5\text{ M } H_2SO_4$ solution containing 0.35 M aniline .

In this case, the first positive potential sweep shows the aniline oxidation occurring in proximity of the working electrode's surface. The distinct irreversible current peak at about 0.9V (SCE) indicates that part of the product of such oxidation is deposited on the electrode and that the growth process is taking place. The subsequent cycles are characterized by a lower oxidative potential due to the fact that PANI growth has an autocatalytic effect, while the peak observed in the first cycle decreases and finally disappears. By looking at the way in which the shape of the curves and the redox potentials vary, it is possible to evidence the regularity of the growth of the polymer. The current peaks characterizing the cyclic voltammograms reflect the possibility of Polyaniline films to change their oxidation state and, consequently, their properties in terms of conductivity and electrochemical response. The first redox peak at around 0.2V (1,1') is attributed to the transformation of

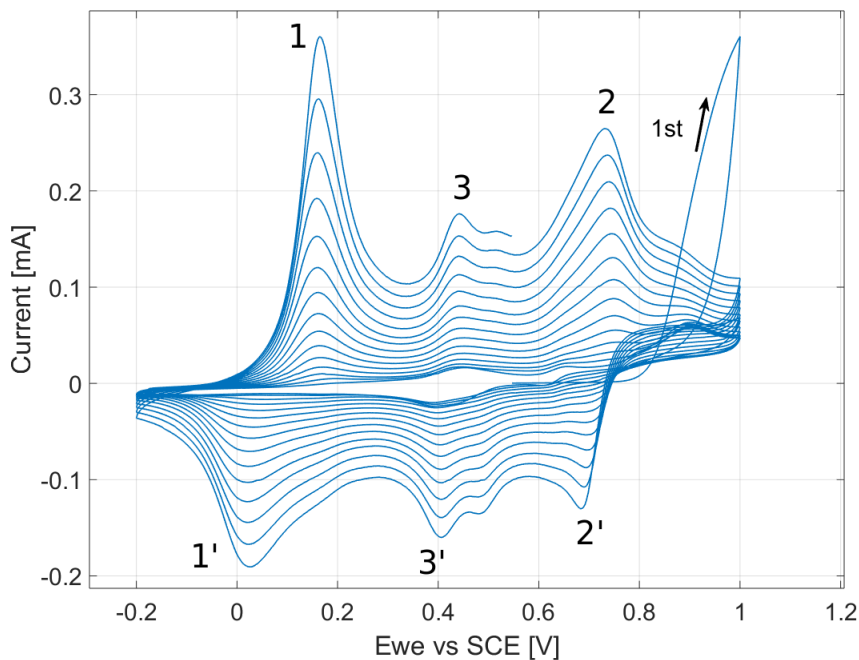


Figure 3.3. CV electrodeposition of PANI on Pt rod.

the full reduced LE (leucoemeraldine) Polyaniline form in the partly oxidized state EM (emeraldine). Instead, the second highest peak (2,2'), at around 0.6V is usually associated to the direct transition from the LE Polyaniline in the full oxidized PE (pernigraniline) state. Thus, looking at the intensity of those peaks it is possible to get useful information regarding the final state of the Polyaniline coatings and, consequently, predict their electrochemical behaviour. It is known that the growth of such polymer leads to the formation of reaction intermediates such as p-benzoquinone, p-aminophenol and some dimers that may be trapped inside the polymeric matrix. The creation of such compounds can be evidenced through the presence of a smaller redox current peak at around 0.4V, which is generally attributed to a redox activity of p-benzoquinone. In ideal cases, the formation of such by-products is limited since they are believed to play an important role in the degradation rate of the synthesized coatings, decreasing their lifetime [18]. The measurement of the total charge involved during the electropolymerization in each sweeping cycle is a strong indication for the growth rate of the polymer, thus it can be used to estimate the reactivity of the different substrates to the Polyaniline deposition. Moreover, the quantity of charge added at each cycle may differ with respect to the other ones, meaning that there is a variation on the growth rate within the same electrodeposition.

3.2.2 Effects of electropolymerization conditions

Scan window and minimum reagents' concentrations. In Figure 3.4(a) it is shown another cyclic voltammogram referred to the deposition of Polyaniline. Even though the solution used for the electropolymerization is the same of the one of Figure 3.3, the plots show some remarkable differences due to the variation of the potential window that has been employed for the sweep. Such result confirms the importance of properly choosing the two switching potentials for the CV electrodeposition in order to modulate the properties of the grown polymer.

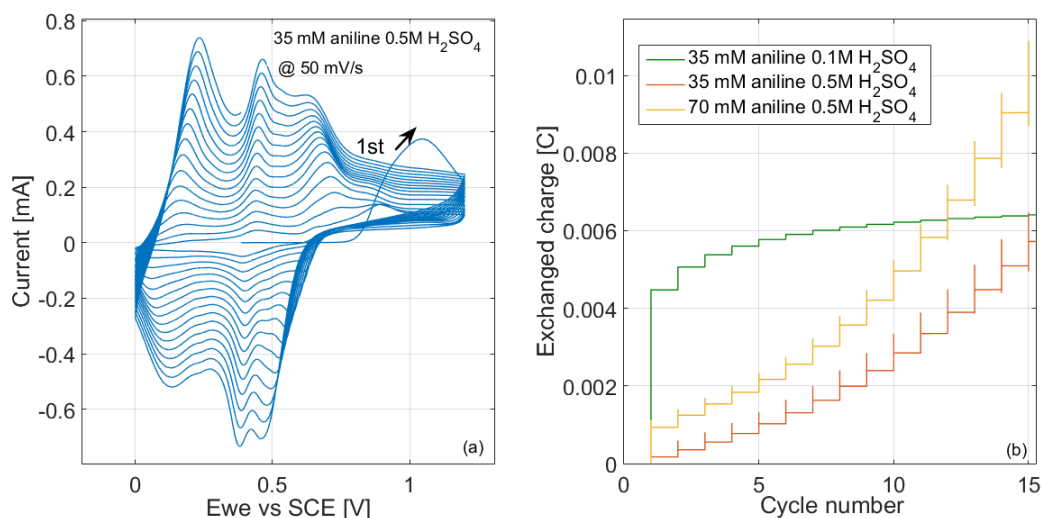


Figure 3.4. (a) Shift of the scan window effect and (b) Impact of precursors' concentration on PANI growth rate.

In fact, as shown in Figure 3.4(a), where the potential window has been shifted of 0.2 V towards positive values with respect to Figure 3.3, it is needed a new analysis of the current peaks to evaluate the effect of such variation. In both cases, the first redox peak is located at around 0.2V and the measured currents are comparable. The main differences involve the other peaks: the one related to the formation of the full-oxidized Polyaniline form (located at around 0.6 V) is not well-defined as in the case of Figure 3.3. The main reason is the great enhancement of the intermediate peak, associated to reaction by-products formation, which is overlapping with the other one due to its higher intensity. As already mentioned, p-benzoquinone synthesis should be avoided since it could remain trapped inside the polymeric matrix. For this reason, all the following Polyaniline electropolymerizations are performed in a sweep range between **-0.2 V and 1 V**, resulting in a more controllable polymer growth. Considering bare surfaces of Pt and Au and regardless of the electrodes' dimensions, electropolymerization was unsuccessful when employing 0.1 mol/L or lower values of acid concentrations. In the same way, a solution containing less than 30 mM of aniline demonstrated not to be effective for an appreciable growth of the

films. Moreover, varying the potential sweep range and scan rate during a cyclic voltammetry deposition, or modifying the applied potential during a potentiostatic experiment, could not allow the electrodeposition with such reagents' concentrations. Figure 3.4(b) shows the total charge exchanged during the polymer deposition. It can be noticed that the growth rate is much more enhanced when the acid concentration is increased, allowing the polymerization with aniline concentration as low as 35 mM . Moreover, the amount of charge that is exchanged increases each cycle, demonstrating the regularity of the growth. On the other side, lower acid concentrations are characterized by strong aniline cations formation in the first cycle. Nevertheless, the charge exchanged at each cycle is reduced more and more, meaning that the polymer has not grown properly. This fact could be demonstrated by investigating the CVs for the deposition, which would not show any characteristic redox peak of the Polyaniline formation.

Electrolyte's concentration. Instead, by increasing the concentration of the supporting electrolyte, the overall measured current can be affected by a huge increase, leading to a greater charge exchange and, consequently, to a thicker polymer formation. In Figure 3.5, CVs for deposition of Polyaniline with different acid concentrations are reported. The curves refer to the electropolymerization on Platinum electrodes with 0.5 mm of diameter. The results show that by doubling the concentration from 0.5 M to 1 M and maintaining fixed all the other parameters, all the current peaks are about four times higher, suggesting a quadratic dependence of the redox peak with respect to the electrolyte concentration.

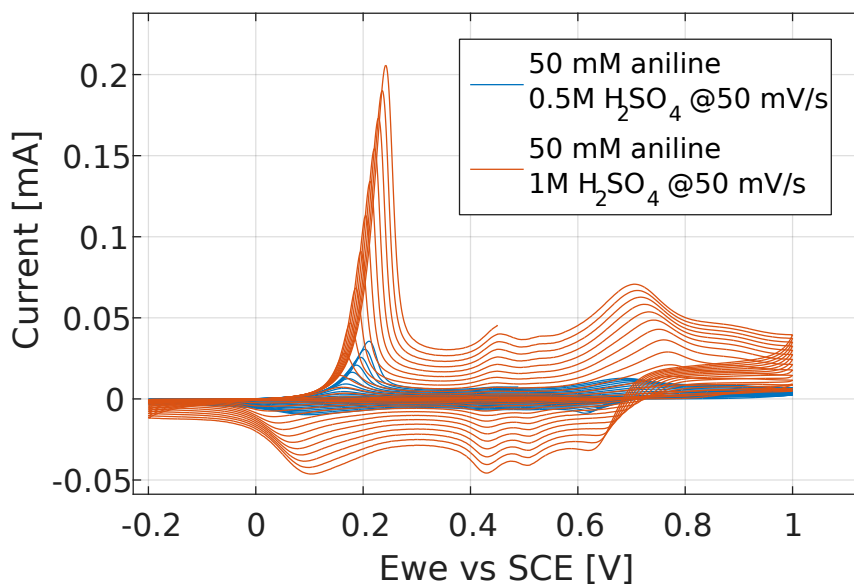


Figure 3.5. Effect of electrolyte's concentration on CV electrodeposited PANI on Pt electrode.

Electrolyte’s nature. The CVs traces can also be employed to study the effect of the supporting electrolyte nature on the electropolymerization. HCl and H_2SO_4 have been both used to evaluate the performances of Polyaniline films doped with Cl^- and SO_4^{2-} anions respectively. In figure 3.6(a) it is reported the cyclic voltammogram for the deposition of PANI using HCl . A comparison between the two acids can be made by evaluating the differences between Figure 3.6(a) and Figure 3.3, which refers to the polymerizations occurring under exactly the same condition except the nature of the supporting electrolyte.

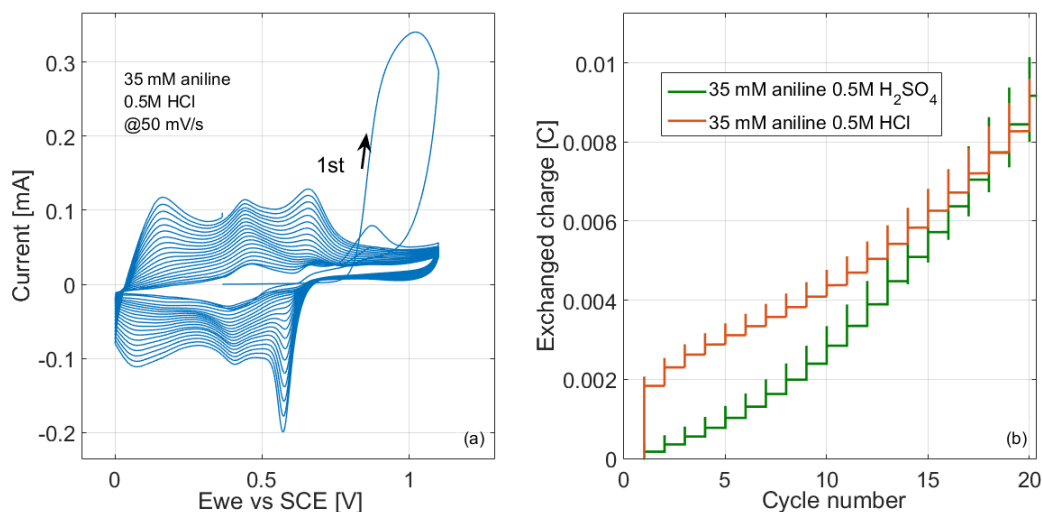


Figure 3.6. (a) Potentiodynamic deposition of PANI on Pt rod with HCl -based solution. (b) Comparison of charge involved in electropolymerization depending on the electrolyte’s concentration.

Regarding the peaks’ positions, it can be noticed that HCl -based Polyaniline growth is not affected by any shift, so that it is possible to associate the redox peaks to the different oxidation state of the film. However, by looking at the relative current intensities, it can be seen that all the peaks reach a similar height, meaning that the redox activity of the different Polyaniline forms is almost the same. On the other side, the H_2SO_4 -based PANI, that has been widely used in the present work, shows the enhancement of the first redox peak, which corresponds to the most conductive form of polyaniline (EM). The higher conductivity of such film with respect to the HCl -based one has already been demonstrated in previous works [19], with a difference of conductivity of three orders of magnitude. Figure 3.6 shows the total charge exchanged during the electropolymerization of the two films based on the different acids. It can be noticed that, after 20 cycles, the two films have grown of the same amount. While the HCl -based curve shows a step increase of the charge during the first cycle due to the formation of radical cations, the H_2SO_4 -based one is characterized by higher increase rate. In both cases the trend of the

exchanged charge with respect to the cycle number is not linear but rather close to a quadratic behaviour. In fact, Cl^- and SO_4^{2-} belong both to the **Class 2** ions for the Polyaniline growth [20]. With respect to the **Class 1** ions (BF_4^- , ClO_4^- and CF_3COO^-) which promote the formation of more compact structures, **Class 2** anions are involved in the formation of more open structures, suitable for potentiometric sensors preparation. However, the morphology of the films can vary a lot within the same class : the SO_4^{2-} anions are responsible for the formation of the high conductive sponge-like films while HCl based solutions lead to the formation of less conductive spaghetti-like structures. Potentiometric responses of the two films were evaluated by measuring the voltage obtained when dipping the polymers deposited on the Pt rod in different concentrations of the same salt solution. In figure 3.7, it shown the comparison between the two films interacting with salts solution containing large ions (Mg^{2+} and SO_4^{2-}).

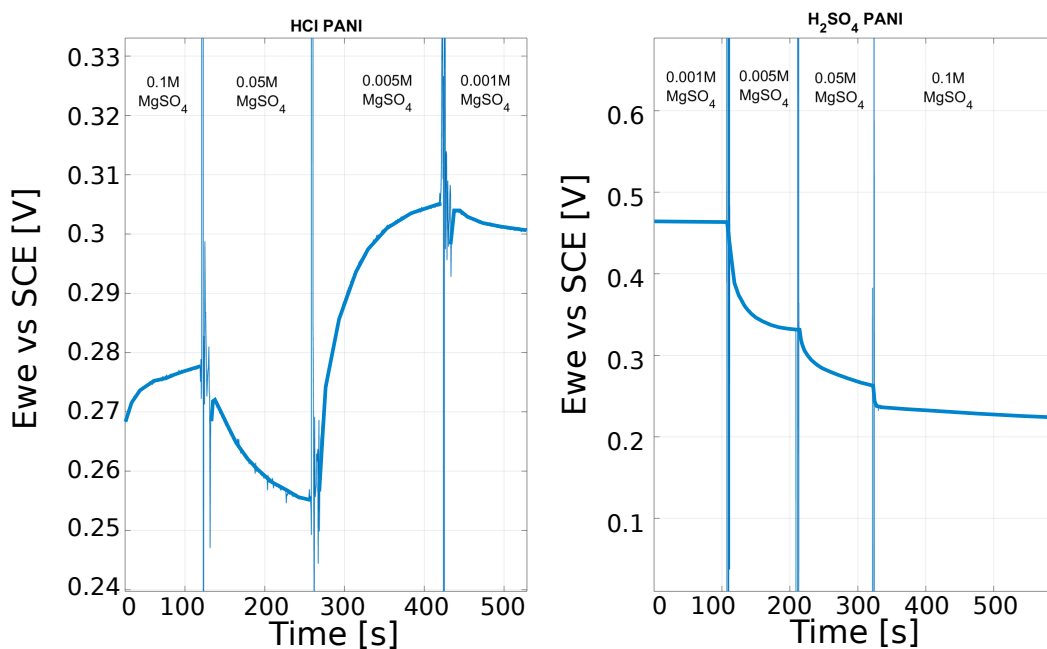


Figure 3.7. Potentiometric response of (a) Cl^- doped and (b) SO_4^{2-} doped PANI in different concentrations of $MgSO_4$

While the H_2SO_4 -based polymer shows a certain sensitivity towards large anions with a decreasing potential trend, the HCl -based one does not provide a clear response towards those charges.

Sweep rate. It is known that the scan rate parameter plays an important role when electropolymerization is performed through cyclic voltammetry. Equations 2.2 and 2.3 suggest that by increasing the sweep rate of the electrodeposition, one should expect higher values of the measured current depending on the type of involved

electrochemical reaction. Many Polyaniline electropolymerization studies report that optimum scan rate values are around 50 mV/s . In fact, the current peaks are lower for slower sweeps, leading to reduced growths of the polymeric films. However, an extensive increase of such parameter may produce unpredictable results: the electropolymerization reactions could not sustain the speed of the scan rates due to the nature of the kinetic reaction and to the variability of the adsorption processes. In figure 3.8, it is shown that the experiments performed at 100 mV/s produces lower current peaks. This fact confirms that 50 mV/s represents an optimum value, that has been chosen for the electropolymerization of Polyaniline in the present work.

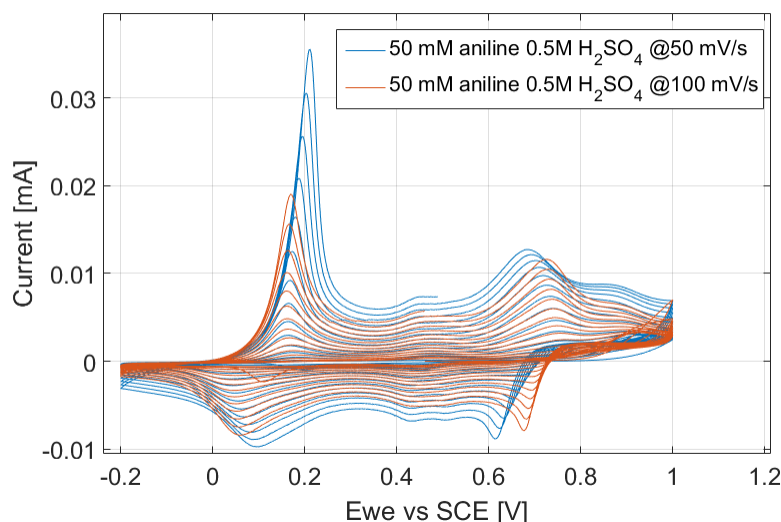


Figure 3.8. CV electrodeposition at different scan rates.

Electropolymerization on Au/ENIG. The CV deposition of Polyaniline on different substrates has been carried out using the recipes reported in the previous sections for Platinum electrodes. However, it has been proven that the deposition on Au with ENIG support is not possible with an electrolyte concentration of $0.5M$ and a scan rate of 50 mV/s . Indeed, multiple attempts have shown that, regardless of all the other parameters and under those conditions, the deposition is unsuccessful and, in some cases, it may cause the corrosion of the electrode surface. Thus, it turns out that the choice of the substrate and its support may affect strongly the electropolymerization conditions and, consequently, the film properties. A successful polymerization has been achieved on Au/ENIG substrates with a scan rate of 100 mV/s , suggesting that at this speed the electropolymerization reaction is more favourable than the corrosion of the electrode. Moreover, the $1M\text{ H}_2\text{SO}_4$ electrolyte solution has shown to produce cyclic voltammograms shapes (Figure 3.9(a)) similar to the ones obtained with Pt, making possible the recognition of the anodic and cathodic peaks.

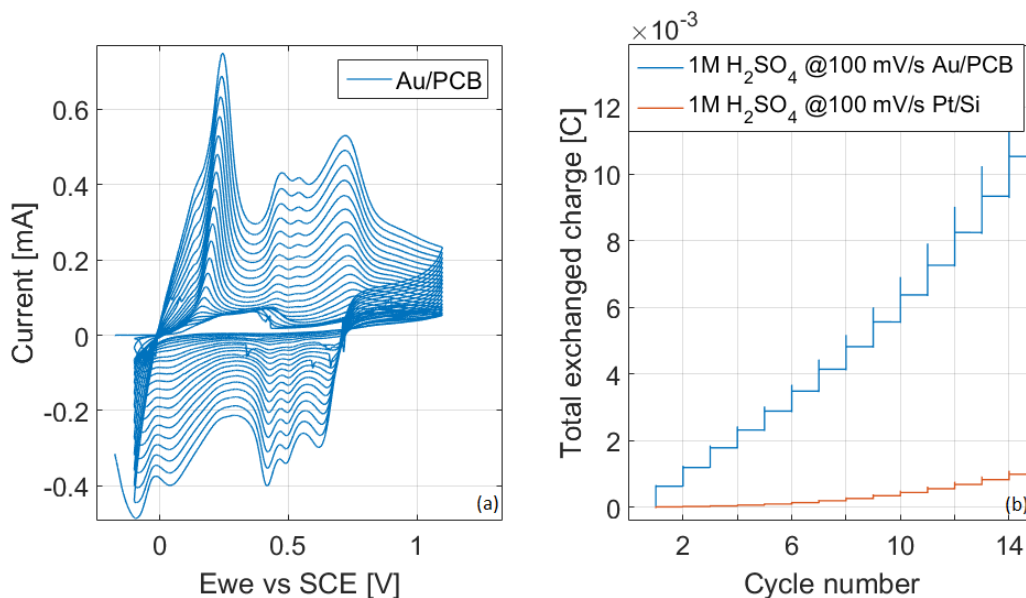


Figure 3.9. (a) Potentiodynamic deposition of PANI on Au/ENIG and (b) comparison with deposition on Pt.

Indeed, while the first polymerization cycles traces differ considerably depending on the substrate, the ones produced in the last cycles are characterized by the same peaks with some small shifts in their positions. The peculiarity of the deposition on Gold is due to the presence of four anodic and cathodic peaks, one more than the ones observed with Platinum [21]. Nevertheless, the exchanged charge at each cycle and the corresponding growth rate is much higher in the case of the Au electrodes (Figure 3.9(b)).

3.2.3 Potentiostatic electropolymerization characteristics

The potentiostatic technique is essentially characterized by pronounced changes in the measured current and in the polymerization rate. The resulting polymer is usually in its doped form and such method allows a flexibility in the obtained structure, leading to multiple possible configurations such as films, nanowires and others. In this work, chronoamperometry method has been proposed for the synthesis of doped PANI membranes. The electropolymerization solution consists of aniline and sulfuric acid, the same reagents used with the previous technique. A constant voltage is applied between the working electrode and the reference one for a well-defined time span. The counter electrode closes the electrical circuit to measure the current flowing through the electrochemical cell, which describes the growth of the polymer on the working electrode's surface. Similarly to the potentiodynamic method, it has been demonstrated that, increasing either the electrolyte's concentration or the monomer one, the electropolymerization is enhanced, leading to the formation of

well-defined films (Figure 3.10).

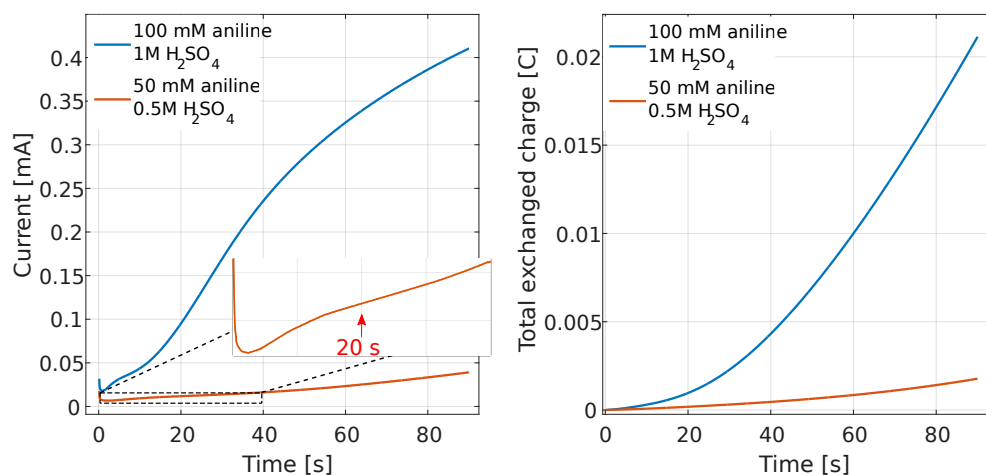


Figure 3.10. Potentiostatic deposition of PANI on Pt varying reagents' concentrations.

The overall measured current results to be about ten times higher when both the concentrations are doubled. The exchanged charge during a chronoamperometric experiment has a monotonic trend, indicating a constant increase of the polymer film. Thus, one could control the amount of synthesized polymer by defining the reagents' concentrations and by finely modulating the electropolymerization time.

The evolution of the current trend during a potentiostatic deposition of Polyaniline gives important information regarding its growth process. The formation of the first radical cations in proximity of the electrode's surface is characterized by the absence of an increasing current value. After few seconds, the synthesized curve tends to rise relatively smooth because there are just a few doped micro-aniline particles formed on the electrode [22]. As soon as the surface has been covered, the polymer starts to grow above the created layers, the slope of the curve changes and the overall increasing current trend appears different after the inflection point. The time required to reach that point depends on the polymerization parameters. In Figure 3.10, the blue curve behaviour is modified after less than 10 seconds, while it takes roughly 20 seconds for the orange one to achieve the inflection point.

Electropolymerization of PANI with chronoamperometry has been also performed on Au/ENIG electrodes as in the case of the potentiodynamic technique. Similarly to the Platinum deposition, it has been noticed a strong influence of the reagents' concentrations on the amount of exchanged charge and film deposited onto the electrode. In particular the monomer concentration demonstrates to strongly affect the polymerization process. The recorded current trend with 100 mM of aniline is very similar to the one obtained in Figure 3.10 for the Pt electrode, demonstrating that the

growth process is the same for both the substrates. Nevertheless, the electropolymerization performed with 50mM precursor's concentration shows some clear differences that are evidenced in Figure 3.11 :

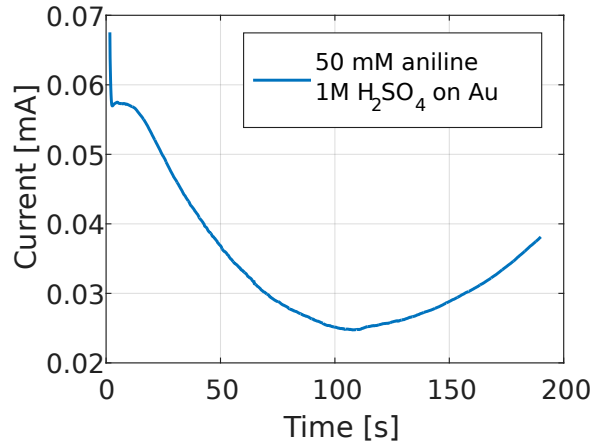


Figure 3.11. Current measured during the potentiostatic deposition of PANI on Au/ENIG.

In this case it is possible to observe that after the initial current maximum, the curve levels off before increasing again at longer times. For this reason, it is possible to separate visually two different stages of growth. The appearance of an initial current maximum, in the course of a phase formation process, is usually associated to the processes of nucleation and growth of the new phase, up to the formation of a full coverage layer [23]. Even though it is not possible to clearly distinguish the two trends due to the overlap in proximity of the minimum value, a normalization can be applied to obtain useful information from the first peak. In fact, by subtracting the exponential current increase achieved at longer times from the original data, it is possible to extract the curve associated to the first growing process (Figure 3.12).

In the previous chapter, instantaneous and progressive nucleation processes have been introduced to explain how the first stages of deposition evolves on bare electrode surfaces. The theoretical current-time relationship, that depends strongly on the kinetics of the reactions, can be used to define which one of those is predominant, based on the different mathematical models:

$$\frac{I}{I_m} = \left(\frac{t}{t_m}\right)^2 \exp\left(-\frac{2}{3} \frac{(t^3 - t_m^3)}{t_m^3}\right) \quad \text{progressive growth} \quad (3.2)$$

$$\frac{I}{I_m} = \frac{t}{t_m} \exp\left(-\frac{1}{2} \frac{(t^2 - t_m^2)}{t_m^2}\right) \quad \text{instantaneous growth} \quad (3.3)$$

The parameters t_m , and I_m in equations 3.2 and 3.3 are the coordinates of the maximum of Figure 3.12. Superimposing the two theoretical expressions with the

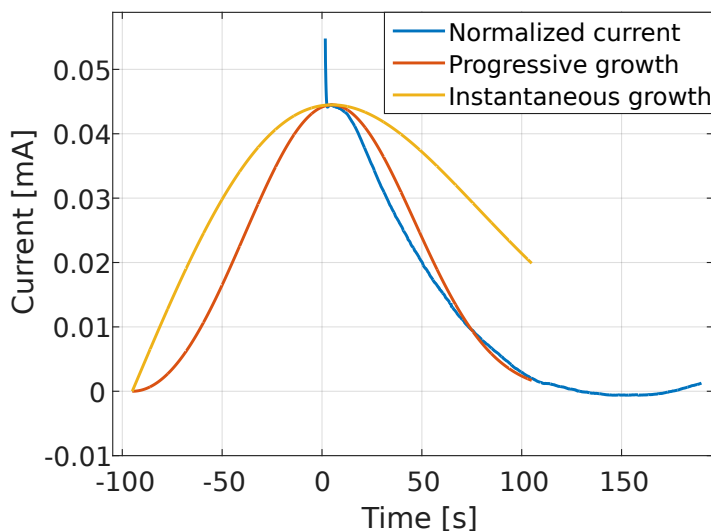


Figure 3.12. Extraction of first growing phase during a potentiostatic deposition on AU/ENIG.

original normalized data (Figure 3.12), it is possible to state that the formation of Polyaniline islands proceeds in a progressive way rather than in an instantaneous one. It should be noticed that with such precursor concentration, the exponential current increase is not completely enhanced after only 180 seconds, meaning that electropolymerization needs higher times for a regular film deposition under those conditions.

3.2.4 Doping of PANI films

It has been shown that doping of conductive polymers represents the fundamental process that allow their effective functioning and use in chemical sensors. Cyclic voltammetry operated in monomer free solutions is often employed to investigate the electrochemical behaviour of polymer films, thanks to the evaluation of the height of the current peaks and the total exchanged charge. Both potentiostatic and potentiodynamic prepared Polyaniline films were used to perform multiple CVs in a $1M H_2SO_4$ monomer-free solution. Figure 3.13 shows the cyclic voltammograms at different scan rates recorded for a PANI film deposited with CV technique.

It is possible to notice that the shapes of the curves recall the ones collected during the electropolymerization, characterized by multiple anodic and cathodic peaks. In fact, it is known that the PANI films are subjected to doping during their formation on the electrode surface, so that some of the peaks in Figure 3.13 are located close to the electropolymerization ones. The peaks' intensities increase with faster scan rates, but all the curves intersect when the current is equal to 0 in the reverse scan. The extraction of each current peak has been carried out with automatic tools

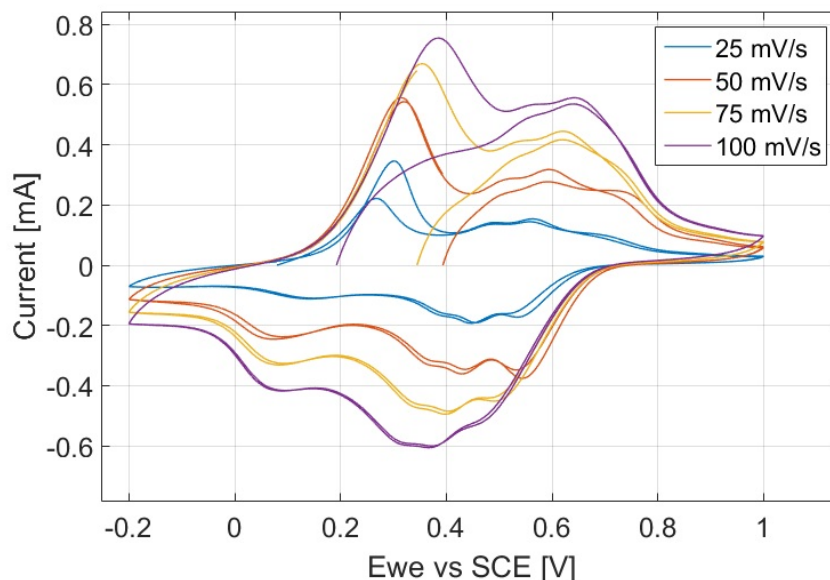


Figure 3.13. CVs recorded at different scan rates in 1M H_2SO_4 solution for a potentiodynamic deposited PANI.

in order to normalize its value with respect to its own baseline. In this way it is possible to make a comparison between all the peaks measured for different scan rates. Generally, the current values are reported with respect to the variation of the square root of the scan rate, to evaluate the behaviour of the reaction and to find out whether it could obey to equation 2.2 rather than to equation 2.3. It is shown (Figure 3.14) that a quadratic interpolation fits accurately the extracted peaks values, meaning that the measured current scales **linearly** with the scan rate.

This fact was expected due to the surface redox character during the doping and undoping of protons and SO_4^{2-} anions in the PANI film [13] [17]. It is interesting to notice that modulating the scan rate allows to control the amount of positive/negative charge that is exchanged and, consequently, to tune the doping mechanism. At very slow sweeps (25 mV/s) the unbalance between positive and negative charge is much higher with respect to faster scans (50 mV/s). However, by further increasing such parameter (75 mV/s and 100 mV/s), the unbalance starts to rise slightly again. Thus, the trend of the total exchanged charge with respect to the scan rate is not monotonic and may be affected by different phenomena, depending on the kinetics of the reactions that take place during the doping and undoping processes. The same considerations can be applied for Polyaniline coatings deposited with different methods. However, since PANI deposited with chronoamperometric techniques generally leads to the formation of fully oxidized forms of the polymer, the CVs recorded in the monomer free acid solution change irreversibly the oxidation state of the polymer, that can be noticed by looking at the way in which the colour of the film evolves (3.15).

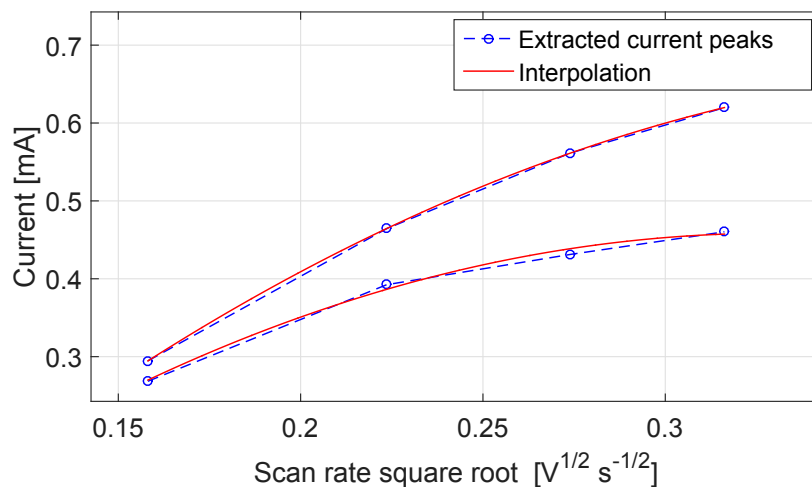


Figure 3.14. Quadratic interpolation of the current peaks trend obtained by varying the square root of the CVs scan rate.

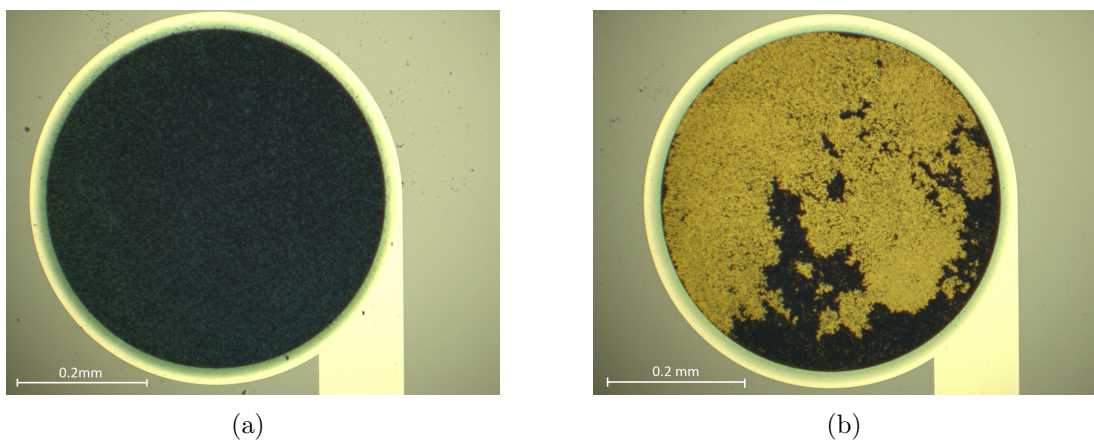


Figure 3.15. Potentiodynamic (a) and potentiostatic (b) PANI after doping/undoping with H_2SO_4 .

3.3 PAPBA: a new multifunctional polymer

Many recent works demonstrated that coupling boronic acid groups to the backbone of Polyaniline represents an outstanding breakthrough in the field of potentiometric sensors. Improvements were observed in multiple applications aimed at sensing a wide range of elements such as small and large ions, saccharides, reactive oxygen species and many others more [24]. The resulting polymer is called poly-3-aminophenylboronic acid (PAPBA) and its backbone contains the structure of Figure 3.16.

Due to its similarity to the Polyaniline polymeric chain, the two polymers share

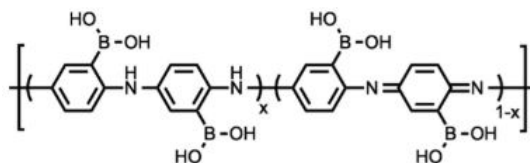


Figure 3.16. Poly-3-aminophenylboronic acid (PAPBA) chain.

the main electrical and optical properties. However, the integration of the boronic group affects remarkably the potentiometric readout of sensors containing PAPBA films. Boronic acid groups are capable of binding a great variety of compounds with high affinity through reversible esterification. Thus, they are suitable for the creation of sensors based on their complexation with other compounds and especially in the field of Molecular Imprinted Polymers (MIP), due to their versatility and capabilities to interact with different templates. While the first studies on PAPBA coatings were made thanks to its deposition as a copolymer with aniline, recent advances in the electropolymerization techniques allow the formation of standing-alone polymeric films. Sensitivity and stability of the polymer are currently being investigated and the main topic is related to the presence of the negatively charged boronic acid moiety, which could enhance the Nernstian slopes only for lower pH range [25]. Nevertheless, PAPBA-based sensors are characterized by fast response time for the detection and analysis of a wide range of components, making useful their study and integration on the *Electronic tongue* presented in this work.

3.3.1 Impact of deposition parameters

The electropolymerization of PAPBA differs from the one of Polyaniline due to the presence of additional elements, which are believed to improve the deposition process and the properties of the resulting films. Indeed, it has been demonstrated that the disruption of the *B-N* bond in the APBA monomer could be achieved when the polymerization solution contains F^- or Cl^- ions. The complexation reaction of those ions with the boronic acid groups has a double effect:

1. the formation of *fluorinated* or *chlorinated boronate anions*, which increases dramatically the solubility of the phenylboronic acid. Thus, the electropolymerization becomes a more favourable process;
2. the switch from *sp²* to *sp³* of the boron hybridization, enhancing the formation of tetrahedral structures, that allow additional bonds with external elements, thus increasing the potentiometric response.

Moreover, it has been demonstrated that the higher the concentration of such ions, the better the sensitivity of the synthesized films. The main reason is clearly

the creation of self-doped structures, given by the formation of those negative ions which are incorporated in the polymeric chain. Further, since the complexation shifts negatively the oxidation potential during the electropolymerization, the number of ions present in the solution has a significant impact on the polymerization rate and, in turn, the morphology and behaviour of the polymer [26]. Electropolymerization of PAPBA has been performed on Pt rod with potentiodynamic technique. Similarly to Polyaniline, the deposition requires the monomer (*APBA*) and a supporting electrolyte (*HCl*, *H₂SO₄*, ...). Figure 3.17 shows the *1st* and the *30th* cycle of the voltammograms recorded during a deposition without *NaCl* (absence of *Cl⁻* ions incorporation). Even though the traces evidence the monomer oxidation and radicals formation, the current values diminish with time, confirming the fundamental role of the small anions for the electrodeposition.

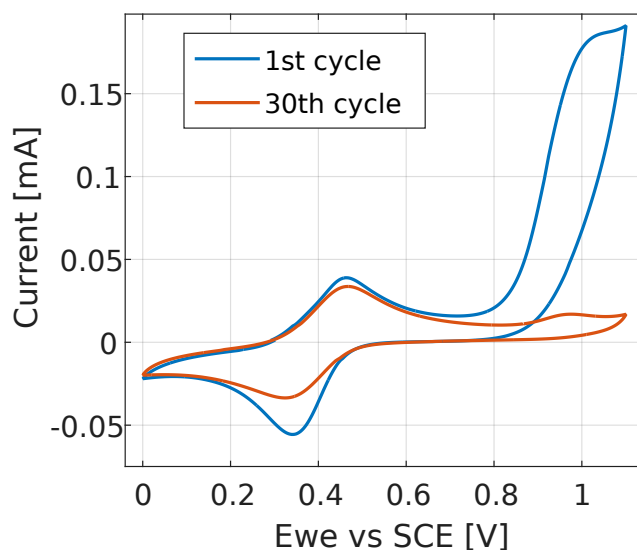


Figure 3.17. Evolution of a PAPBA deposition without *Cl⁻* incorporation

It has been found that the addition of polyanionic materials could enhance the stability and pH range of the polymeric films. A good candidate for this purpose is represented by the **Nafion** complex, and previous works demonstrated that electrochemical polymerization can be achieved both in a Nafion suspension and at a Nafion-coated electrode [27]. In the present study, the polyanionic complex was added to the electropolymerization solution containing APBA monomer, the supporting electrolyte and *NaCl*, necessary for a proper polymer growth. It is worth mentioning that the monomer precursor, available in solid phase, has been dissolved in the electrolyte prior to the insertion of Nafion, which otherwise can decrease its solubility. The electropolymerization CVs, displayed in Figure 3.18, show the impact of the presence of that complex in solution.

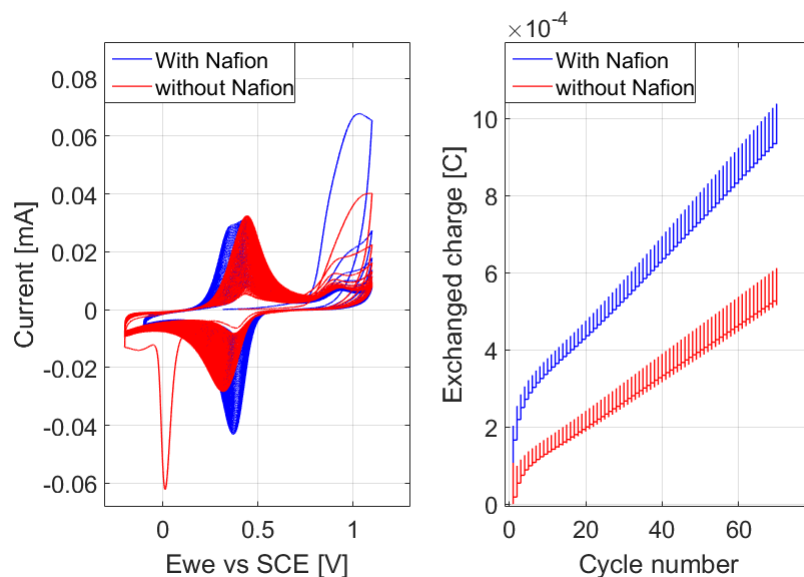


Figure 3.18. Current and total charge measured during PAPBA electropolymerization (50 mM APBA and 200 mM NaCl) with and without Nafion.

It can be noticed that the polymer growth rate is enhanced and a higher reduction peak can be observed in the reverse scan. Regarding the anodic traces, the Nafion-based polymerization introduces an additional oxidation peak with respect to the one shared with the Nafion-free recipe. It is known that the film produced with the former should have better stability due to the electrostatic interaction between PAPBA and Nafion. Moreover, degradation and delamination due to less adhesion should be associated with the absence of the polyanionic complex.

However, it has been demonstrated that the role of such component can be mitigated by increasing extensively the concentration of sodium chloride in the polymerization solution and thus, of Cl^- ions. In fact, according to *Shoji et al.* [26], the effect of Nafion is remarkable when the ratio of the concentrations of APBA monomer and NaCl is only around **1:1**. Hence, an excess of Cl^- ions may influence the electropolymerization and polymer stability, in the same way as a polyanionic component. The potentiometric response in $MgSO_4$ of PAPBA produced with and without Nafion is depicted in Figure 3.19. The ratio of the concentrations of APBA and NaCl is **1:4** in both cases.

It can be noticed that the behaviour of the films, in terms of sensitivity slope, is almost preserved after one week from the polymerization for both coatings, while the shift of the absolute values has been associated to the polymers conditioning. Thus, when the salt concentration is four times higher than the monomer one, it could be obtained a stable polymer regardless of the Nafion incorporation.

It is also worth noticing that removing Nafion allows to get rid of spikes in the open circuit voltage measurements like the one shown in Figure 3.20. Such signal features have already been noticed [26] and associated to the Nafion permselectivity, whose

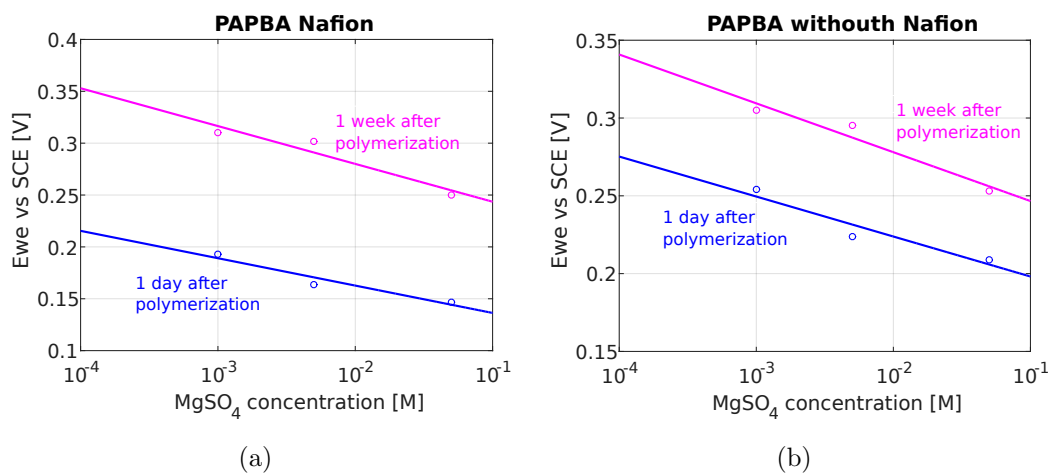


Figure 3.19. Potentiometric response of PAPBA films deposited with (a) and without (b) Nafion for different concentrations of $MgSO_4$.

negatively charged sulfonated groups, attached to the polymer backbone, may repel instantaneously solution phase anions.

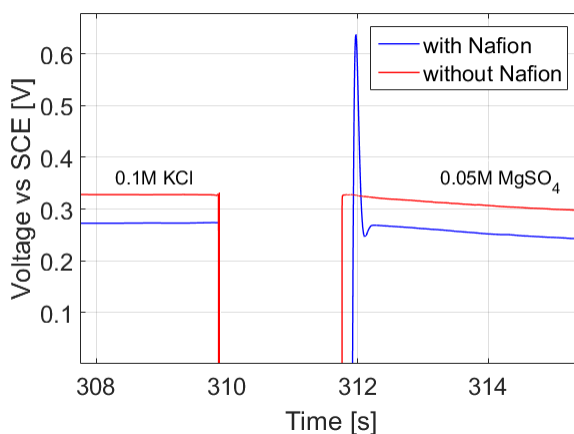


Figure 3.20. Spike in the OCV measurements for Nafion-incorporated PAPBA.

Regarding the other electropolymerization parameters, the potential scan window of the potentiodynamic deposition has been fixed between **-0.2V and 1.1V** in all the experiments. Such range allows to get the oxidation of the monomer, which results to require a slightly higher voltage with respect to aniline. The cyclic voltammograms showed in the previous figures clearly demonstrate that the PABPA growth rate is much lower than PANI, since the current traces recorded at each cycle are much closer. For this reason, all the experiments presented in this section have been performed with **at least 40 cycles**. Moreover, contrary to Polyaniline, the maximum growth rate has been achieved with the sweep rate fixed at **100 mV/s**, that has been chosen as optimum value in all the electrodepositions. Regarding the supporting

electrolyte, PAPBA has been electropolymerized by using HCl and H_2SO_4 . In Figure 3.21, CVs for the deposition with $0.2M$ concentration of both acids are reported.

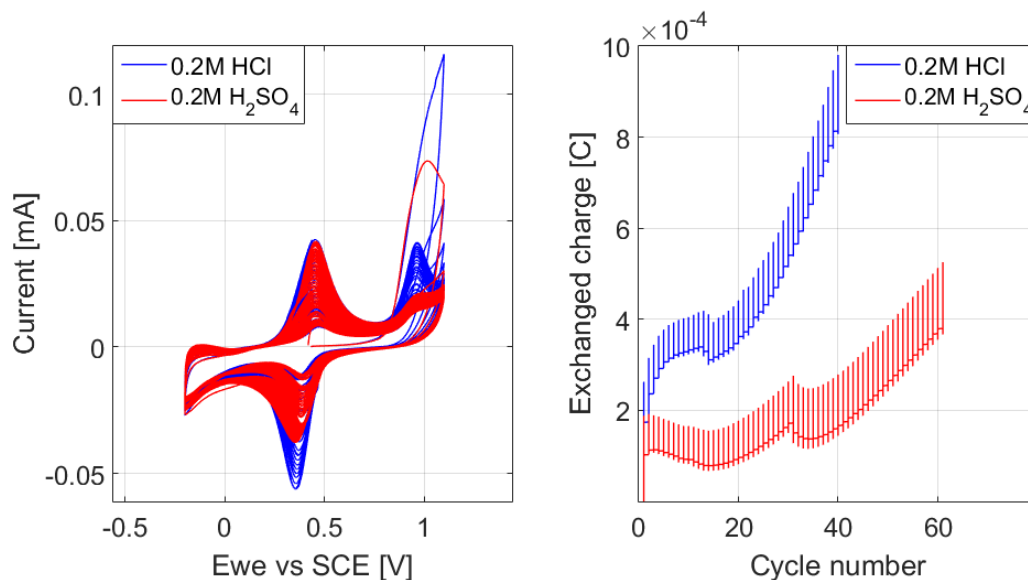


Figure 3.21. Current and total charge measured during PAPBA electropolymerization (50 mM APBA and 200 mM NaCl) with different supporting electrolytes.

By looking at the amount of exchanged charge, one can deduce that the polymerization rate achieved with the HCl recipe is higher than the H_2SO_4 one. As shown in the figure, the same value of the current oxidation peak reached after 60 cycles with sulfuric acid can be obtained after only 40 cycles with the hydrochloric one. The main differences between the two traces is given by the fact that the amount of oxidized monomer is higher with HCl in each cycle. This result confirms the capability of small ions, such as Cl^- ones, of breaking the B-N bonds to favour the polymerization and improve the overall process, as discussed in the previous section. Nevertheless, the different nature of the supporting electrolyte does not seem to affect the position and the shape of the cathodic and anodic peaks, so that it is expected to obtain similar properties of the two films. For instance, the following figure 3.22 reports the open circuit voltage measurements of the two films varying the concentration of KCl. The two linear fits that indicates a cationic sensitivity in that salt are characterized by almost identical sensitivity slopes.

Similarly to PANI, PAPBA electropolymerization on the Au/ENIG substrates results to be much more challenging than the Pt deposition. Further studies are needed to find out the optimum values of the deposition parameters to allow a more versatile integration of the polymer on different substrates.

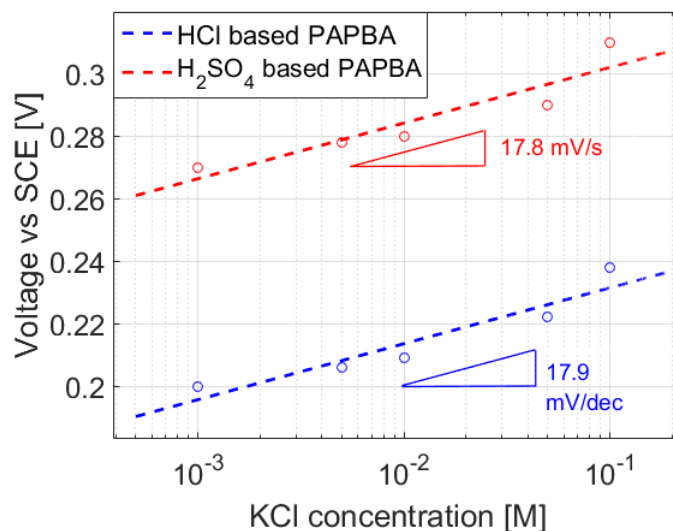


Figure 3.22. Potentiometric response of *HCl*- and *H₂SO₄*-based PAPBA films for different concentrations of *KCl*.

3.4 Study of polypyrrole growth and stability

The possibility to integrate Polypyrrole films in the *Electronic tongue* described in the next sections had already been studied. The present work is intended to reproduce some of the obtained results and to analyse the potentialities and the limits of those membranes for the fabrication of the cross-sensitive polymer arrays.

Polypyrrole (PPy) is one of the most studied conductive polymers. It has been employed in a wide range of applications due to its easy deposition from aqueous and non-aqueous media, high adhesion to many types of substrates, enhanced conductivity and stability [28]. Its properties can be properly modulated by varying accurately the synthesis parameters. For these reasons, it has been integrated in cross-sensitive electrochemical sensors, gas sensors, fuel cells, corrosion protection coatings, rechargeable batteries, supercapacitors and many other devices. As far as the synthesis is concerned, different electrochemical techniques such as cyclic voltammetry, galvanostatic, potentiostatic, reversal potential pulsing techniques etc. have been successfully used for the deposition on noble metals, inert materials and on other metal supports by tuning the electropolymerization conditions. Similarly to the other conductive polymers, the film preparation sequence includes the monomer oxidation and the consequent coupling of the formed radical cations, deprotonation and cascaded reactions following the same steps. Functionalization techniques follow polymer preparation in applications such as electrochemical sensors. Those processes could be carried out in two different ways: either by involving the polymerization of a functionalized monomeric molecule or by taking advantage of the anion exchange properties of the oxidized form of the polymer [29]. The former requires the introduction of a substituent on the nitrogen atom or on the 3-4 positions of the monomer.

A supporting electrolyte containing anionic species is needed instead in the latter. While the nature of the substituent can be quite variable and specifically chosen accordingly to the target application, the anions incorporated in the polymeric chain derive either from salts constituted of small ions, or from metal complexes that can modulate the electrochemical properties of the conductive polymer. Although large anions are believed to be strongly retained inside the polymer frame, such electrode materials are less stable than those in which the substituents are covalently attached to the polymeric chain.

3.4.1 Integration of anionic species in the polymer matrix

PPy have been successfully deposited on Platinum electrodes with different sizes using water-based electropolymerization solution. The supporting electrolyte contained also additional elements in order to modulate the properties of the conductive films. In particular, calcium chloride ($CaCl_2$) and potassium hexacyanoferrate ($K_4Fe(CN)_6$) have been dissolved in millipore water prior to adding the monomer in solution. Figure 3.23 compares the two chronoamperometric electropolymerizations performed with the same monomer concentration ($0.1M$) and for one minute on a Platinum rod.

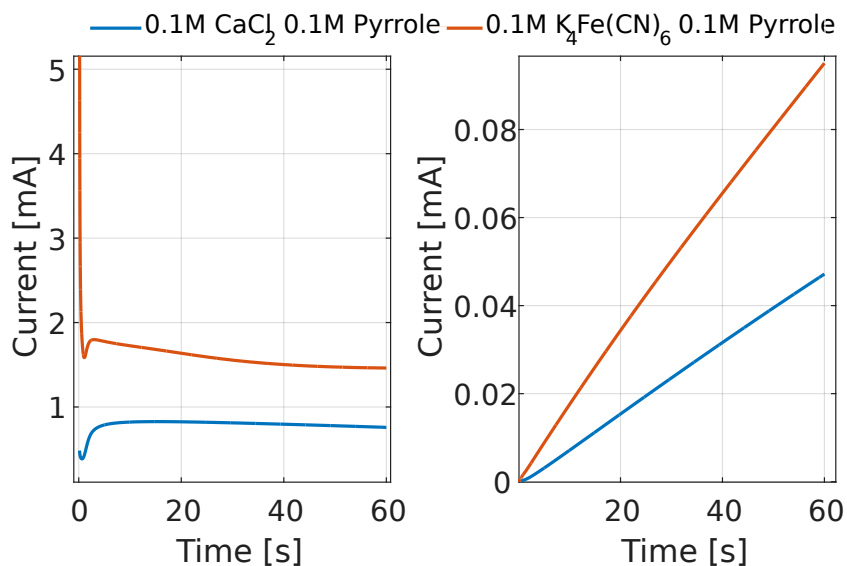


Figure 3.23. Potentiostatic deposition of Polypyrrole with $CaCl_2$ and $K_4Fe(CN)_6$.

It can be noticed that the current measured for the hexacyanoferrate membrane is higher than the case of the $CaCl_2$. Thus, it is also expected to get a thicker film by looking at the consumed charge. Except for the initial peak of the former, the shapes of the current trends is quite similar, meaning that the growth process is expected

to be quite similar, and the morphology being different only due to the presence of different ions. A potentiostatic deposition produces a fully oxidized form of the polymeric film. Indeed, by fixing a positive constant voltage, the continuous extraction of the electrons from the chains leaves an excess of positive charges that must be balanced by the ions which are in solution. For this reason, it is believed that Cl^- and $Fe(CN)_6^{4-}$ anions interact with the polymeric backbone during the electropolymerization. The result of this doping process is quite dependent on the anion nature. In fact, Cl^- ions are small particles which can diffuse quite easily inside and outside of the polymer matrix so that whenever the Cl^- -doped PPy gets in contact with a test liquid, they can migrate in order to establish a potential equilibrium. However, such electrochemical behaviour seems to challenge the reproducibility of potentiometric devices. In fact, if a chemical interaction perturbs heavily the small ions concentration, there may be a strong change in the response of the sensor for the same test liquids. For instance, it has been noticed that a PPy membrane prepared with $CaCl_2$ as the one of figure 3.23 can switch over time its anionic sensitivity to a cationic one. On the other side, hexacyanoferrate anions are characterized by larger dimensions, so that they are most likely to be trapped in the polymeric matrix during the electropolymerization. For this reason, the corresponding sensitivity is expected to be preserved and, for this reason, such polymer has been chosen to be integrated in the array presented in the next chapters.

The electrochemical reaction activity of a conductive polymer can be influenced by the preparation method. Indeed, the CV deposition of PPy involves the redox couple PPy/PPy^+ , where PPy^+ is the radical cation species or polaron. During the electrodeposition, when the polymer is in its oxidized state, some anions get migrated from the solution into the polymer matrix to maintain its electroneutrality. On the other side, the chain reduction involves injection of electrons with a consequent quenching of positive charges on the polymeric chain. As a consequence, some doping ions can be released and enter in the solution and the synthesized film remains in its partly doped or undoped state. A CV deposition of PPy with $K_4Fe(CN)_6$ is shown in Figure 3.24.

The potentiodynamic electropolymerization has been performed with a cycles number much lower with respect to PANI and PAPBA. In fact, the amount of exchanged charge and the recorded current values are consistently enhanced, meaning that PPy deposition has produced thicker films. The CV peaks are characteristics of the pyrrole oxidation and following electropolymerization. The amount of charge exchanged at each cycle is almost the same, meaning that the polymer is characterized by a pretty regular growth. In the next chapters, it will be shown that the differences in the doping degree with respect to the potentiostatic deposition would be reflected in a change of the corresponding polymer properties.

Electropolymerization on Au has been possible using exactly the same recipes for both potentiostatic and potentiodynamic depositions. Figure 3.25 shows that PPy deposition is more favourable on Pt substrates where the exchanged charge is higher

regardless of the techniques. Thus, it is expected to get thinner films on Gold. Finally, it is possible to notice that the CV deposited polymer is thicker than the CA one, regardless of the substrate.

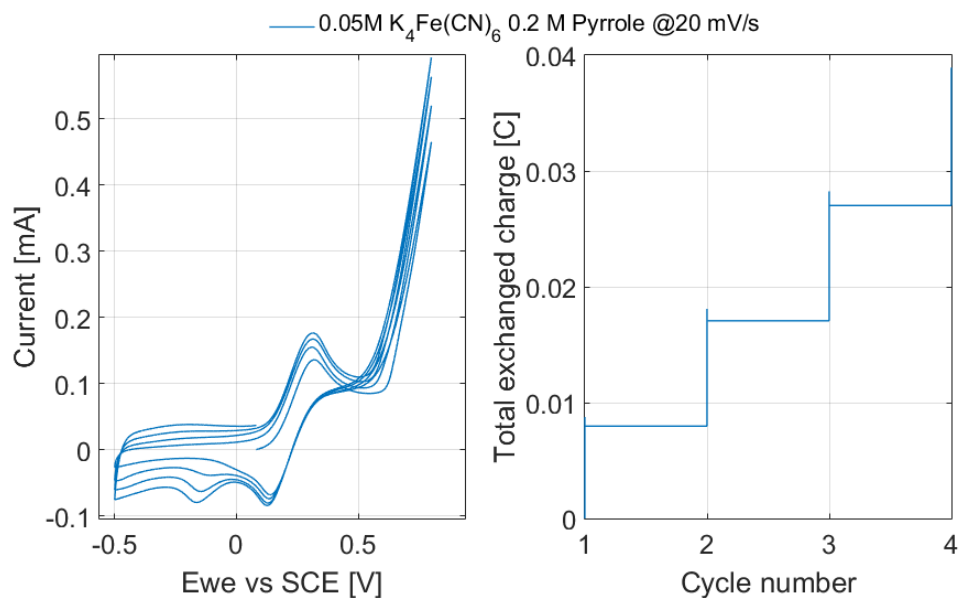


Figure 3.24. CVs plot and total exchanged charge of a potentiodynamic deposition of Polypyrrole with $K_4Fe(CN)_6$ on Pt.

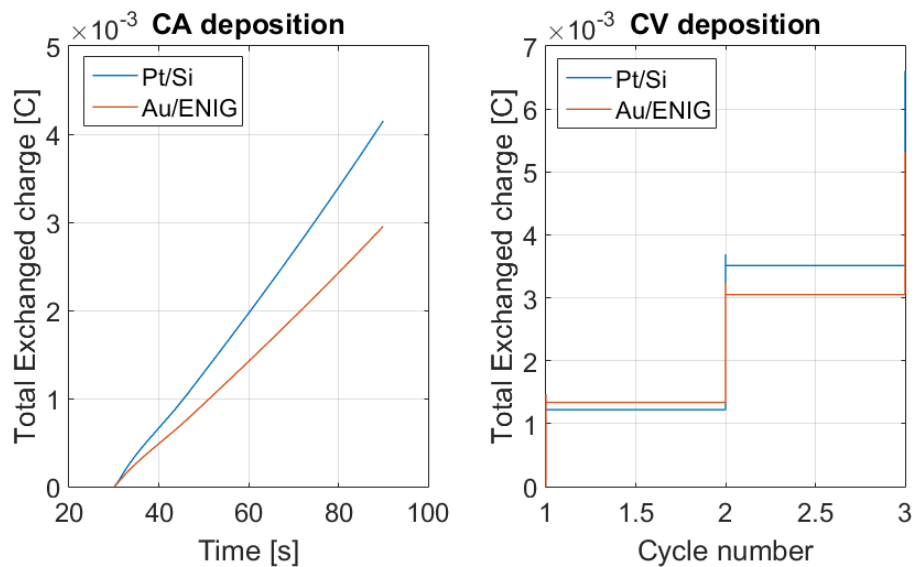


Figure 3.25. Comparison of the potentiostatic and potentiodynamic deposition of PPy on Pt and Au/ENIG.

3.5 Characterization of electrodeposited polymers

3.5.1 Profilometric analysis

Veeco Dektak 6M Profilometer has been used to analyse some basic properties of the produced films, such as their thickness and roughness. In the previous sections of this chapter it is shown that by varying the electropolymerization parameters (precursors' concentration, voltage sweeps, scan rate, etc.) it is possible to exchange a different amount of charge, so as to obtain polymeric films with variable thickness. The surface profiles for seven electrodeposited PANI electrodes is reported in Figure 3.26. The eighth blank electrode has been used as reference for the evaluation of the height for each of the seven profiles. In particular, the thickness for each polymer has been computed taking the mean value of the profiles and normalizing it to the height of the blank electrode.

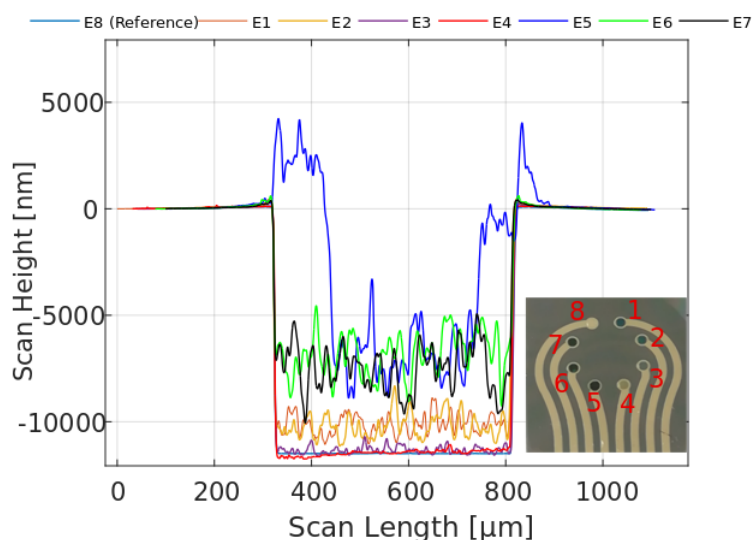


Figure 3.26. Surface profile recorded for different PANI films deposited with CV technique.

A link between the amount of polymer deposited on each electrode and the quantity of charge exchanged during the electropolymerization is possible by applying Faraday's law of electrolysis, assuming a current efficiency of 100 %:

$$t = \frac{(M_m + 0.5M_a)Q}{\rho F A z} \quad (3.4)$$

Thus, it is expected a linear dependence of the polymer thickness t on the total charge Q involved during the synthesis. In equation 3.4, M_m and M_a are the monomer and acid molar mass respectively, ρ is the polymer density ($1.36 \text{ g} \cdot \text{cm}^{-3}$), F is the Faraday constant ($96500 \text{ C} \cdot \text{mol}^{-1}$), A is the surface area of the electrodes

(in this case $2 \cdot 10^{-3} \text{ cm}^2$) and z is the number of negative charges involved in the polymerization process. Chemical reaction expressed by equation 3.1 shows that two electrons need to be released to allow electro-oxidation. However, since doping of the polymeric film happens concurrently to the deposition, it is expected that z is higher than two and its value is mostly determined experimentally [30]. The following figure 3.27 shows the linear interpolation for the correlation between the two parameters. From figure 3.26 it can be seen that deposition on electrode 5 has experienced an irregular growth. For this reason, it has not been included in figure 3.27.

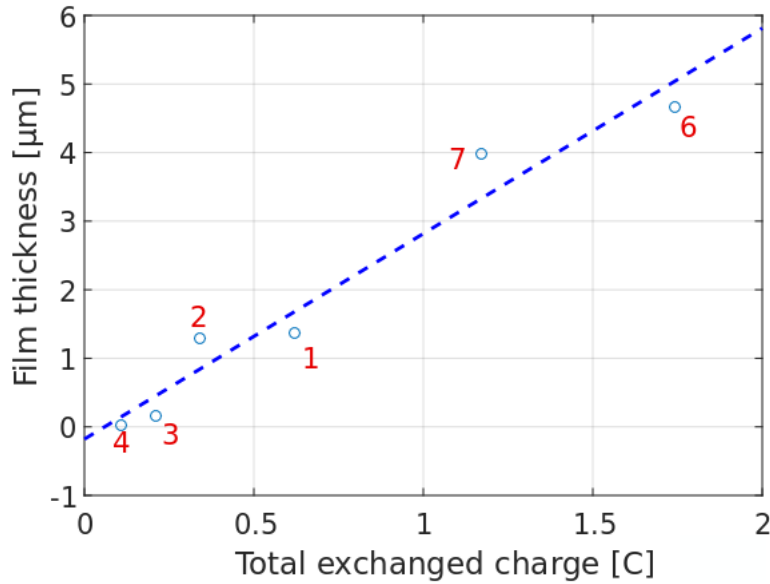


Figure 3.27. Linear dependance extraction of the relation between exchanged charge and polymer thickness.

The z parameter extracted from the linear interpolation is equal to **2.38** which is in accordance with the ranges reported by other authors [31] [32].

The surface profile could also be used to extract the roughness parameters, which are strictly linked to the morphology of the films. The following set of equations allows to calculate the most common parameters, which are: the arithmetic mean deviation (R_a), the root mean square deviation (R_q), Skewness (R_{sk}) and Kurtosis (R_{ku}):

$$R_a = \frac{1}{N} \sum_1^N |z_i - z_m|$$

$$R_q = \sqrt{\frac{1}{N} \sum_1^N (z_i - z_m)^2}$$

$$R_{sk} = \frac{(\frac{1}{N} \sum_1^N (z_i - z_m)^3)}{R_q^3}$$

$$R_{ku} = \frac{(\frac{1}{N} \sum_1^N (z_i - z_m)^4)}{R_q^4}$$

where N is the number of scans performed for each profile, z_i represents each measurement and z_m is the average of the scan profile. The previous four parameters contain information regarding the *height distributions* for all the surface profiles and can be exploited to make a comparison with a *normal distribution*. While R_a gives an estimation of the roughness of the surface to be compared with the thickness of each polymer, R_q is more sensitive to the presence of high peaks, representing the standard deviation of the height distribution. The Skewness parameter (Figure 3.28 [33]) is related to the asymmetry of the distribution of heights :

- For a normal distribution $R_{sk} = 0$
- $R_{sk} < 0$: the mean value is negatively shifted respect to the peak of the corresponding normal distribution
- $R_{sk} > 0$: the mean value is positively shifted respect to the peak of the corresponding normal distribution

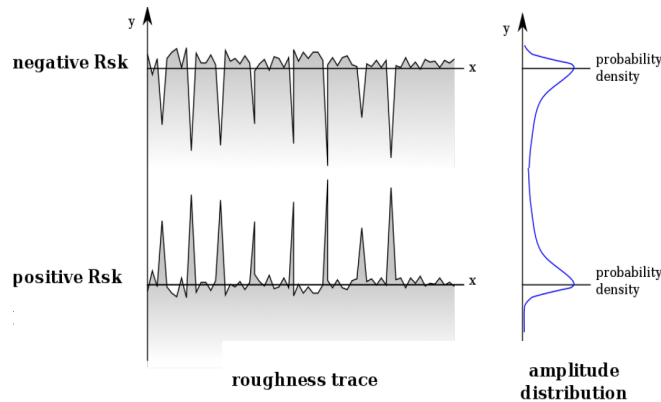


Figure 3.28. Skewness dependence on surface profile.

The Kurtosis parameter (Figure 3.29 [34]) is used to evaluate the tails of the height distribution. Hence, it is not related to the intensity of the central peak but to extreme values of height, far from the mean line, that will give the greatest contribution.

- For a normal distribution of heights $R_{ku} = 3$
- $R_{ku} > 3$: higher contribution of extreme values with respect to a normal distribution
- $R_{ku} < 3$: lower contribution of extreme values with respect to a normal distribution

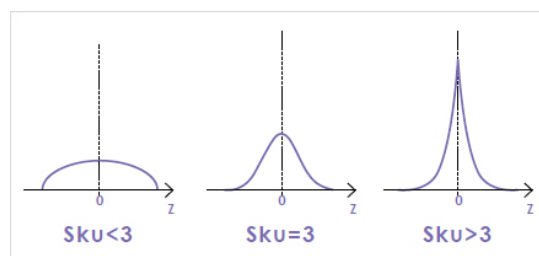


Figure 3.29. Height distributions depending on Kurtosis.

The following Table 3.1 reports the roughness parameters along with the thickness and the electropolymerization charge for the seven *PANI* films deposited on different electrodes. It can be noticed that the polymer deposited on the fourth electrode is the thinnest and R_a and R_q are much higher than its thickness. It means that the normalization with respect to the reference electrode has an uncertainty comparable to the polymer thickness, which in turn would need a further investigation. The other polymers are characterized by comparable roughness except the fifth one, whose irregular growth results in a *Kurtosis* way far from 3. By analysing the *Skewness* parameter, it can be noticed a certain tendency of the polymers produced with lowest electrolyte concentration (E1,E2,E3) to have a positive asymmetrical shift of the mean value with respect to the height distribution, meaning that the profile is mainly characterized by flat surfaces with some positive peaks. On the contrary the *Skewness* of the others (E6,E7) suggests surfaces characterized by negative peaks.

Electrode	Charge [mC]	Thickness [μm]	R_a [nm]	R_q [nm]	R_{sk}	R_{ku}
E1	0,62	1,36	365	450	0.29	2,63
E2	0,34	1,28	451	560	0.78	3,34
E3	0,21	0,16	133	168	1,00	3,82
E4	0,11	0,03	100	128	-0.13	3,02
E5 ¹	3,72	7,71	3696	4051	0.53	1,72
E6	1,74	4,67	806	992	-0.21	2,46
E7	1,17	3,99	953	1272	-1.51	2,95

¹ Polymer thickness has been estimated even though it is characterized by an irregular growth.

Table 3.1. Roughness analysis for seven potentiodynamically (CV) deposited *PANI* films.

A profilometric analysis has been also conducted on the other polymers presented in the previous sections of this chapter. Since the amount of charge exchanged during the electropolymerization can vary significantly depending on the polymer nature, it has been found a noticeable difference in the thickness of the obtained films.

Figure 3.30 shows that the *Polypyrroles* coatings are much thicker than the other two polymers. Moreover, potentiostatic deposition of *Polyaniline* has produced a thicker film with respect to the ones deposited with cyclic voltammetry (Figure 3.26). The measured *PAPBA* profile is almost overlapping the reference one, meaning that the film is so thin that the thickness normalization could produce wrong results.

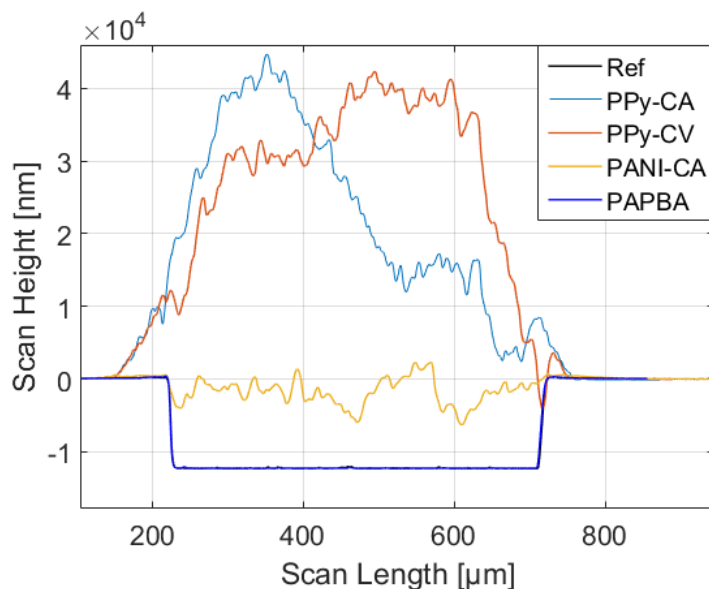


Figure 3.30. Surface profiles of PPy, PANI and PAPBA.

Table 3.2 summarizes the profilometric results of four different films.

Electrode	Charge [mC]	Thickness [μm]	R_a [μm]	R_q [μm]	R_{sk}	R_{ku}
PPy-CA	7,1	32,8	11,3	12,9	0.3	1,79
PPy-CV	6,5	38,7	10,9	12,7	-0.69	2,13
PANI-CA	31,5	10,5	1,43	1,83	-0,22	2,83
PAPBA ¹	0,04	0,03	0,01	0,02	5,48	40,0

¹ Roughness parameters are strongly affected by contaminations on the electrode surface, where it is expected to have a thin polymeric film of few nanometers.

Table 3.2. Roughness analysis of different polymeric films.

In the case of the PPy's electrodes, the lateral walls have been taken into account for the evaluation of the roughness parameters. For this reason, the R_a and R_q are in the same order of the polymer thickness. However, the surface profile shows a preferential 2D-electropolymerization of PPy rather than a 3D one, since the polymer does not grow on the lateral walls. As concerns Polyaniline deposited with chronoamperometry, it is characterized by an extreme profile regularity as shown by

R_a and R_q , which are close to the ideal values of a normal distribution. If one tries to apply equation 3.4 to the PPy films to calculate the theoretical polymers thickness, the results will be $19 \mu m$ for PPY-CA and $18 \mu m$ for PPy-CV respectively. Such mismatch with the actual values is due to the limit of the application of Faraday's law of electrolysis, which gives a correct estimation only in case of very compact films with low porosity. A calibration curve based on multiple electropolymerizations, as in the case of Figure 3.27, represents the most accurate method for the extraction of the thickness parameter.

3.5.2 SEM characterization: film morphology

Figure 3.31 shows the SEM photographs for Polypyrroles films deposited with different techniques.

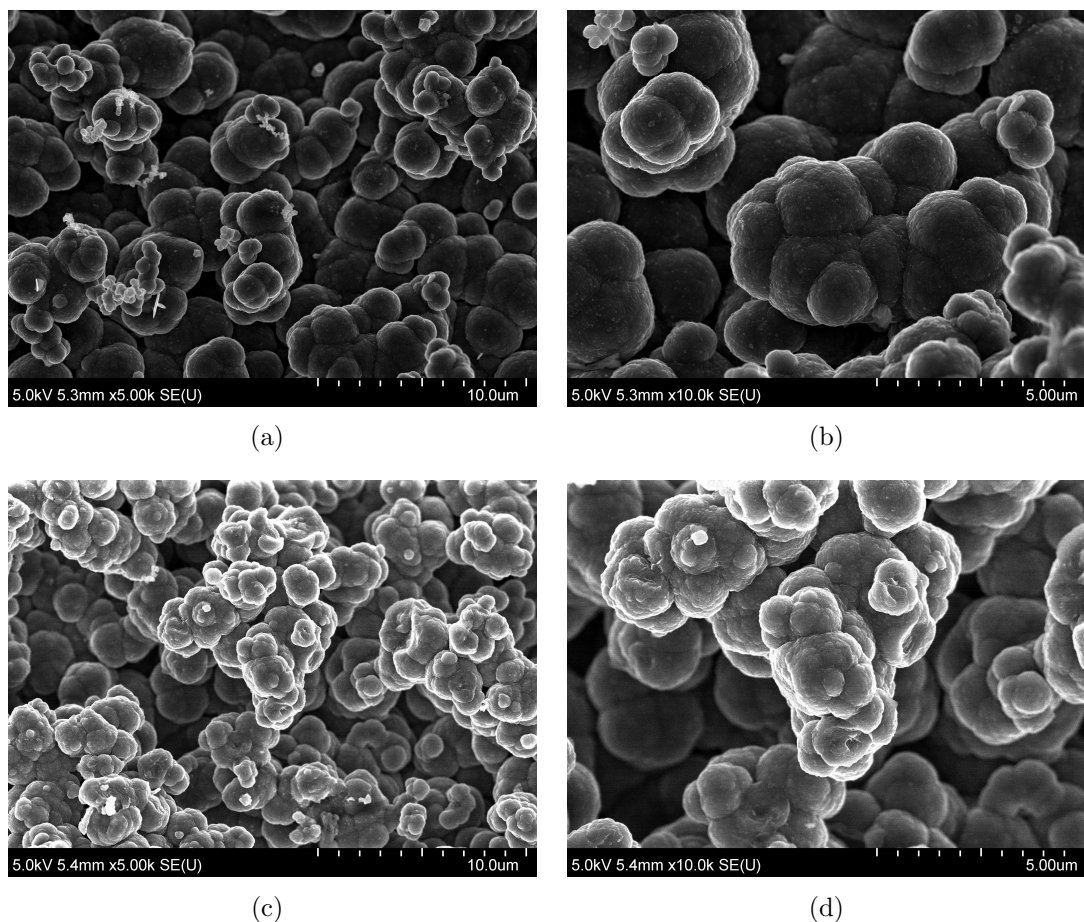


Figure 3.31. SEM characterization of Polypyrrole deposited with CA ((a) and (b)) and CV ((c) and (d)) methods .

Figures 3.31(a) and (b) show a potentiostatic (0.8V for 60 seconds) produced film

on Pt electrode (0.1M *Pyrrole*, 0.1M $K_4Fe(CN)_6$) at different scales, while 3.31(c) and (d) refer to a film deposited with 3 CV cycles (-0.5V to 0-8V sweep range) on another Pt electrode (0.2M *Pyrrole*, 0.05M $K_4Fe(CN)_6$). Both films have been conditioned in a 0.1M *KCl* solution for two weeks before being dried for the characterization. The deposition method does not seem to affect the obtained morphology which is characterized by granular structures, arranged to form a porous membrane. The conditioning effect is not visible in terms of the deterioration of the structural features of the two polymers. It can be noticed the presence of some salts residuals, especially in Figure 3.31(a), which are linked to the final extensions of the polymer. The morphology of Polyaniline deposited with chronoamperometry (0.8V for 90 seconds, 0.5M aniline and 1M H_2SO_4) has been investigated as well (Figures 3.32(a) and (b)). It has been subjected to the same soaking conditions of the two previous films.

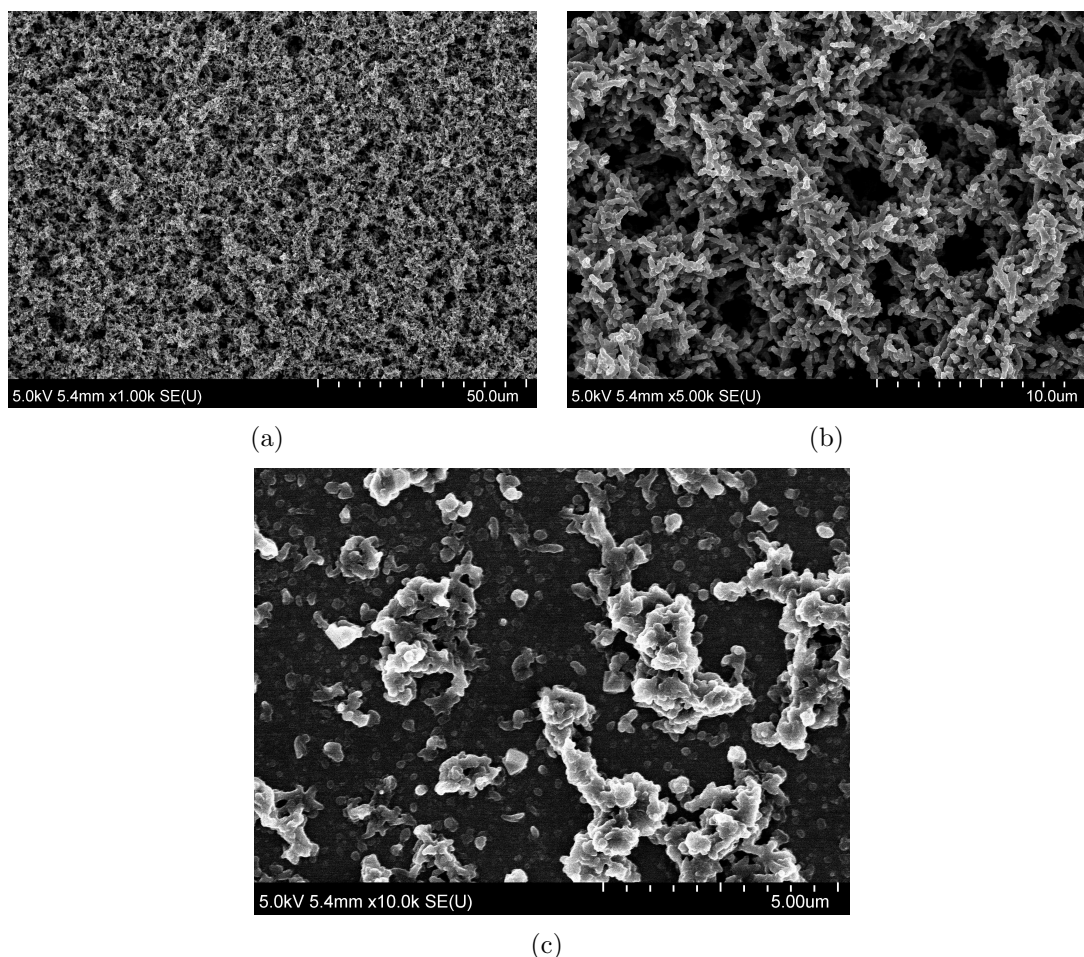


Figure 3.32. SEM characterization of Polyaniline deposited with CA ((a) and (b)) and CV (c) technique.

The pictures show that the structural arrangement of PANI differs substantially with respect to the PPy one. In this case, the result of the electropolymerization is a more compact and dense film, characterized by a completely different morphology. The Pt electrode is well-coated by H_2SO_4 doped PANI bars which are crossed and overlap on each other. The brighter edges visible on the surface of the polymer are usually associated to HSO_4^- doping ions which are incorporated in the matrix. The cross-linked micro-bars have a length of about 0.5-1 μm and the width of 0.1 μm . This three-dimensional network is typical of Polyaniline grown on bare electrodes with H_2SO_4 as supporting electrolyte. In fact, it is known that HCl films are characterized by less dense structures with more spaghetti-like features, resulting in a less conductive polymer. The characterization of PANI prepared with cyclic voltammetry resulted to be more challenging due to the lowest conductivity of the resulting thin film 3.32(c).

3.5.3 Raman spectra of electrodeposited polymers

Raman characterization was mainly employed for the investigation of possible structural changes of the polymeric chains due to differences in the electropolymerization conditions or due to polymers ageing. Figure 3.33 shows that the Raman spectra acquired for Polyaniline deposited with different techniques are almost identical, meaning that their backbones' structures are the same. This fact was expected since the effect of different electropolymerization methods is mainly associated to the doping level, which does not affect strongly the vibrational modes of the chain. Moreover, the effect of the polymer ageing is not evidenced since the position of the peaks are preserved for both high and low frequencies.

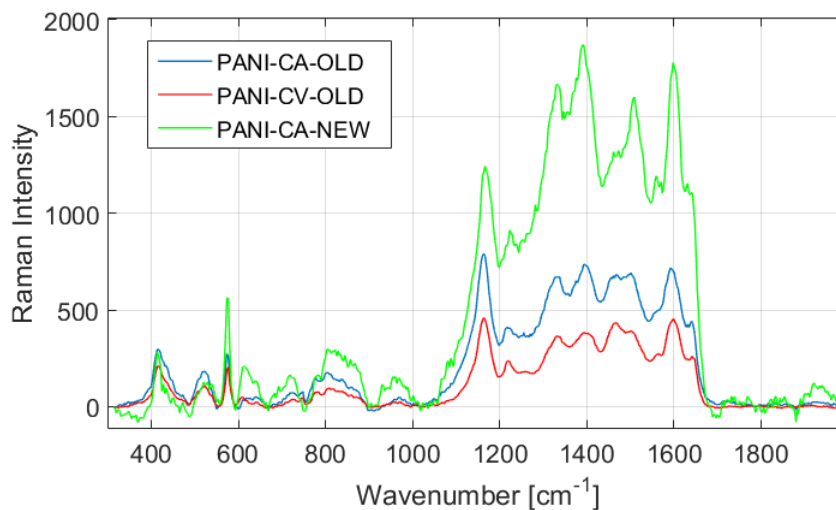


Figure 3.33. Raman spectra of PANI deposited with different techniques and after ageing.

The peaks at higher wavenumbers are associated to the vibration of the single and double bonds between the Carbon atoms. Instead, the peaks comprised between 1000 cm^{-1} and 1500 cm^{-1} are mainly associated to the bond between the carbon atoms and nitrogen atoms for both the amine and imine sites. Peaks at lower wavenumbers indicate the deformations of the ring structures or of the $C-N-H$ bonds [35]. Since PAPBA deposition resulted in thin film formation on Platinum, its Raman characterization has been more challenging. In fact, the reflections coming from the electrode surface created a background signal at high intensity so that it was almost impossible to extract information from the sample. Nevertheless, after the background subtraction, the Raman spectrum of Figure 3.34 has been obtained.

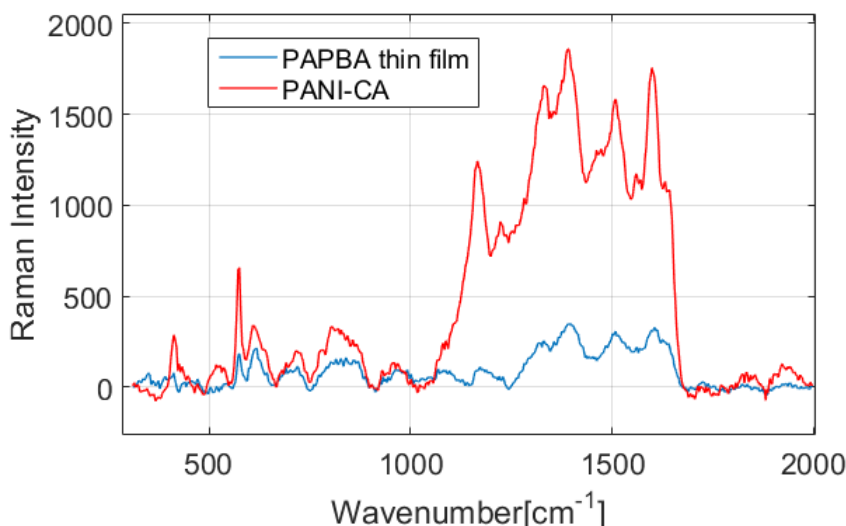


Figure 3.34. Raman spectra of PAPBA thin films.

In the previous sections it was explained that the polymeric chain of PAPBA is essentially derived from the one of PANI with the insertion of boronic acid substituent. For this reason, by comparing the two spectra, it is possible to notice a high correlation of the position of the peaks with only some small modifications. However, an accurate analysis for the detection of the boronic acid component can't be performed simply by using the spectrum of Figure 3.34.

Concerning the Polypyrrole films, the Raman results allow to distinguish the presence of the different salts that have been used for the electropolymerization and that are described in the previous sections. In fact, even though the two spectra depicted in Figure 3.35 share most of the peaks and their relative intensities, the incorporation of the $Fe(CN)_6^{4-}$ anions can be observed at lower frequencies. While the PPy prepared with $CaCl_2$ shows more pronounced peaks, the other trace is rather characterized by broader bands which are associated to the different interactions brought by the complex anion. Similarly to the case of Polyaniline, the peaks

at higher wavenumbers are mainly dependent on the vibration of the carbon atoms bonds while the other peaks are associated to the deformation of the rings that form the polymeric chain [36].

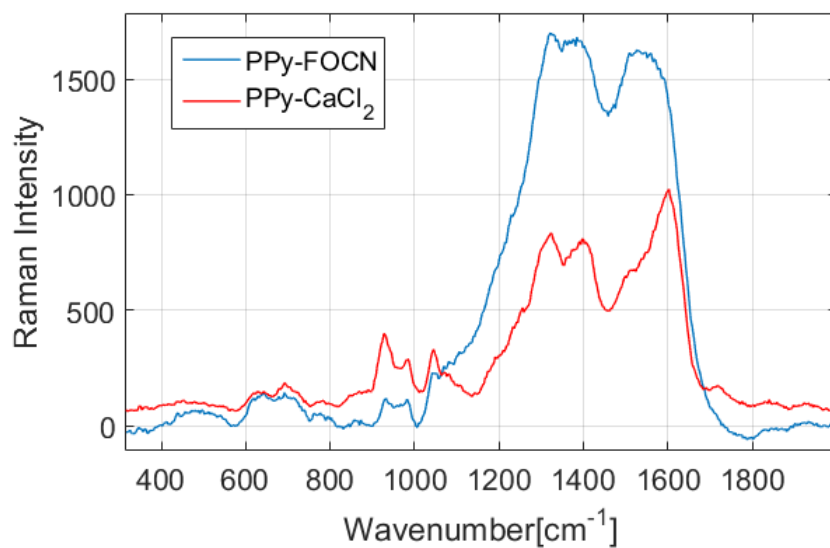


Figure 3.35. Raman spectra of PPy deposited with different salts.

Chapter 4

Microfluidic system for automated testing of liquids

Characterization and tests of *Electronic tongues* require to deal with a great variety of liquids. Indeed, the evaluation of the sensor response comes from the direct interaction of the active materials with different classes of test fluids. For this reason, it is often required to employ microfluidic setups in order to handle those liquids as well as manipulate them, accordingly to different applications. In particular, in addition to commercial classes of liquids, which could actually be provided directly to the sensor, for research purposes it is fundamental to modulate properly the test solution characteristics by mixing or adding certain quantities of other components. If the microfluidic setup is accurately calibrated, it allows a more reliable characterization of the device as well as easier tests and data creation. Multiple accessories enrich the functionalities of the instrumentation and, depending on the application, additional components may be needed. In the following sections, the main instruments employed for the experimental microfluidic setup are presented. Then, the calibration procedure is discussed before presenting the basic operations, needed for testing different liquids.

4.1 Microfluidic components integration

4.1.1 Flow sensors

Measurement of the flow rate plays an important role in many applications, ranging from the biomedical and environmental fields to the automotive and process control ones. More specifically, flow sensors are used to measure mass, average velocity, differential pressure, temperature or volumetric flow of a gas or a liquid. The simplest and basic approach is to measure the heat loss from a hot body exposed to a fluid flow. Thus, exploiting the convective heat transfer, it is possible to get specific information regarding the input flow. When a hot wire is inserted inside the stream,

two types of measurements are possible:

1. **Open loop:** a constant heating power is provided, and the temperature of the wire is measured as a function of the flow;
2. **Closed loop:** the wire is maintained at constant temperature and the required power is measured.

In this case sensors are placed in a half bridge configuration to enhance temperature compensation. The output characteristic of the sensor is basically dependent on its Temperature Coefficient of Resistance (TCR) which defines the output resistance that is given by a variation of temperature with respect to a reference:

$$R = R_{ref}[1 + TCR(T - T_{ref})] \quad (4.1)$$

Their main drawback is due to the loss of linearity when high flow rates are applied, since the sensor is not fast enough to respond to such variations. A differential version of this sensor is made of three elements: a central heater which is exactly between an upstream and a downstream sensor (Figure 4.1 [37]).

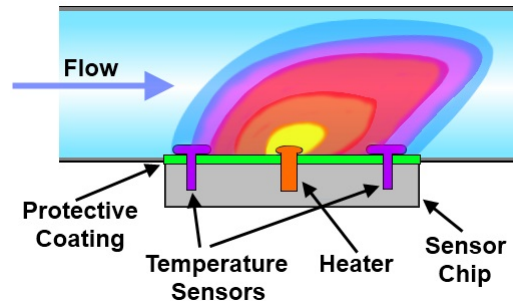


Figure 4.1. Working principle of a differential thermal flow sensor.

While the flow cools the former, the latter gets in contact with the heated fluid and its temperature is sensed. In this case the output is given with respect to the variation of temperature of the sensors pair, minimizing the common mode effect. However, it is still limited when considering high flow rates, and increasing the distances of the temperature sensors would reduce the sensitivity and the minimization of the common mode effect, even though it enlarges the linearity. On the other side, the time of flight technique demonstrates to be more suitable for large flow rates values. The principle is based on the measurement of the time needed for a heat pulse, generated at an upstream heater, to be detected by the downstream one. Even if the sensor shows lower resolution, it allows large ranges measurements as well as good long-term stability. In general, commercial flow sensors based on the previous principles can be either unidirectional or bidirectional and include a thermal isolation of the heating element from the substrate, in order to reduce the power consumption

and to let the fluid to conduct most of the power. In this case, the sensors are placed on standing bridges made of silicon oxide or silicon nitride, which shows lower thermal conductivity with respect to silicon. Dust filters are usually needed to enhance the life time of those sensors, and thermopiles demonstrate to be one of the best candidates for temperature sensing. Some other flow-velocity microsensors are based on semiconductor field-effect structures like ISFETs, which are sensitive to ions concentration variation. An ion generator is placed upstream and two ISFETs are placed at different distances, so that the variation of time difference between the sensor's response gives information related to the input flow.

Instead, the operating principle of the Coriolis flow meter is basic but very effective. It contains a tube which is energized by a fixed vibration. Such tube is subjected to a twisting whenever a fluid (gas or liquid) passes through it. The mass flow momentum is the responsible of this change in the tube vibration resulting in a phase shift. A linear output, proportional to the flow, can be derived by measuring such vibration. As this principle measures mass flow independent of what is within the tube, it can be directly applied to any fluid flowing through it, whereas thermal mass flow meters are dependent of the physical properties of the fluid. Furthermore, it is possible to measure the actual change in natural frequency, in parallel with the phase shift in frequency between inlet and outlet. This change in frequency is in direct proportion to the density of the fluid, generating a further output signal. If both the mass flow rate and the density are known, it is possible to derive the volume flow rate (Figure 4.2).

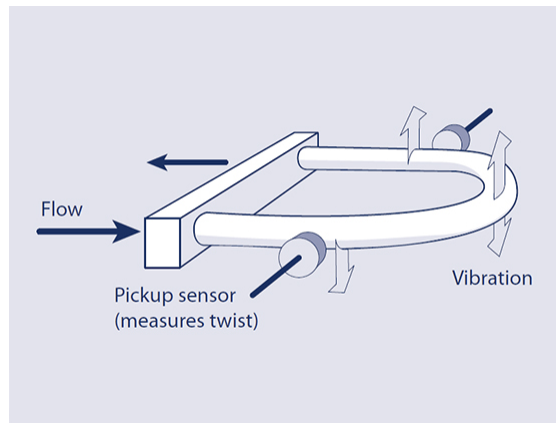


Figure 4.2. Working principle of a coriolis flow sensor.

The advantage of measuring the mass flow rate instead of the volumetric one is due to the fact that the former is completely independent from the effects of temperature and pressure on fluids properties. For instance, the same mass of air occupies half of the volume when it is subjected to the double of the pressure. Coriolis flow sensors' response in time can be really fast, in the order of 50 to 100 milliseconds

and they are characterized by high accuracy ($\pm 0.2\%$ of rate for liquids and $\pm 0.5\%$ for gases). Commercially available flow sensors often exploit one of the previous principles or similar approaches. However, the choice is highly dependent on the application and on the ranges of flow rates to be measured.

The experimental set up presented in the next sections includes two different flow sensors:

1. a thermal flow sensor integrated in the *Fluigent Flow Rate Platform*;
2. a coriolis flow sensor *Bronkhorst mini Cori-Flow*.

4.1.2 Micromixers

One of the main scaling effects to be considered in microfluidics is the increasing difficulty to mix multiple fluids. In fact, fluids moving with a laminar flow are characterized by different interface properties with respect to the turbulent ones. However, the mixing could be enhanced by the diffusion process of the liquid streamlines. Micromixers are usually employed to increase the contact between the two fluids by multiplying the interface subdividing, twisting, distorting and expanding the microchannels or the small tubing connections. Those devices are usually called *chaotic* micromixer. Another possible mechanism is based on a pulsatile flow: the streams of the fluids are alternatively switched on and off and, after some cycles, the fluids profile may be completely distorted due to the upstream and downstream movement that characterize the interface of the initially separated fluids. Micromixers are fundamental in those applications that require manipulation and smart modifications of liquids by adding other ones in small microchannels connections.

4.1.3 Additional components

In addition to the above mentioned components, the microfluidic system presented in the following sections comprises:

- **microfilters** at the inlet and outlet of the Coriolis flow sensor;
- **microvalves** that allow to switch the path followed by the flow inside the system;
- a **vacuum pump** (*KnF Lab Liquiport, PML 10865-NF-130*) that allows sucking and moving the liquids along precise directions.

4.1.4 Pressure-controlled flow

The *Fluigent Microfluidic Flow Control system (MFCS)* is a pressure-based flow controller for microfluidic and nanofluidic applications (microchannels, nanochannels,

capillaries, lab on chip. . .), and allows stable flows with short response times down to 40 ms and settling times as low as 100 ms. The instrument is capable of extracting specific quantities of liquids coming from different flasks to which it is connected. It enables the flow actuation of fluids by pressure regulation, exploiting the principle based on the pneumatic pressurization of multiple reservoirs. Indeed, liquids can be forced to flow inside the tubes through the application of a certain nitrogen pressure inside each flask. Such operation can be achieved through the so called *Fluiwells*, which are microfluidic accessories enabling a precise pressurization (Figure 4.3).

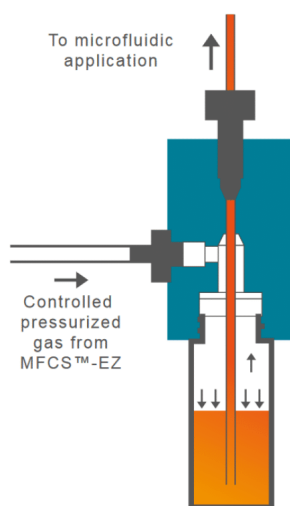


Figure 4.3. Pneumatic pressurization of a flask.

The versatility of the system comes from the fact that it consists of multiple channels that can be activated or not at the same time. Moreover, the size of the microfluidic tubes for each channel is different, so that they are characterized by different fluid flow ranges:

- Channel 8: Size XL, +/- 5 mL/min;
- Channels 7,6,5: Size L, +/- 1 mL/min;
- Channels 4,3,2: Size M, +/- 0.08 mL/min;
- Channel 1: Size S, +/- 0.007 mL/min.

Multiple tests described in the following sections were made in order to calibrate the channels and to minimize the mismatch of the ones with the same size. The actual flow of the liquid can be controlled through **8 switches** that can activate or close the valves to which the tubes are connected. For instance, the flow of the liquid contained in the flask corresponding to channel 5 (*CH5*) is possible only if applying

a certain pressure to that channel and by opening the switch that controls *valve # 5*. A flow sensor is placed between the flasks and the valves so that when the flow of the liquids starts, the instrument measures the flow rate for each of the channels. The system can be set to provide a specific flow rate on the different channels thanks to the *Flow Rate Control Module*: upon the completion of a *channels' identification* procedure, the controller is capable of modulating the pressures on all of them at the same time in order to satisfy the flow rate requirements.

4.2 Complete experimental setup and calibration

Microfluidic components introduced in the previous sections have been connected in the way depicted in Figure 4.4.

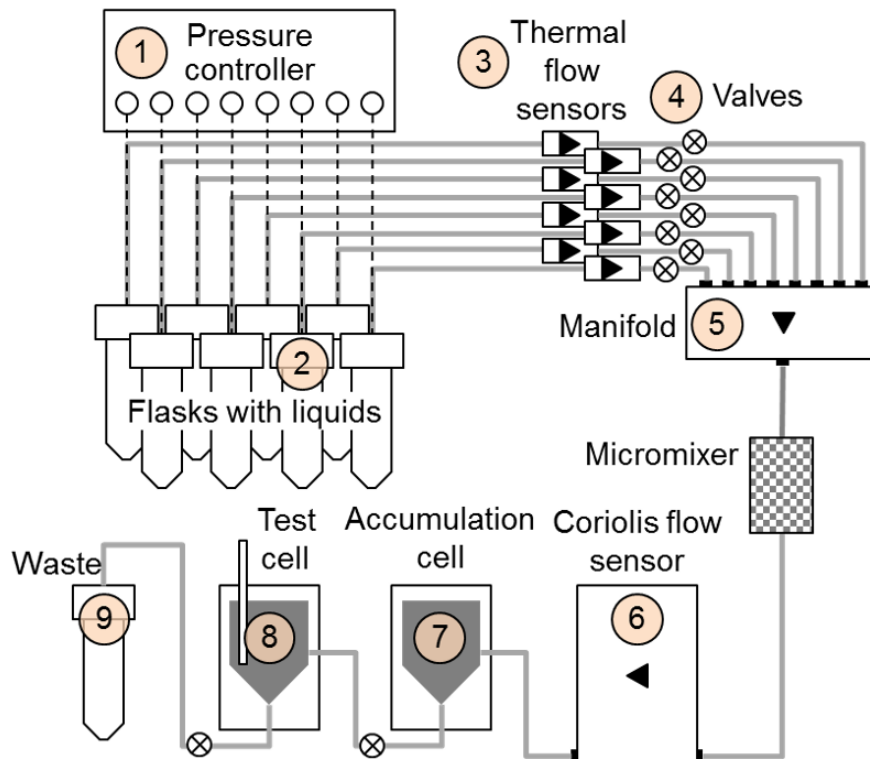


Figure 4.4. Complete experimental set-up for liquids handling. *Credits: Patrick Ruch.*

The pressure controlled mechanism (1) allows to extract liquids contained in the initial flasks (2). Thermal flow sensors (3) are connected to each of the eight channels, that upon activation through switching valves (4), can fill up a manifold chamber (5) where the liquids start to mix. A micromixer is then placed ahead of the Coriolis flow sensor (6), which provides a more accurate value of the flow rate related to the total

liquid flowing into the system. The test liquid is collected inside the accumulation cell (7) while the measurement is running in the test cell (8) with a previous test liquid. Finally, the test cell is evacuated thanks to a waste flask (9) and the new test liquid can be moved from the accumulation cell to the test one, where the sensor has been placed during all the measurements. Accumulating the liquid in another cell, before providing it to the sensor, has been proposed as a solution to mimic the way in which the actual device could work. Indeed, the removal of the previous test liquid and the injection of the new one would be fast enough to cause the sudden change of the collected signals as in a real application.

A calibration of the experimental setup has been necessary in order to accurately control the amount and type of liquid that can be provided to the accumulation cell prior to each test. The *Fluigent Maesflo Software* is capable of adjusting the pressure values so that the flow rate measured by the thermal flow sensors is close to the value requested by an external user. For this reason, the first calibration step has been mainly oriented towards the verification of the proper functioning of the thermal flow sensors through the measurement operated by the Coriolis one, characterized by higher accuracies for the reasons explained in the previous sections. However, the measurement of the flow rate performed by the latter is obtained after the collection of the liquid inside the manifolds chamber, i.e. measured regardless of the channel size and with a full range of $3.33 \text{ mL}/\text{min}$. Tests on multiple channels have been conducted in different days, involving *CH8*, *CH7*, *CH6*, *CH5* and *CH4*. Isopropanol has been injected inside all the involved channels prior to each test with water to remove possible salts residuals inside the microfluidic extensions. Moreover, the first test with water for each channel needed always to be discarded due to the strong variation of the flow rate recorded with both the sensors when two different liquids were injected one after the other. The most accurate calibration process requires the evaluation of the weight of the liquid obtained at the outlet of the entire system and comparing this value with the ones measured by the two flow sensors. The activation or deactivation of a channel lead to a ramp up and a ramp down of the flow rate measurement respectively, which should anyway be taken into account for the estimation of the total collected volume. The evaluation of the ratio between the actual weighted volume (V_w) and the measured one (V_m) makes possible to adjust the calibration of the flow sensors. Indeed, knowing the scaling factor ($\frac{V_w}{V_m}$), it is possible to determine automatically the amount of volume that is actually provided by the system.

4.2.1 Volumes estimations of the microfluidic connections

The positions of the two calibrated flow sensors in the experimental setup of Figure 4.4 makes possible to evaluate with high precision the volume of the setup microfluidic connections. When fluids stop to flow inside those sensors, the recorded flow rate suddenly drops to zero so that, whenever a reservoir of liquid becomes empty (one

of the input flasks), the sensors would acquire such decrease in different times. The span of time that separate such event for both of them is dependent on their physical distance. In Figure 4.5 flow rates for the two sensors are reported during one of those experiments.

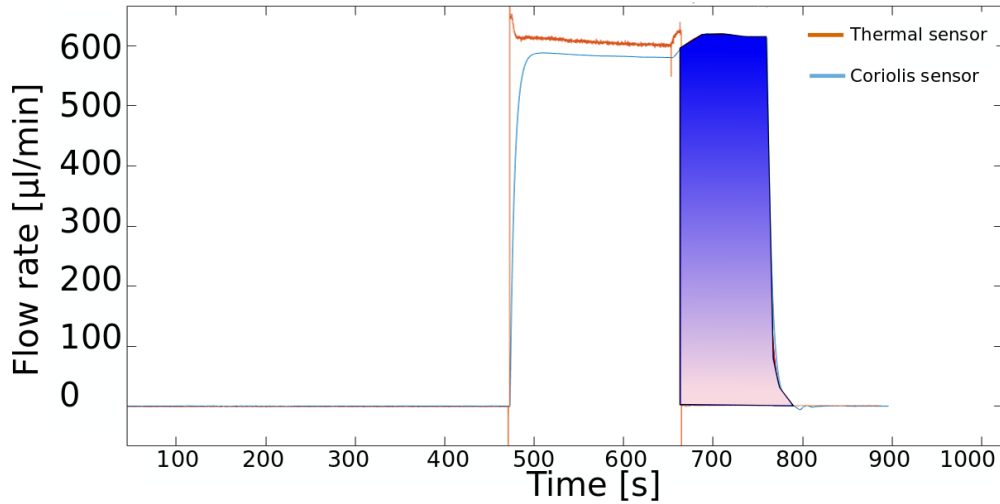


Figure 4.5. Estimation of volumes through integration of flow rates.

The moment in which the thermal flow sensor signal drops indicates the fact that the sensor does not acquire additional liquid. The flow rate of the Coriolis sensor is then integrated for the remaining time up to its decrease. The estimation of the volume of the connections between the sensors is then around $1059 \mu\text{l}$. Similar experiments allow to get estimation of other connections of the entire setup:

- volume of liquid that flows from the flasks to the flow sensor: $196 \mu\text{l}$;
- volume between the outlet of the Coriolis sensor and the inlet of the mixing chamber: $460 \mu\text{l}$;
- volume of the entire path of a liquid coming from a reservoir and directed towards the accumulation cell, obtained by summing all the contributions of the previous experiments : $1715 \mu\text{l}$;

All the previous estimations are affected by an uncertainty of $\pm 0.2\%$, given by the accuracy of the volume counter of the Coriolis sensor. A validation of the methods used for this purpose comes from a rough estimation of the volume of some connections, which could be obtained directly knowing the diameter and the length of the connections. However, the experimental procedure results to be more accurate and necessary, since not all the connections could have been measured manually without dismantling the entire set-up, or by knowing a-priori some values related to

the path followed by the liquids inside the flow sensors. Thus, the full investigation and characterization of the setup has been remarkably fundamental for all the actual tests performed with the sensor array.

4.2.2 System validation and limitations

The possibility to control directly the flow rate values on all the channels at the same time gives to the system a certain flexibility, in terms of the types of tests that can be performed. It is possible, not only to collect a test liquid from a reservoir and provide it to the test cell, but also to extract liquids simultaneously from multiple channels according to user-defined ratios. Thus, the validation of the calibration of the instrument can be performed by verifying the mixing capabilities of the setup. Figure 4.6 shows an example for the validation of the mixing procedure. It is shown that the $0.05M$ KCl solution created by mixing $0.1M$ KCl ($CH7$) and millipore water ($CH6$) produces the same potentiometric response of a $0.05M$ KCl solution injected directly into the system.

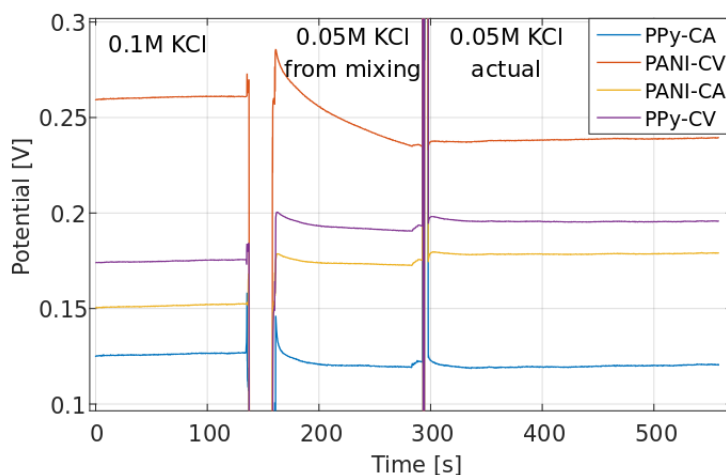


Figure 4.6. Validation of mixing capabilities.

The reliable operation of the system can be affected by some **sources of contamination** and by **speed and flasks volume limitations**:

- at each test iteration the channels are set to provide the correct amount of liquids and the valves are set open to fill the mixing chamber. However, all the internal tubing connections are still filled with the liquid of the previous transition. In this sense, a key role is played by the insertion of an intermediate outlet from the mixing chamber to the waste. Once the correct solution replaces entirely the previous one, the actual filling of the accumulation cell can

start. The precise estimation of the volume of the tubing connections allows to minimize the excessive liquids' waste;

- tests' speed is limited by the maximum flow rate that can be measured by the thermal flow sensors. Moreover, those limits are strongly dependent on the number of employed channels, since the system can't satisfy high flow rates requirements on multiple channels simultaneously. In fact, the identification procedure that assure the proper contribution of each channel to the final mixed liquid, could also cause the cross contamination of the liquids. This phenomenon occurs whenever a low identification quality leads to negative flow rates values on some of the channels;
- reservoir of liquids have a limited volume. Replacement of the flasks is needed during the system operation in case of tests that, overall, requires greater volumes.
- the accumulation and test cell should be made of materials that can sustain the continuous wetting without affecting the tests. Some 3D-printed materials have demonstrated to leach some compounds in the collected liquids, so that some sensitive polymers could eventually be deteriorated or irreversibly modified due to prolonged exposure to contaminations.

4.3 Fully automated tests

The full automation of the tests has been accomplished thanks to the possibility of automatically instructing the components of the experimental setup through multiple script functions. Instruction codes have been written following the software guidelines. Test timings have been determined by defying activation or deactivation periods of the valves connected to two switchboards. The first one has been placed after the valves, at the outlet of the thermal flow sensors to trigger or prevent the fluid flow. The second switchboard has been connected after the Coriolis flow sensor. The corresponding valves have been devoted to different purposes, according to the necessary steps for each test. Throughout all the experiments, the vacuum pump needs to be switched on. In this way the liquid ejected by the accumulation or test cell is pushed towards the waste flask.

Different tests share some basic common operations:

1. Pre-defined flow rates values are requested through the software control module. Pressure is automatically applied to satisfy the user requirements. Liquids start to flow from the flasks to the system following the channels connections;
2. Flow rates can be monitored through the flow sensor to verify the correct operation of the set-up and of the simultaneous channels employment;

3. Liquids are then first mixed inside the manifolds chamber, which receives all the channels connections as inlets and let the mixed solutions to flow through its outlet;
4. The micromixer improves the mixing of the solution coming from the manifold before it could flow towards the collection chamber;
5. The solution passes through the Coriolis flow sensor which has been placed between two microfilters. Accurate flow rate measurement is necessary to monitor the mixed solution flow towards the collection chamber.
6. The liquid reaches **Valve # 1** of the second switchboard. Opening such valve allows the flow of liquids into the collection chamber. At this point all the other valves of the same board must be switched off to make possible the chamber filling;
7. Flow of liquid has to be stopped after a fixed time to assure that the correct amount of liquid has been provided. The time is defined depending on the specified total flow rate and on the required volume. **Valve # 1** has been switched off while **# 2** could be set depending on the operation to be accomplished. It could either allow the transfer of the collected liquid directly into the waste or to let it flow towards the test cell where the sensor has been placed;
8. **Valve # 6** is switched on to allow the movement of the liquid from the collection chamber towards the waste. As already mentioned before, the employment of this valve allows to get rid of the contamination liquid coming from the previous tests.
9. The evacuation of the test cell is possible by opening **Valves # 3** and **# 5** as well as by switching on the pump. In this way the liquid can be sucked and collected into the waste flask and the test cell is emptied to allow a new liquid test.
10. The flow of the liquid from the mixing chamber is possible by opening **Valve # 2** that connects the collection chamber to the test cell. Liquid flow could be accelerated by the opening of **Valve # 4** which allows nitrogen flux to push the liquid out of the collection chamber.

A representation of the filling procedure of the test cell is presented in Figure 4.7. In all the tests, the maximum achievable total flow rate is $1500 \mu\text{l min}$. For this reason, the minimum test time is limited by the time needed to refill the accumulation cell with the following test liquid. As a consequence, the volume of the test cell directly influences the speed of the operations, since the system timings must assure a certain liquid level to reach the sensor position. For a glass vial chosen as test cell, the minimum amount of required liquid is $3600 \mu\text{l min}$. Finally, the total testing time

must take into account the intermediate filling and emptying of the accumulation cell to preserve the new test liquid.

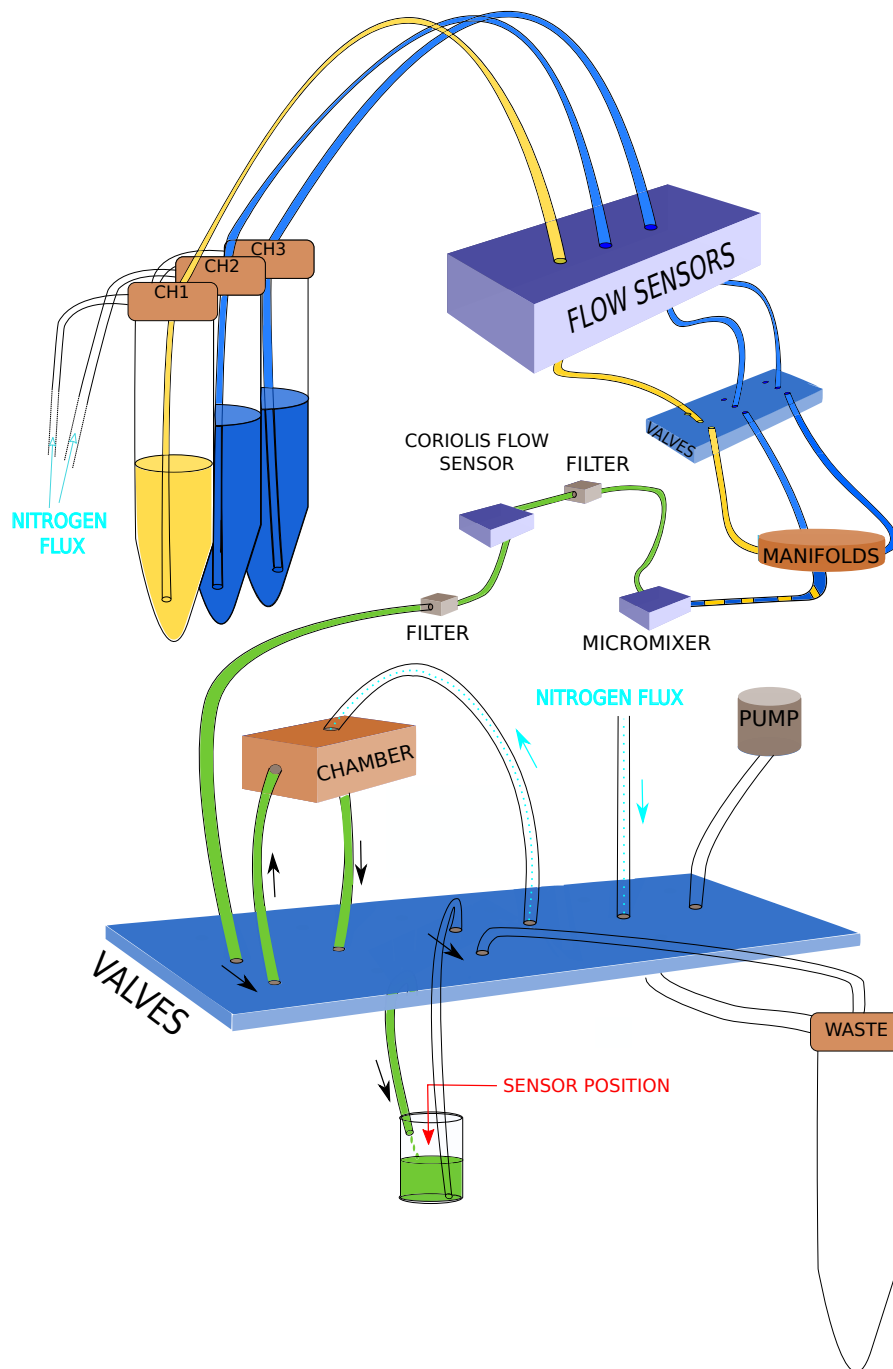


Figure 4.7. Representation of the test cell filling

Chapter 5

Cross-sensitive arrays fabrication and characterization

5.1 Sensors design

In Chapter 3 it has been discussed the possibility to produce polymers by electrodeposition on different substrates. Thus, the design of the sensors arrays takes advantage of such flexibility and allows the fabrication of multiple versions that share some common characteristics. It has already been mentioned that one of the main advantages of electropolymerization is the miniaturization of the entire system, since it provides a local and well-defined deposition of the active materials. For this reason, the dimensions of the electrodes' pads can be largely scaled and polymers have been successfully deposited on electrodes with diameter down to $0.5mm$. Hence, the study of the cross-sensitive arrays has been performed either on 4-electrodes arrays ($\varnothing 2mm$, Figure 5.1) or 8-electrodes ones ($\varnothing 0.5mm$).

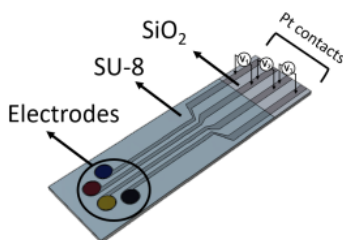


Figure 5.1. A four electrodes ($\varnothing 2mm$) array and contacts for voltage read-out.

The disposition of the platinum-sputtered pads recall the circular structure of the O-rings, which are usually placed on top of the chip during the electropolymerization inside the electrochemical cell. Electrical tracks are designed to connect the electrodes to an external component for the measurements, while an insulating

layer of SU-8 has been deposited to expose only the circular electrodes for the electropolymerization. Concerning the fabrication process, a $525\ \mu\text{m}$ thick silicon wafer is subjected to thermal oxidation at $1050\ ^\circ\text{C}$ to get an oxide layer of roughly $500\ \text{nm}$ for the creation of an insulating substrate, in order to prevent electrical interaction between the electrodes. Then, the wafer is coated by a $2.4\ \mu\text{m}$ layer of positive resist and, after depositing $10\ \text{nm}$ of Ti and sputtering $100\ \text{nm}$ of Pt on the entire wafer, the tracks for the electrical contact are created through a lift-off process. A O_2 plasma etching enhances the surface cleaning. In a second lithographic step, a $15\ \mu\text{m}$ SU-8 layer is deposited on top of the wafer and, after curing, part of it is removed in order to let exposed the electrodes pads and the external edges of the platinum tracks. A further protective layer of $200\ \text{nm}$ is deposited at the end of the fabrication process.

Chips are released from the wafers after dicing with a diamond blade tool and prior to the deposition of the polymer coating, the removal of the protective layer is achieved by dipping the chips in acetone and IPA. Nevertheless, it has been found that when the final protective layer is not fully removed from the chip's surface, it may partially or completely prevent the electrodeposition of all the polymers. For this reason, it has been proposed a O_2 plasma treatment to make sure that the electrodes surfaces have been cleaned properly. Indeed, in many applications requiring cleaning and activation of surfaces, plasma technology has demonstrated to lead to many advantages. The main issue for the fabricated sensor array is the presence of residual of organic components, also after the acetone/IPA baths, consisting of loosely bound hydrocarbons. For this reason, the O_2 plasma would cause the reaction of hydrogen and carbon that would leave the Pt surface in the form of volatile H_2O and CO_2 . Such treatment has demonstrated to improve drastically the deposition processes, and it has been widely employed before the creation of new arrays of polymer coatings. The effect of the plasma treatment can be evidenced during the potentiodynamic deposition of polymers, in which the voltage is scanned in a precise window. Only the first cycle of the electropolymerization results to be affected by the cleaning process, since a reduction peak is evidenced during the first reverse scan. On the contrary, a deposition on a Platinum rod does not show any remarkable spurious current peak. For instance, Figure 5.2 shows the first cycle of a CV-electrodeposition of PANI on the two different surfaces.

While the process on Pt rod shows the redox peak associated to the oligomeric chains formation of aniline, the trace related to the surface of one of the electrodes of the sensor array shows a reduction peak, probably due to the residuals of the oxygen plasma activation. However, starting from the second cycle of the potential scan, the redox peaks formation would clearly follow the standard Polyaniline electropolymerization that has been described in Chapter 3. Thus, the plasma treatment has been employed extensively to allow the activation of the sensor array.

In the framework of the creation of a device that can be scaled for commercial and industrial application, Electroless Nickel Immersion Gold (ENIG) is a more suitable

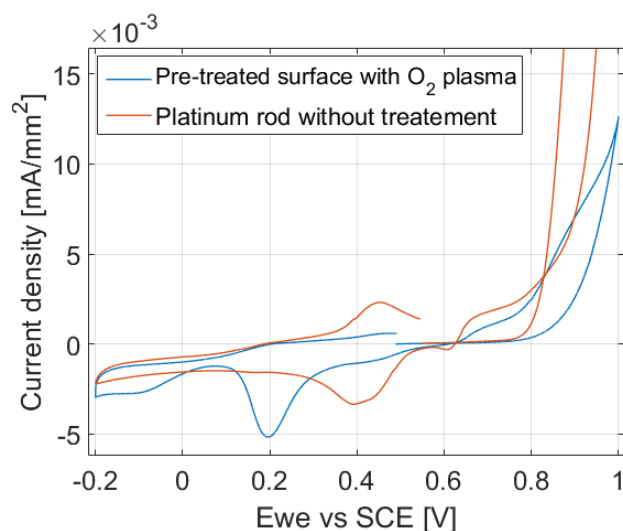


Figure 5.2. Effect of the oxygen plasma surface treatment on the first deposition cycle of PANI.

substrate and a type of surface plating, commonly used for printed circuit boards. The first step for the fabrication is an auto-catalytic process that involves depositing nickel on the palladium-catalyzed copper surface. Then, during the immersion gold step, a thin gold adheres to the nickel-plated areas through molecular exchange. In the Au/ENIG version of the sensor array, the main structure of the electrodes is preserved with respect to the Si/Pt one, with a circular disposition of the eight electrodes ($\varnothing 0.5\text{mm}$, Figure 5.3).



Figure 5.3. Sensor array based on Au/ENIG electrodes.

5.2 Limitations of multiple polymers integration

The design of a cross-sensitive arrays of polymers requires the integration on the same chip of multiple sensing materials. The chips fabricated in the way described in the

previous section have been functionalized by the deposition of different conductive polymers through electropolymerization. The first concern, when dealing with this procedure, is to verify the feasibility of the simultaneous presence of polymers of different natures on the electrodes that form the arrays. Electrodepositions occur one at a time, so that the complete array is in contact with a polymerization solution, but only the electrode connected to the Potentiostat can be actually polymerized through the application of a certain voltage. Nevertheless, the fact that the chip is dipped inside different solutions must be taken into account. Indeed, the pre-treated surfaces result to be ultra-fine cleaned, so that possible sources of contamination, that might modify the electrodes quite easily, can be derived by the electropolymerization of other electrodes. Moreover, one must consider the influence of the solution for the deposition of one polymer that gets in contact with a pre-deposited one.

In Chapter 3, there have been introduced three different types of polymers : PANI, PAPBA and PPy. It has already been mentioned that the PAPBA polymeric chains constitute modifications of the Polyaniline structure, with boronic acid substituents. The polymerization process of these two polymers is quite similar and based on H_2SO_4 . For this reason, it is expected that the electropolymerization of one of those does not affect the other one and viceversa. This fact has been confirmed through the successful deposition of PANI and PAPBA on different electrodes of the same array. However, the integration of Polypyrrole seems to entail a certain number of issues to be investigated.

5.2.1 Effect of PANI/PAPBA deposition on PPy electropolymerization

It has been noticed that Polypyrrole deposition on one of the electrodes, following the other two electropolymerizations using the H_2SO_4 -based solutions (PANI and PAPBA) on other ones, may be unsuccessful. In some cases, the deposition is incomplete, with part of the electrode surface that is not fully covered or the measured current values, during either a potentiostatic or a potentiodynamic experiment, have demonstrated to be much lower than the ideal ones (Chapter 3). Thus, it is expected that the surfaces of the electrodes, which are not involved directly in the polymerization, experience some sort of modification that prevents the PPy coating deposition. Those surfaces have been investigated to get a full understanding of this contamination issue. Figure 5.4 shows the optical microscope images, in which it is possible to notice the presence of some residuals on the edge of one of the electrodes different from the one of the electropolymerization. Those contaminations are not equal in all the electrodes and, in some cases, they may cover more extended areas of the entire surface. The presence of those elements have been also evidenced through electrochemical techniques. Cyclic voltammogram in a $0.1M$ KCl solution have been recorded on one of the electrodes of the array, before and after the deposition

of Polyaniline of a neighbour electrode. In Figure 5.5, the two CV traces differ considerably due to the presence of some residuals from the contact of the electrode with the PANI electropolymerization solution.

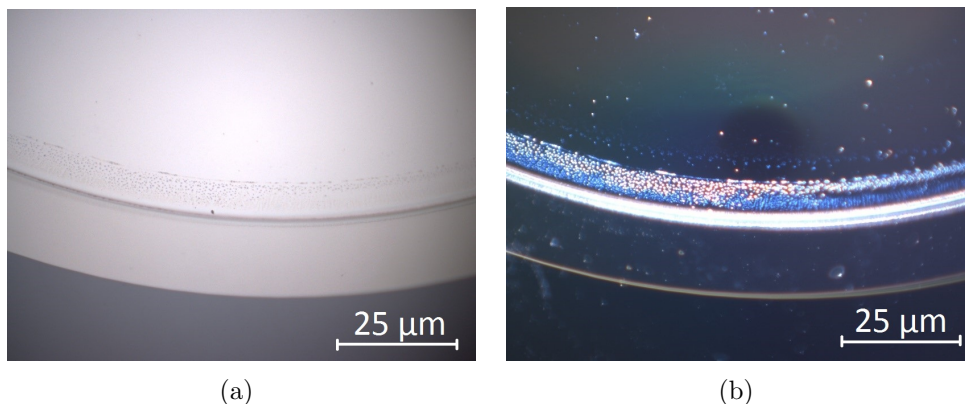


Figure 5.4. (a) Brightfield and (b) darkfield optical images of one of the electrodes' edge after the electrodeposition of PAPBA on another electrode.

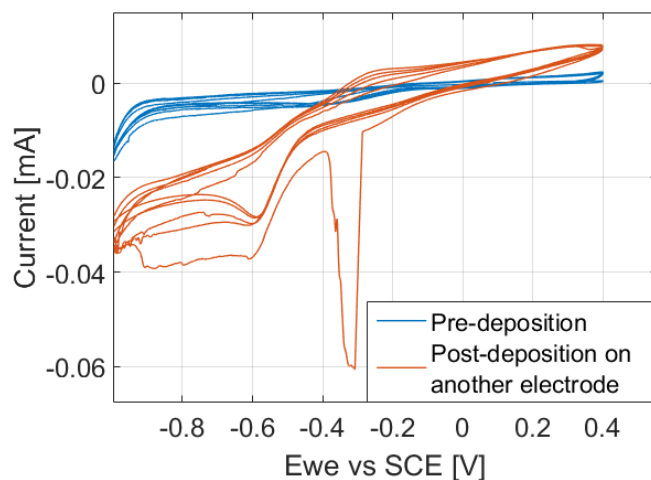


Figure 5.5. CV in $0.1M$ KCl of an array's electrode before and after electropolymerization of PANI on another one.

Even though the nature of those residuals has not been fully investigated, it is expected that they are H_2SO_4 -soluble components. Indeed, multiple treatments of the electrodes have revealed that dipping the sensor inside sulfuric acid has the same effect of other electrochemical procedures, such as reduction or oxidation of the electrode in the same solution. Thus, it can be concluded that a successful electropolymerization of PPy films can be achieved on those electrodes if they are subjected to further chemical cleaning steps.

5.2.2 Effect of PPy deposition on PANI/PAPBA electropolymerization

A similar effect to the previous case can be noticed when PANI and PAPBA needs to be electrodeposited on other electrodes, different from the ones in which PPy has been already polymerized. However, the contamination of the surfaces is more evident, and all the electrodes of the array result to be profoundly affected by the contact with the Polypyrrole electropolymerization solution. A similar approach to the PANI/PAPBA case has been adopted to clean the electrodes. Nevertheless, dipping in sulfuric acid for prolonged time does not release the residuals and electrochemical cleaning can help partially in the removal of those contaminants to allow the PANI/PAPBA deposition. Figure 5.6 shows the effect of an attempt of cleaning the electrode surface by electrode reduction at $-1V$ for 60 seconds in $0.05M\ H_2SO_4$. Only part of the deposition residuals has been successfully removed.

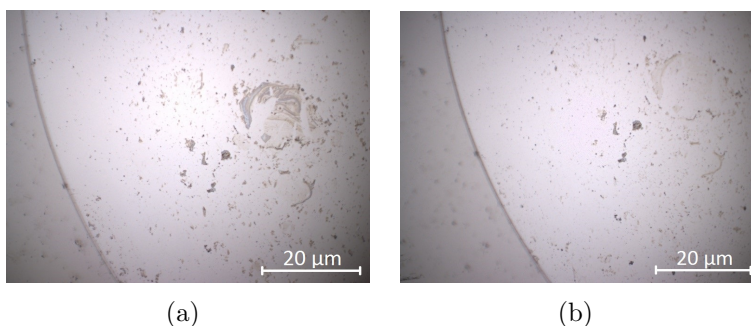


Figure 5.6. Electrode surface before (a) and after (b) the electrochemical cleaning following the ePPy electropolymerization on another array's electrode.

As a consequence, one could think that, since cleaning the electrodes after the PPy deposition results to be more challenging than the same operation after the PANI/PAPBA polymerization, Polypyrrole should be the last polymer to be produced, when all the other electrodes have been already coated with Polyaniline and PAPBA. However, an additional effect must be taken into account, that is the influence of the PPy electropolymerization solution in contact with the other polymer coatings. Figure 5.7 displays the microscope image of a portion of a purple PAPBA thin film after the deposition of PPy on another electrode. It is expected that the contamination of the polymer could modify its initial properties and that the alteration could be unpredictable, preventing from gaining reproducibility of such effect.

In Chapter 3, the profilometric analysis reported that Polypyrrole films are at least ten times thicker than the other ones. Thus, the impact of the contamination on the thinner polymers would be more relevant than the opposite situation. For this reason, a trade-off solution must be adopted. Since the deposition of PPy as last polymer could ruin irreversibly the other films, the best choice would be to polymerize PPy before all the others. Regarding the other electrodes pre-treatment

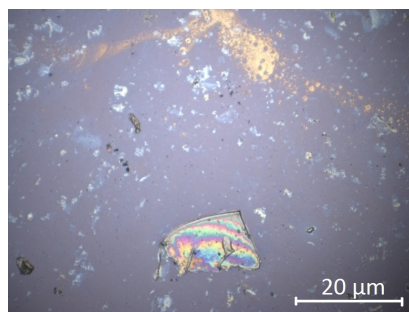


Figure 5.7. PAPBA film contaminated by residuals of PPy electropolymerization on another electrode.

to enhance the deposition of PANI/PAPBA, multiple cleaning steps could be followed to improve the surfaces' quality as much as possible. For instance, it is possible to dip the sensor in acid or leave the chip in water overnight, so that most of the residuals could be dissolved. Nevertheless, it has been proved that, rinsing vigorously with water and IPA the electrodes to be cleaned, electropolymerization of PANI/PAPBA can be successful with a full surface coverage. The extensive surface treatment may prevent from growing the polymers with the same rate described in Chapter 3, but it has been proved the most reproducible way to integrate all the polymers on the same array (Figure 5.8).

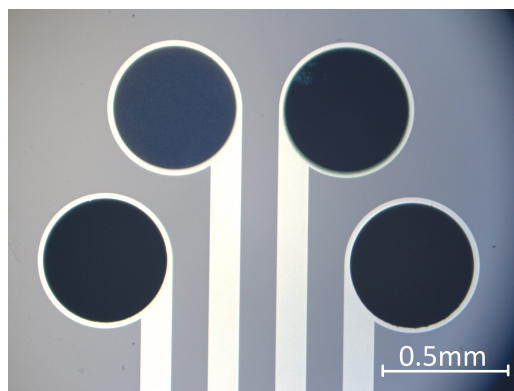


Figure 5.8. Complete array of four polymers: PPy-CA, PANI-CV, PANI-CA and PPy-CV.

5.3 Electrochemical characterization of polymeric films deposited on the arrays

In Chapter 3, the polymers introduced in the present study have been mainly characterized from the structural and morphological point of view. Monomer nature and

polymerization conditions seem to play an important role for the determination of the final film properties. Depending on the electrodes' number and on the substrate (Pt/Si or Au/ENIG) the microfabricated arrays comprise all the studied polymers or a subset of them:

- PPy-CA: Polypyrrole deposited with chronoamperometric technique and doped with $Fe(CN)_6^{4-}$. ($0.1M$ Pyrrole, $0.1M$ $K_4Fe(CN)_6$ at $0.8V$ for $60s$).
- PPy-CV: Polypyrrole deposited with CV technique and doped with $Fe(CN)_6^{4-}$. ($0.2M$ Pyrrole, $0.05M$ $K_4Fe(CN)_6$ in the range -0.5 to $0.8V$ for 3 cycles at $20mV/s$).
- PANI-CA: Polyaniline deposited with chronoamperometric technique and doped with SO_4^{2-} . (50 mM Aniline, $1M$ H_2SO_4 at $0.8V$ for $90s$).
- PANI-CV: Polyaniline deposited with CV technique and doped with SO_4^{2-} . (50 mM Aniline, $0.5M$ H_2SO_4 in the range -0.2 to $1V$ for 15 cycles at $50mV/s$).
- PAPBA: Polypyrrole deposited with CV technique and doped with $Fe(CN)_6^{4-}$. (50 mM APBA, $0.5M$ H_2SO_4 in the range -0.2 to $1.1V$ for 70 cycles at $100mV/s$).

Moreover, it has already been shown that the potentiometric response of the membranes represents a fundamental figure of merit to define the parameters which would enhance a greater impact in their sensing performances. A better understanding of the array's cross-sensitivity can be achieved by fully characterizing all the polymers electrochemically, since it represents the transducers' principle governing the read-out of the *Electronic tongue* signals.

5.3.1 Cyclic voltammetric studies

Potentiometric sensors' responses are strongly driven by the exchange of charges occurring between the active materials and the liquids with whom they are in contact. For this reason, cyclic voltammetry is a suitable technique to investigate the interaction of the polymers with different ionic species. Figure 5.9 shows an example of a CV recorded for one of the PPy electrodes immersed in a $0.1M$ KCl solution.

When the potential is scanned towards more positive values, the electrodeposited polymers gets in contact with anionic species and the measured current gives an estimation of the strength of such interaction. Thus, a current peak observed at higher potentials represents an anionic exchange activity between the polymer and the salt solution. For the same reason, the presence of a peak observed during the reverse scan towards lower potentials is an indication of a cationic exchange. Thus, cyclic voltammetry performed in different salts solutions paves the way for estimating the interactions of different polymeric films with multiple ionic species. The polymer

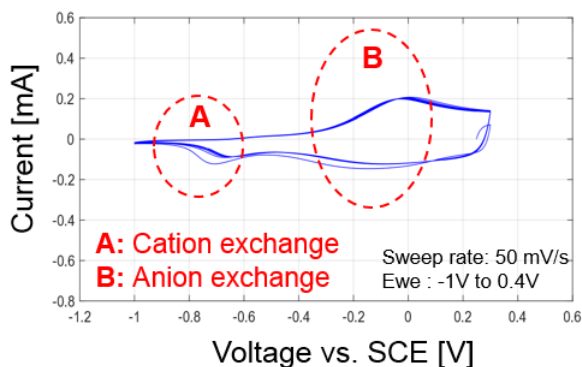


Figure 5.9. CVs of a $\text{PPy}(\text{CaCl}_2)$ film recorded in 0.1M KCl at 50 mV/s .

response may depend on many factors in addition to the type of charge that it can exchange and multiple phenomena must be taken into account. Hence, the shape of the voltammograms is a powerful description of the polymers' behaviour. The same polymer shows different CVs when it is in contact with another salt solution, due to the fact that the sensitivity changes based on the ions which are dissociated (Figure 5.10).

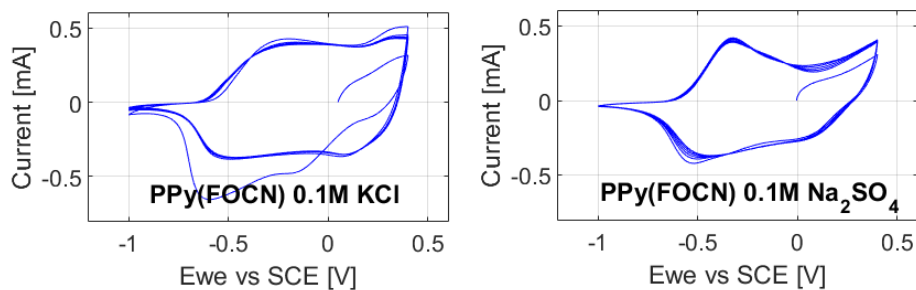


Figure 5.10. PPy-CA interaction with a 0.1M KCl and a $0.1\text{M Na}_2\text{SO}_4$ solution (four CVs cycles at 50 mV/s).

Moreover, all the polymers to be integrated into the array show different interaction levels with the same salt solution and consequently, the CVs recorded for PPy, PANI and PAPBA films display remarkably dissimilar shapes (Figure 5.11).

5.3.2 Potentiometric sensitivity

A quantitative evaluation of the interaction of the electrodeposited polymers with multiple ionic species could be obtained through the *sensitivity slopes values*. Whenever a membrane gets in contact with a salt solution, it may respond in a certain way such that the electrode potential, measured against a reference electrode one

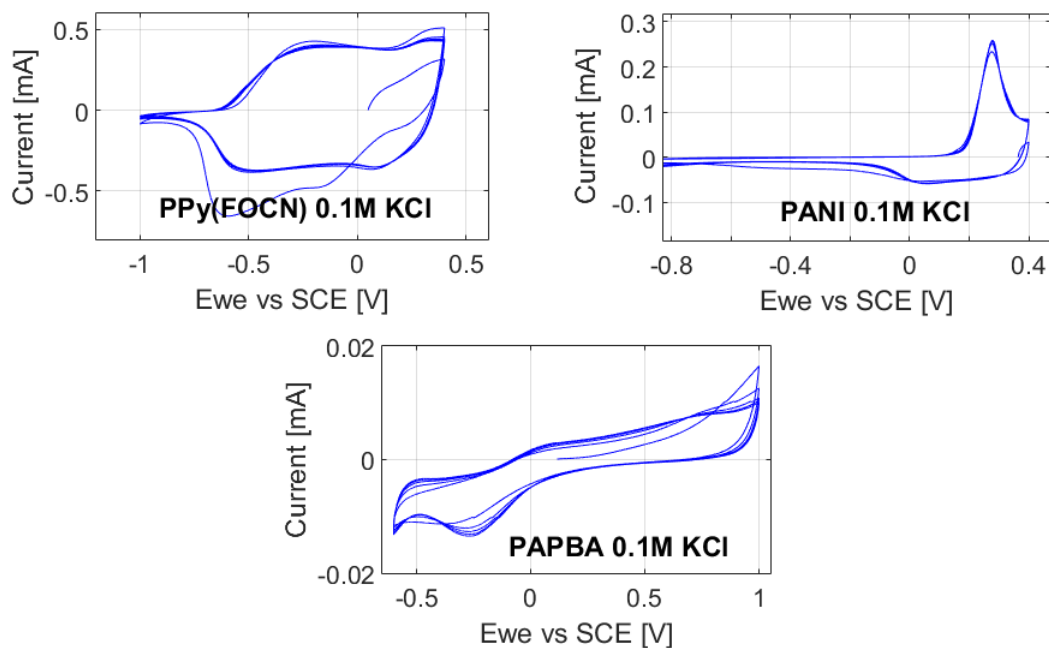


Figure 5.11. CVs at 50 mV/s in 0.1M KCl solution of PPy-CA ($Fe(CN)_6^{4-}$), PANI-CV and PAPBA films.

(SCE), varies to reach a new equilibrium condition. Thus, the corresponding signal results to be profoundly dependent on the nature of the ionic components of the solution as well as to their dimensions. Indeed, it has already been explained in the previous chapters that the potentiometric response depends on the movements of charges interacting with the polymers, due to electrostatic forces (migration), concentration's gradients (diffusion) and some other processes at lower order. However, the contributions of those effects are directly linked to the polymeric films structures, doping levels and thickness. For this reason, a potentiometric response should be evaluated for each of the electrodes forming the sensor array and for a wide range of salts solution. A conductive polymer is said to be **cation-sensitive** in a specific salt if by increasing the salt's concentration, the voltage read-out rises up as well. On the contrary, a falling level of the measured potential is an indication of the fact that the membrane is **anion-sensitive**. The evolution of the signal collected from each of the array's electrodes by varying a salt concentration can be studied to evaluate the sensitivity level of each polymer for a particular salt, containing one cationic and one anionic species. By plotting the voltage values (vs. SCE) achieved by varying logarithmically the concentration of the solutions, it is possible to compute the sensitivity slopes, which are the slopes associated to the linear interpolations of the potentials' variations.

The experiments have been conducted automatically thanks to the microfluidic set-up presented in Chapter 4. After positioning one of the arrays comprising multiple deposited conductive polymers, the concentration of a certain salt injected into the system was varied and tested. Four different salts concentrations ($0.05M$, $0.01M$, $0.005M$ and $0.001M$) have been created through the system starting with a $0.1M$ solution prepared in the lab. The dilutions series involved three different channels ($CH5$, $CH6$ and $CH7$) and the filling of the accumulation chamber has been accomplished setting the flow rate to $900 \mu l/min$, to assure the stability of the system with a certain margin. Thus, in order to collect enough liquid into the accumulation cell ($3600 \mu l$) and to remove the previous test liquids from the internal connections ($1800 \mu l$), the system takes **6 minutes**, which then corresponds to the testing time for each solution, concurrent to the preparation of the next concentration. Such value seems reasonable to achieve a condition close to the electrochemical equilibrium of all the sensors. Measurements have been repeated more times and the average potentials, achieved for each salt concentration, have been used for the evaluation of the sensitivity slope. It is known that the electropolymerization conditions affect strongly the potentiometric responses of the films. In Figure 5.12 the values of the sensitivity slopes for different PPy films are reported. The dots represent the mean of the multiple tests conducted for the same salt concentration.

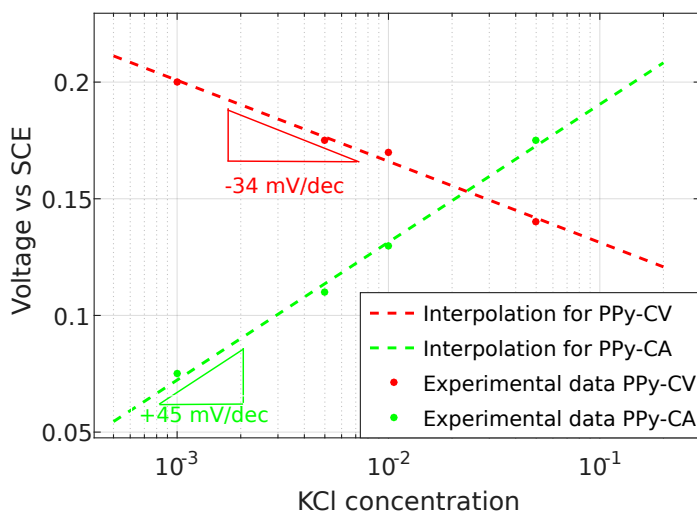


Figure 5.12. Sensitivity slopes in KCl for PPy films deposited with different techniques (CA and CV).

The trend of the linear interpolations of 5.12 could have been predicted due to the different techniques that have been employed for the deposition of the polymers on the array. Indeed, a potentiostatic electropolymerization is capable of creating fully doped polymers due to the higher degree of oxidation of the polymeric chain, which results to be linked to anionic species. An excess of those negative charges tends

to attract more positive elements from the solution in contact with the membrane, providing a cationic sensitivity. Instead, depositions occurring through the scanning of the potential, such as cyclic voltammetry, creates undoped films in a more reduced form, where most of the incorporated ions are released during a reverse scan. As a consequence, the response of the polymer is mostly diffusion-based and it may eventually lead to an anionic-sensitive behaviour, like the one of the PPy-CV film of Figure 5.12. However, it is expected that the values of such slopes can strongly change with other salts solution. It has been noticed that Polypyrrole shows much reduced sensitivity slopes when interacting with ions of greater dimensions. While Figure 5.12 shows that K^+ and Cl^- ions interact strongly with PPy films, a different behaviour characterizes those polymers when they are in contact with a solution containing ions such as Mg^{2+} or SO_4^{2-} . Indeed, sensitivity towards those ions results to be quenched due to their polymeric structure, which does not seem to sustain that kind of interaction. Nevertheless, the other polymers integrated in the array, such as PANI and PAPBA, show a great enhancement of an anionic sensitivity in $MgSO_4$ solutions. In Figure 5.13 it is evidenced that Polyaniline and PAPBA strongly interact with larger ions in solution, compared to the smaller slopes obtained for PPy.

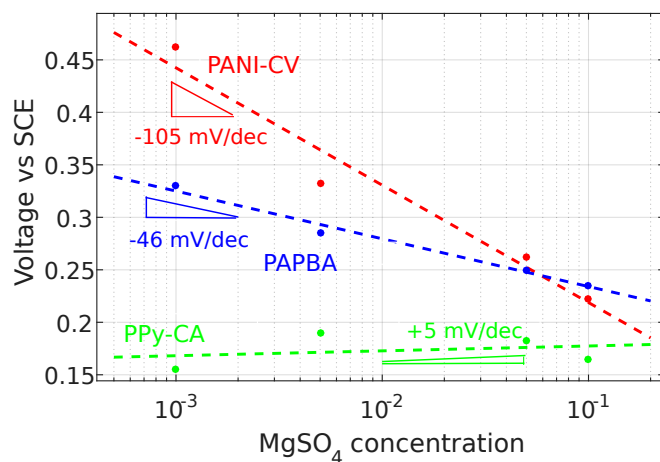


Figure 5.13. Sensitivity slopes in $MgSO_4$ for PANI-CV, PAPBA and PPy-CA films.

Moreover, the sensitivity of those polymers could also be evidenced in KCl solution, as already mentioned in Chapter 3 (Figure 3.22), where a cationic sensitivity of the polymers has been observed for such salt. It is worth mentioning that the values of the slopes have been obtained for specific polymers deposited on one sensor array. Small variability in the growth process could cause slight variations of those values and most importantly, the reported experiments have been conducted the same day of the electropolymerization. All the polymers have been stored in a 0.1M KCl solution over days. The influence of this soaking process is not yet well-understood,

but it must be taken into account for a correct evaluation of the sensitivity of all the membranes. However, for the purpose of demonstrating the general trend in the responses that one could get from such potentiometric sensors, the previous figures have been created from testing the solutions soon after the deposition of all the polymers on the array.

5.4 Towards a miniaturized portable "Electronic tongue"

In the previous sections of this Chapter it has been demonstrated how the polymers integrated on the arrays and deposited according to Chapter 3 show a remarkable sensitivity rather than a selective response towards specific elements. Conductive polymers have not been deposited with appropriate functionalizations as it would have been with ISEs. Thus, their response is based on the compensation of electrostatic and diffusive forces, which enhance the interaction with a certain multitude of elements, and not only one. Then, if more active materials are deposited on the same array, each with a certain sensitivity, a **cross-sensitive device** can be built, and qualitative and quantitative analysis of the test liquid can be extracted by considering the evolution of the responses of all the elements composing the array.

The miniaturization of a device, based on those types of arrays, requires certain further studies to allow such technological development. Arrays of small dimensions have already been presented. However, two main concepts need to be carefully explained to understand the limits of a practical realization of an *Electronic tongue* for chemical analysis of liquids:

1. Sensing of a reference liquid for tests normalization and sensor storage;
2. Clearance of bulky Reference electrodes for voltages read-out.

Indeed, preservation of the active materials is a crucial concern to enhance device lifetime as well as its reliability. For this reason, polymers need to be continuously in contact with a solution, limiting the exposure to air and contaminants. Moreover, it is evident the need of a reference point for the measurements performed over time for the same liquids, maintaining the sensors starting conditions. Ideal reference solutions fix the responses of all the elements of the array, so that the measured electrical signals show stability before and after each test. Training, calibration and studies of the arrays presented in this work have been conducted employing *KCl*-based reference solutions.

In Chapter 2, it has been explained that reference electrodes such as SCE are essential to measure absolute voltage values related only to the changes occurring at the interface of the working electrode with the solution comprised in the electrochemical cell. However, those electrodes are usually employed in a laboratory environment

and, after their use, they are immersed back in a saturated salt solution to preserve their functionality. Hence, they result inappropriate in those applications where portability is a design specification, and their volume might apply a constraint in the scalability processes that involve miniaturized devices. As a consequence, a new approach must be followed to allow reliable measurements and consistent results.

5.4.1 Dynamic signals' components

Tests for the characterization of the arrays to be integrated in such miniaturized devices require that the analysis of the liquids are preceded and followed by the immersion of the sensors in the reference solution. This operation entails certain consequences in the way in which the polymers respond and, consequently, in the analysis of the potentials read-out. Figure 5.14 shows a series of tests performed with a Polyaniline (CV) electrodes immersed in different concentrations of *KCl*.

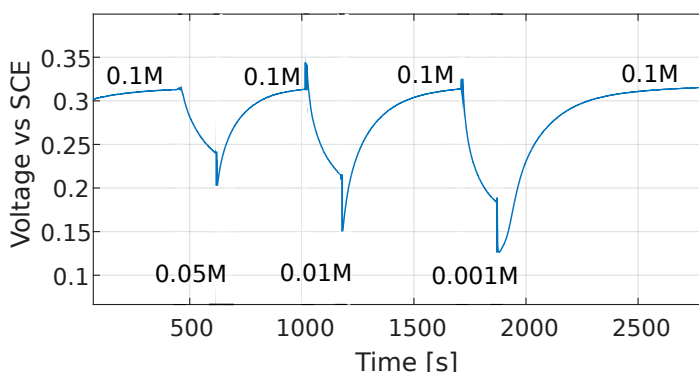
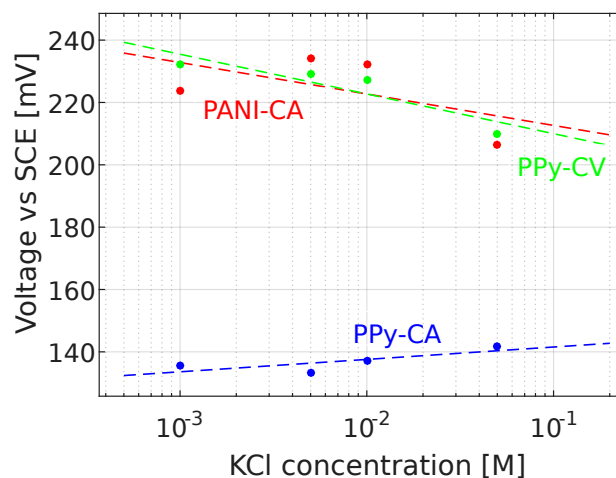


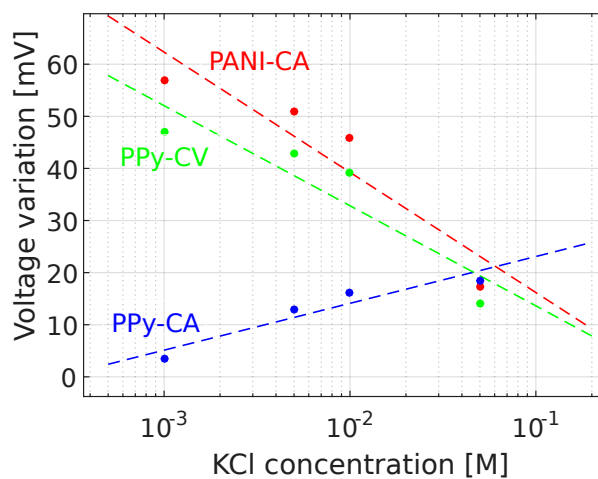
Figure 5.14. PANI-CV potentiometric response for a sequence of *KCl* concentrations interspersed with *0.1M KCl*.

Ideally, one would wait for the stabilization of the voltage signals in the reference (*0.1M KCl*) before changing the test solution. As it can be noticed, the time required to recall the reference potential depends on the amount of potential variation to which the electrode has been subjected. Indeed, the lowest salt concentration causes the highest voltage drop, which would need enough time to be recovered. Thus, testing liquids in this way is affected by a certain variability that may be unpredictable. Most importantly, when all the polymers are continuously moved from one solution to another, they might experience some sort of modifications which would result to a variation of the reference potential over time. For this reason, in most cases it is worth considering the voltage variation with respect to the reference rather than the absolute potential values. In this sense, a dynamic analysis of the voltage signals enhance robustness and consistency of the results. In figure 5.15 it is shown that the same or higher sensitivity slopes can be obtained when considering the potential variation instead of the equilibrium potential measurement at the end

of the test of each liquid. The variation has been calculated by subtracting each time the equilibrium potential obtained in the test liquid with the voltage measured in the reference one.



(a)



(b)

Figure 5.15. (a) Equilibrium potential and (b) potential variations from $0.1M$ KCl reference signal.

Values of the slopes are in the range between 10 mV/dec to 30 mV/dec, slightly lower than the ones obtained in the previous sections. This fact is due to the switch to the reference solution, which is the highest concentration, so that the polymers would need more time to reach equilibrium in diluted solutions, with one or more decades of concentrations' differences. However, for the reasons explained above, such types of measurements are fundamental for the reliability of the device and the sensitivity values would be still enough to allow qualitative and quantitative analysis.

5.4.2 Differential cross-sensitive signals

The absence of the reference electrode from the electrochemical measurement requires another mechanism to establish the potential variation of the polymers-covered electrodes in different test liquids. The most convenient approach is to take the difference for each couple of the electrodes placed on the array. Since the electrodeposited materials show a great variety of sensitivities towards multiple species, by considering a linear combination of their responses, one could expect to collect signals expressing *artificial sensitivities*. In principle, the main drawback of employing this technique would be the loss of information regarding each polymeric film performance. However, it is necessary to recall that the *Electronic tongue* concept disregards the traditional chemical sensing principle of employing selective and well-defined values for a complete liquids' characterization. Rather, the simultaneous evolution of signals is analysed for a complex evaluation, which would need further data processing steps to allow components discrimination. Hence, while experimental set-ups for each polymer characterization would be performed in a lab environment with cells containing a reference electrode, the transfer of those polymers' functionality on a portable device could be achieved based on the differential cross-sensitive signals coming only from the array.

In figure 5.16 there have been reported some of the potentiometric responses coming from differential measurements performed for three different polymers (PPy-CA, PPy-CV and PANI-CA) that have been successfully deposited on Au/ENIG substrates. The differential voltages shows sensitivity towards different ionic species. Four different salts have been chosen to show the influence of both cations and anions interaction with the three different membranes. The values of the sensitivity slopes for the differential signals are reported in Table 5.1. The signal comprising Polyaniline and PPy deposited with CV shows the highest sensitivities for all the tested salts solutions. However, the fact that the sensitivity varies considerably changing only one of the ionic species is fundamental for the detection of all the components and, most importantly, the highest slopes for each signal does not correspond with the maximum sensitivity of another one. This mixed behaviour endorses the cross-sensitive property of such array and it would look more promising when considering the integration of more than the three polymers shown in this example. Thus, it is expected that those materials could be suitable for application in portable devices based on potentiometric measurements without reference electrodes.

Nevertheless, the analysis of the potential equilibrium, achieved after a certain amount of time the sensor has been dipped inside the test solution, could be not sufficient for correct interpretation of the results. Indeed, it may happen that, when interacting with different *complex* liquids, the array could show similar final responses due to the way in which the multiple ions interact and hide or compensate other effects. For this reason, during data processing, pattern recognition methods should take into account the complete evolutions of the signals to perform more accurate

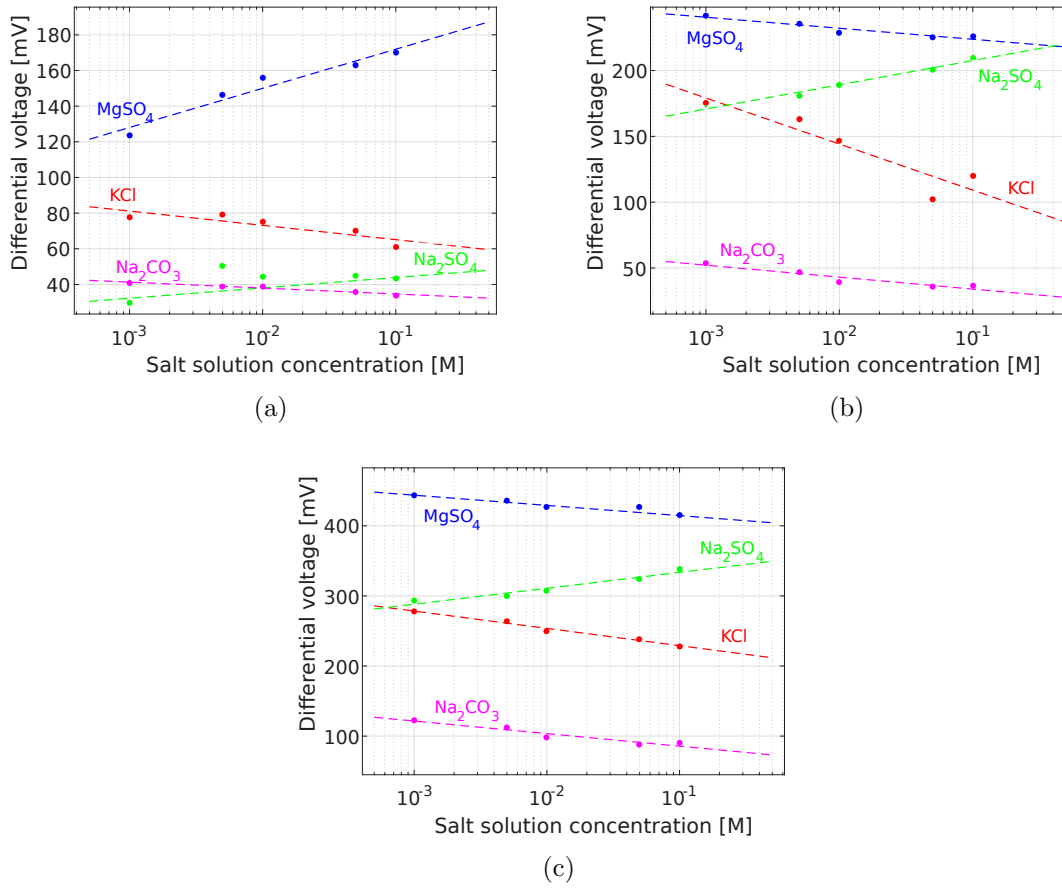


Figure 5.16. Equivalent sensitivity for couples of polymers deposited on an Au/ENIG array: (a) PPy-CA vs PPy-CV, (b) PANI-CA vs PPy-CA, (c) PANI-CA vs PPy-CV. Tests for KCl , $MgSO_4$, Na_2SO_4 and Na_2CO_3 .

Salt solution	PPy-CA vs PPy-CV [mv/dec]	PANI-CA vs PPy-CA [mv/dec]	PANI-CA vs PPy-CV [mv/dec]
KCl	-8	-25	-24,3
$MgSO_4$	-22.2	-8	-15
Na_2SO_4	+6	+19	+22,1
Na_2CO_3	-3,1	-9	-18

Table 5.1. Sensitivity slopes of differential voltages in Figure 5.16.

evaluations. Figure 5.17 shows the dynamic signals during a test performed with different SO_4^{2-} -based salts solutions, interspersed with a reference KCl dipping. It can be evidenced the importance of the shapes of the voltage traces in addition to the

tests final values. Some of the signals experience considerable drops or growths as soon as the test solution is changed, before drifting back to minimize their variation. Thus, in some cases a stable equilibrium value could not be achieved even after some minutes, so that the potentiometric response should be entirely studied for more accurate analysis and to overcome the limitations of the slow equilibrium recovery of all the differential voltages. Moreover, since the dynamic signals features depend on the way in which the membranes trap and release ions, in principle it could be possible to analyse the trend of the traces when the sensor is moved back in the reference solution. For instance, the orange signal of Figure 5.17 shows perceptible differences in its evolution after the $CaSO_4$ and $MgSO_4$ tests.

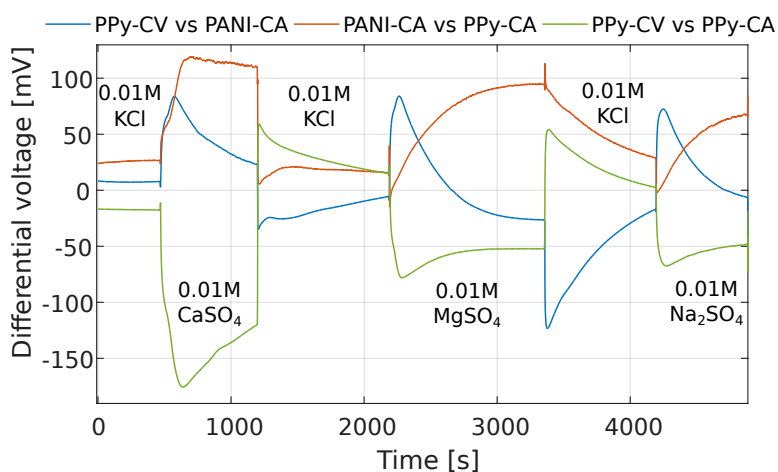


Figure 5.17. Dynamic evolution of differential voltages for different salts tests.

Chapter 6

Machine Learning and device implementation

The focus of this chapter is the practical application of the sensor array introduced in the previous chapters in a qualitative analysis problem. Multi-species solutions investigation results in discrimination, classification or identification of different samples. Machine learning methods are well-known in this field and have demonstrated to be suitable for processing of multivariate experimental data of chemical sensors [38]. Electronic tongues implementation requires statistical approaches for data processing and pattern recognition methods to accomplish the qualitative classification objective. The most common algorithms have been employed in this work and some additional elements have been specifically designed to improve **liquids fingerprinting** performances for the array introduced in Chapter 5.

6.1 Processing of a sensor array response

In a classification problem, a certain number of liquids' classes has to be distinguished. Many observations for each class are fundamental for the application of the machine learning techniques. Once a data set contains a reasonable and consistent amount of tests, then it is possible to apply some known algorithms for the actual recognition process. The explanation of those techniques are out of the scope of the present work but some concepts need to be clarified before presenting the contributions for the improvement of the classification results.

- A **PCA** (*Principal Component Analysis*) is applied for data structure exploration and visualization. Its operation can be thought of as revealing the internal structure of the data in a way that best explains their variance. Indeed, supposing that each test is described by a certain number of variables, then its representation would need a high-dimensional data space. PCA is capable of providing a low-dimensional picture of the tests performed by calculating the

so called *principal components*, which constitute a set of linearly uncorrelated (orthogonal) variables that maximizes the variance. To each component it is associated a certain score, which is a measure of its ability of separating the data set observations;

- **LDA** (*Linear Discriminant Analysis*) is one of the simplest supervised machine learning approaches. It produces an inferred function by analysing the training data and the corresponding labelling (i.e. each test is associated with its liquid class). In particular, LDA creates a linear combination of features that characterizes or separates two or more classes of objects or events. The resulting combination may be used as a linear classifier, so that it is possible to make a prediction for a test external to the training data set. In this sense, LDA induces clustering of a set of tests in such a way that the ones belonging to the same group are more similar to each other.
- **Decision trees** build a classification model through a series of binary separations of the samples according to some characteristics. Based on a particular threshold for a specific feature, the samples are split into two subsets and this process continues recursively, with the objective being to create child nodes containing only samples of the same class. To each node it is associated an impurity level, that measures the capability of a specific split to separate properly the samples [39]. Since the creation of the tree is stochastic, it is probable to get very different models even if the underlying data are the same. This instability can be addressed by averaging predictions over many trees which is the core concept of **Random Forests**. Each of those trees takes a *random* subset of the overall data set to generate uncorrelated predictions through a *voting classifier*. The idea of employing multiple *weak learners* to create a strong predictor characterizes all the **Ensemble Learning** methods and different approaches allow to construct the most accurate and complex system of trees.

Thus, application of machine learning approaches presupposes the creation of a data set comprising multiple samples of the same class and a certain number of classes to be distinguished. As a result, a **classification model** can be built and the functionality of a device, that provides information for the class recognition, could be verified by applying that model to a new liquid test and compare its true label with the predicted one.

6.2 Intelligence transfer: Electronic tongue training

The analytical procedure required to collect and process the data produced by the array for qualitative analysis consists of precise steps:

1. sensor is inserted in a test cell containing the reference solution;
2. after a certain time interval (set for the particular test) the sensor gets in contact with a test solution and the response is collected. This operation can be achieved either by using the experimental set-up presented in Chapter 4 or manually, depending on the dimension of the classification problem to be solved;
3. the sensor is dipped back in the reference solution to recover its starting condition;
4. steps 2 and 3 are repeated to test the same class of liquids and the other classes more times;
5. the data set is organized so that at each test it is associated the correct label. Machine learning algorithms create a classification model based on the data set with a certain recognition confidence, called *classification accuracy*. The more the number of tests for each class increases the more the accuracy improves;
6. device training is completed and a classification model is built.

6.3 Reduction of high-dimensional features spaces

The response of the *Electronic tongue* consists of *time series* of differential voltage measurements, obtained for couples of electrodes placed on the array. The collected data contain time stamps with the corresponding voltage readings and the final data set consists of an enormous amount of time series collected for each test liquid, to which it is associated a certain label. Thus, the input variables for the machine learning algorithms are represented by the values of those voltages obtained at each time stamp. For tests conducted for m seconds at 1 Hz the resulting vectorial space would contain $m \times n$ variables where n is the number of measured differential voltages. Even though only few signals could be recorded, a meaningful test should last several seconds resulting in a massive variables number. A machine learning high-dimensional problem could end up in the *curse of dimensionality* issue. Such phenomenon refers to the fact that the volume of the variables space could be so extensive that the available data become sparse and, in order to obtain a statistically reliable result, the amount of additional data needed often grows exponentially. Since the number of automated tests cannot be increased indefinitely to satisfy those strict requirements, the predictive power of a classifier first increases as number of dimensions used are increased but then decreases (*Hughes phenomenon*) due to sparsity and dissimilarities of the data [40]. Generally, a powerful method to limit such issue is the features selection and extraction to produce a more balanced data set,

to be provided to the algorithms for the classification. Dimensional reduction approaches for the time series signals coming from the sensors array are presented in the following sections.

6.3.1 Down-sampling and polynomial interpolations

Down-sampling represents the simplest way to reduce the number of variables to be analysed. A subset of the recorded data points is actually extracted and provided to the algorithm for the classification purposes. Signal reconstruction to allow the visualization of the original curves' shapes is often performed through splines interpolation. A *spline* is a set of polynomial functions of a certain order which are commonly used to describe data that would require a high order polynomial fit. Data points are split in a prescribed number of intervals and a polynomial fit of a certain degree is built for each of them. In particular, cubic splines are constructed from third order polynomials and are employed in a wide range of applications due to their convergence properties and regularities. Even though down-sampling can be accomplished quite easily, its drawback is related to the possible loss of signals information. In the previous Chapter, it has been proved that the complete shape and evolution of the voltage traces, after switching the liquid from a reference solution to a test one, carry some relevant features that should be analysed for more accurate results. Figure 6.1 shows the effects of an excessive reduction of the data points for the analysis of a voltage signal, whose peak cannot be always detected.

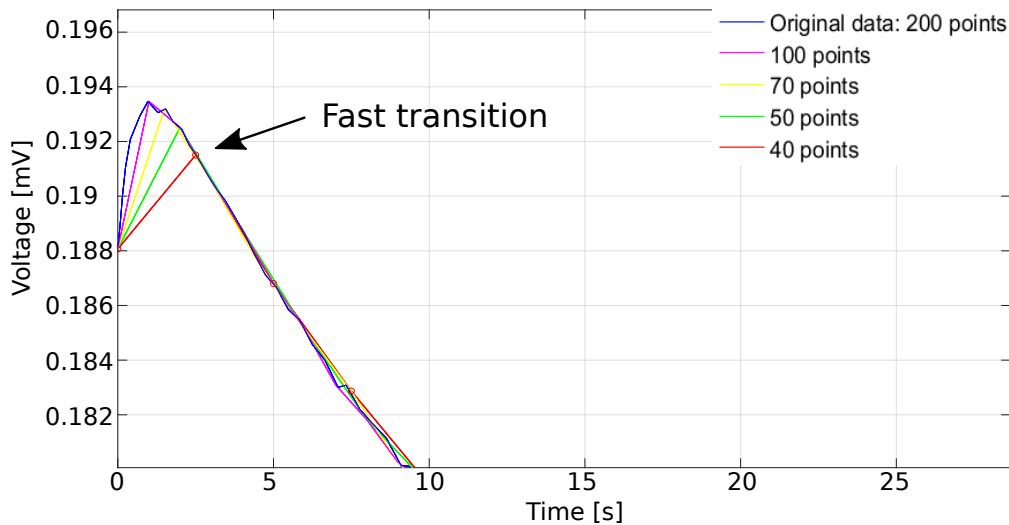


Figure 6.1. Down-sampling on a fast signal transition.

Hence, reducing number of data points must be limited and the number of data points must be chosen to avoid any possible loss. Moreover, since the appearance

of specific signals features is unpredictable, it is not possible to operate different down-sampling rates depending on the test time or test iteration. Another powerful technique to reduce the dimensionality of the problem is the polynomial interpolation of the signals transitions. In this case, the reduction is much harder since polynomials need only their coefficients to be defined. For a third order interpolation it has been noticed an high correlation of the coefficients associated to the same test solution (Figure 6.2), so that it could be possible to perform the classification methods only with four variables for each differential voltage measurement.

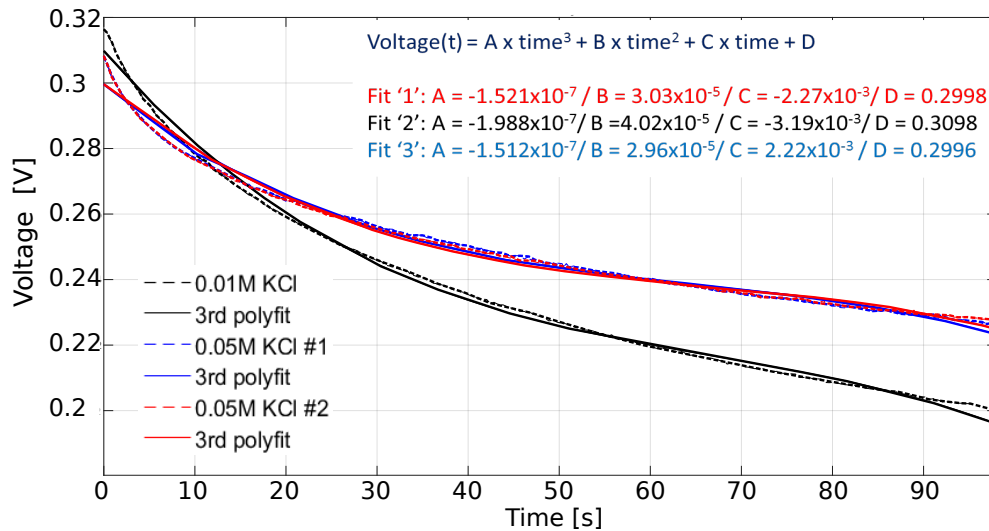


Figure 6.2. Third order polynomial interpolation and coefficients correlation for two tests performed on the same liquid (0.05M KCl).

However, the accuracy of such methods decreases drastically when the signals are not monotonic or when they do not show a specific regularity. In that case, higher polynomial interpolation orders would be needed in order to describe more accurately the shape of a recorded trace. In Figure 6.3 it is possible to notice an example of signal reconstruction through a *15th* order interpolation of a signal containing an initial peak as the one of Figure 6.1. In this case, it would be necessary to compare sixteen coefficients to distinguish different transitions.

6.3.2 Assisted features selection

Due to the instability of the previous reduction principles, a more accurate features extraction could be obtained taking into account the types of signal that are expected to be collected. Such mechanism should prevent any loss of signal information providing, at the same time, a reasonable *summary* of its trend and shape. The most significant signal elements depend on its roll-off or the rate at which it rises up. The potential presence of any initial peak should be considered as well, since the way in

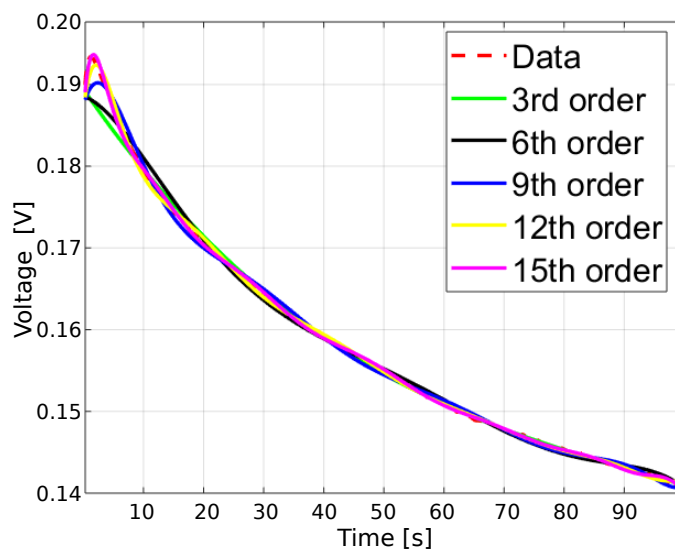
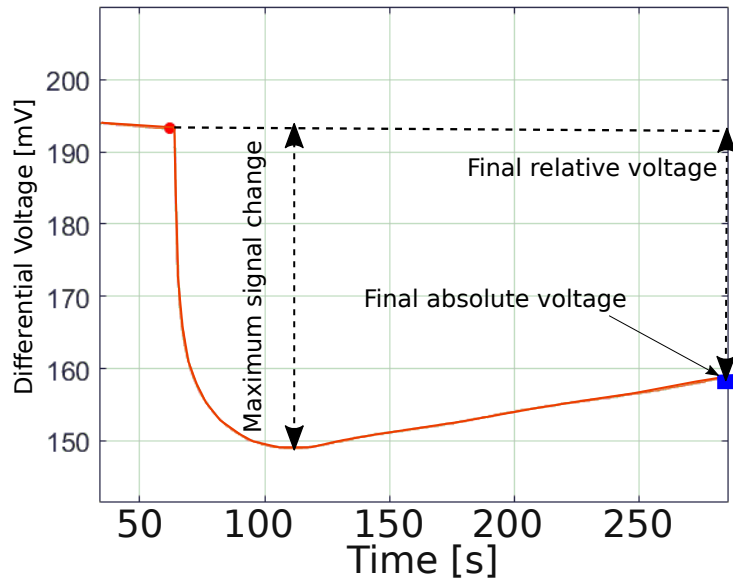


Figure 6.3. Polynomial fits of different orders.

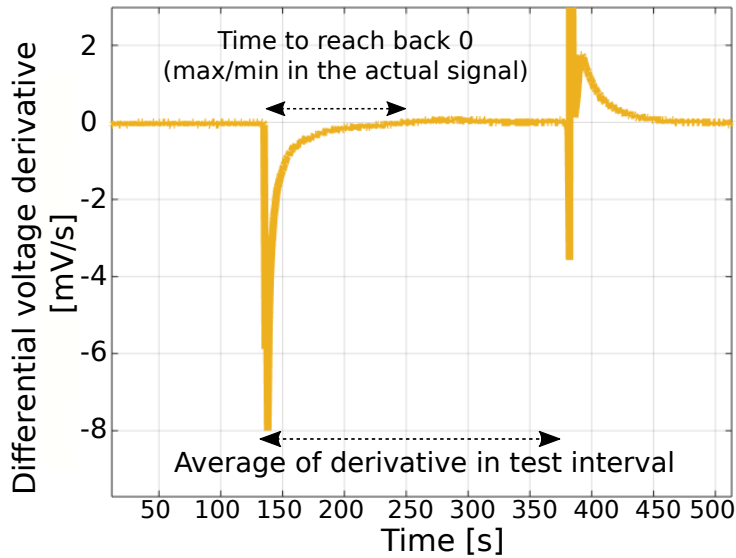
which the polymers release some ionic species and start to trap other ones is described by that kind of feature. Thus, in addition to the evaluation of the voltage signals, one could consider analysing their derivatives to investigate some reproducible aspects of their variation. Five different features (Figure 6.4) have been selected for the experiments presented in the next sections:

1. **Final absolute differential voltage** value as in the common potentiometric sensors;
2. **Final relative differential voltage**, taken as the difference between the final absolute voltages values of reference and test solution;
3. **Maximum signal change**, computed as the voltage gap between the final reference solution value and the signal maximum or minimum achieved during the test when the curve increases or decreases respectively;
4. **Average of the derivative of each signal** during test time, to estimate its overall rate of change;
5. **Time required to achieve a maximum or minimum** in the signal trend, related to the polymers speed of interaction with the different ionic species.

Considering testing time of 100 seconds with 100 data points collected from each signal, employing the above-mentioned five features would mean reducing the features of twenty times, scaling down the complexity of the corresponding machine



(a)



(b)

Figure 6.4. Extraction of features from signal (a) and derivative (b) traces.
learning problem. The functionality of the assisted features selection must be validated through a practical implementation of the device.

6.4 Mineral waters showcase

The sensor array of Figure 6.5(a) has been employed to prove the functionality of the device in terms of classification capabilities. In particular, different classes of mineral waters (*Aquella*, *Contrex*, *MBudget* and *Vlaser* in Figure 6.5(b)) have been tested by dipping repeatedly the electronic tongue inside the same water brand sample and all the other ones to train the array for the recognition process. Each measurement has been preceded and followed by a reference solution immersion to recall a starting potential for all the tests.

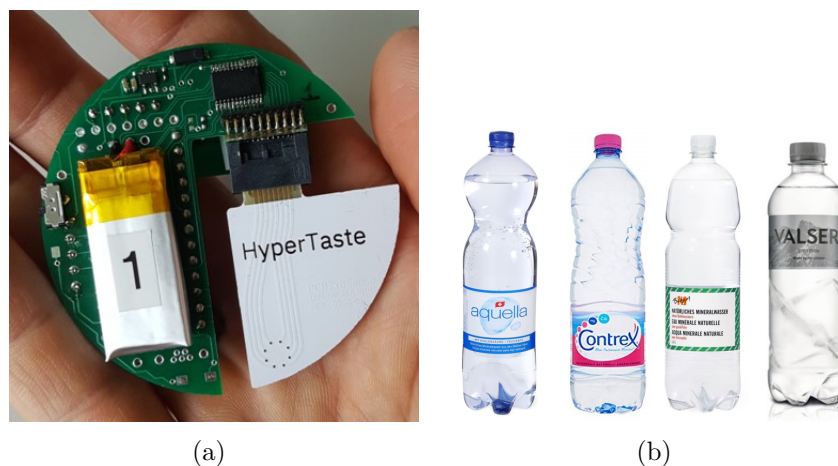


Figure 6.5. Electronic tongue device for mineral waters classification (a) and water brands (b).

All the eight electrodes have been fully covered by conductive polymers introduced in the previous Chapters. In particular, the most reliable electropolymerizations on AU/ENIG substrates allow for the deposition of Polypyrroles with different techniques (potentiostatic and potentiodynamic) and Polyaniline with chronoamperometric method. The same coatings have been produced with different thickness to avoid polymers redundancy on the same array. Nevertheless, only three differential voltages (four electrodes) have been sufficient for the proof of concept demonstration. Training and calibration can be obtained in few hours after the array preparation and tests have been performed continuously before storing the device in the soaking solution after a reasonable data set creation. The read-out mechanism is embedded in the device (Figure 6.5(a)) and allows the collection of accurate measurements of the differential voltages at a certain frequency. For the mineral water showcase, the recording time has been set to **4 min** while the sensor has been immersed in the reference solution for **6 min** to enhance the potential recovery. The three signal traces are displayed in Figure 6.6.

In such tests, a 0.01M KCl solution has been chosen to replace the 0.1M KCl standard reference. Indeed, a diluted solution could be useful to induce less perturbation of the signals with respect to the voltage measured with the mineral waters.

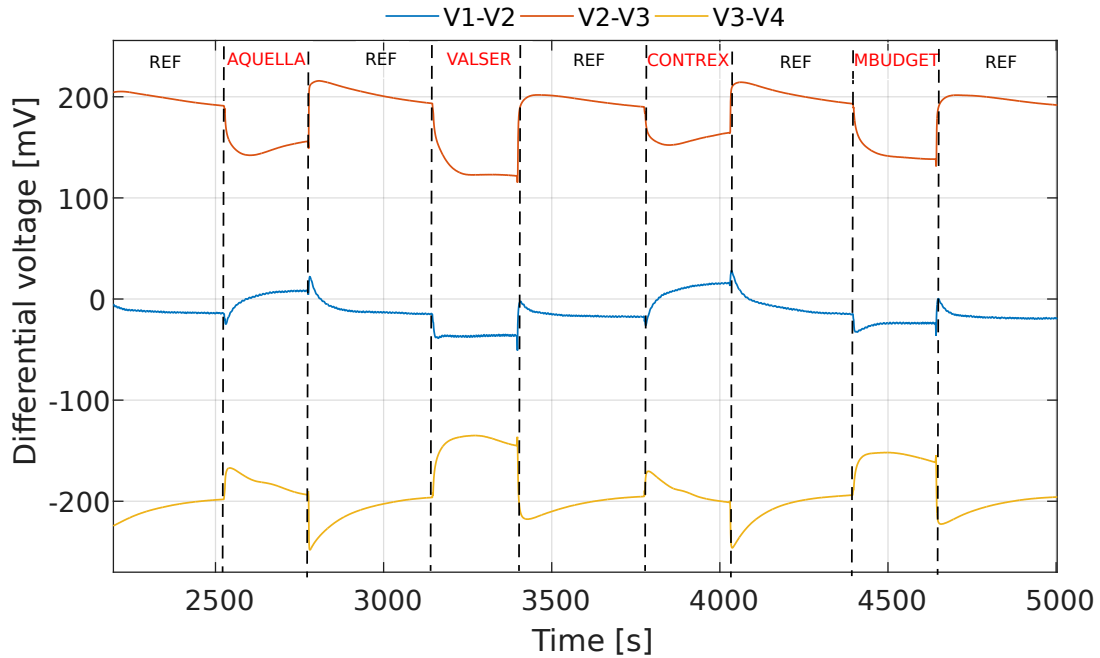


Figure 6.6. Differential voltages traces recorded by dipping the sensor in different mineral water brands and $0.01M$ KCl reference solution.

Those samples are characterized by a fairly low ionic concentration. Consequently, it is expected that the interaction of the polymers with the test solutions is less affected by the release of ionic components coming from the reference solution dipping. Moreover, the conductivity of the polymers results not to be quenched by such dilution since the voltage traces in a reference measurement are quite stable. Once the tests have been completed, the following steps consist of:

1. cropping each test transition data with the previous corresponding reference data points from all the measurements;
2. labelling each test with the corresponding water brand;
3. extracting the five features introduced in the previous section by considering the reference signal and the derivative data (repeated for all the three signals);
4. visualizing each test described through the features variables in the PCA space;
5. applying supervised machine learning algorithms (LDA, Ensemble Learning,...) to create a classification model;
6. evaluate the classification accuracy and apply the model to further tests with unlabelled samples to verify the correct operation of the *Electronic tongue*.

6.4.1 Classification results

A consistent data set should contain as many tests as possible for the same liquid class. The reported results have been obtained with **18 tests** for each water brand. Features' extraction allows tests representation in a new dimensional space, whose specific projections are called *scatter plots*. In Figure 6.7 all the tests have been placed in the projection of the first two extracted features to show the interrelation between them. The 2D-plot demonstrates that a certain clustering can be obtained even considering a limited number of characteristics, which is promising for the overall recognition result. Since the number of recorded voltage traces has been set to three, and that for each of them there have been extracted five features, the overall descriptors' number is fifteen, so that the correct representation of the tests should be in a *15-dimensional space*. Thus, the best data visualization in a 3D-plot could be given by the principal component analysis , displayed in Figure 6.8.

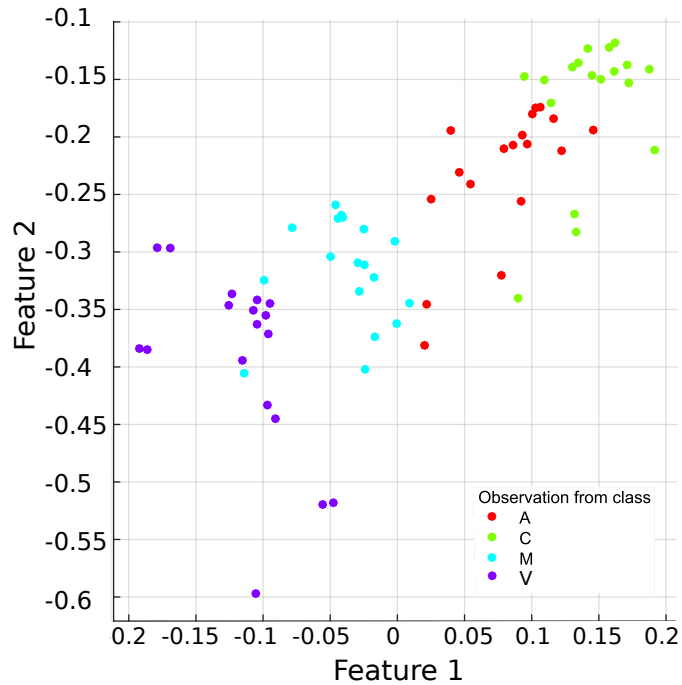


Figure 6.7. Scatter plot of 72 water tests for two features.

The PCA reveals that there are essentially two groups of tests which are well-distinguished by the first principal component, whose score is as high as 89 %. Each group contains two waters' clusters which are pretty close, but almost completely distinguishable. Such result could have been predicted by analysing accurately the voltage traces of Figure 6.6. In particular, the blue curve ($V1-V2$) shows a distinct shape since the reference potential is pinned between the two groups of mineral

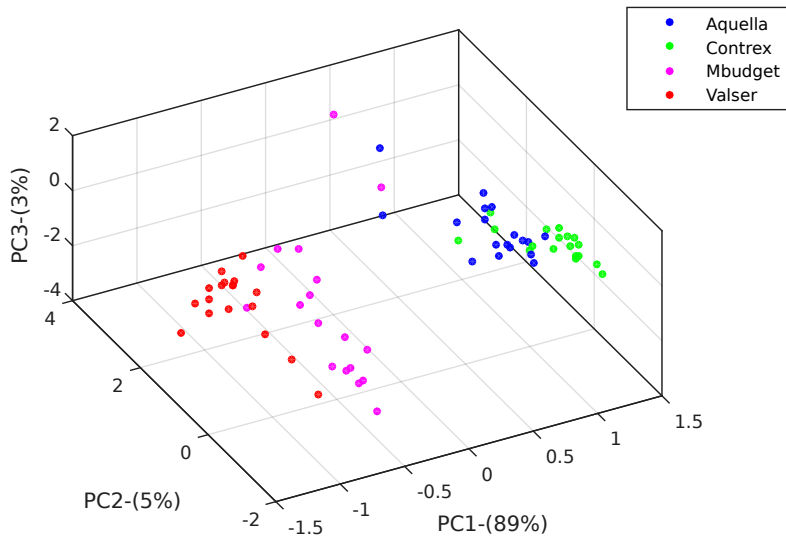


Figure 6.8. Principal component analysis for 72 water tests after feature extraction.

waters. Indeed, the differential voltage related to *Contrex* and *Aquella* rises with respect to the reference value, while it falls down for the other two brands. Thus, since the extracted features exhibit remarkable sensitivity to such behaviour, the visualization and classification performances indicate to be affected as well. In Figure 6.9 there have been reported the results for the *Random forest* and *LDA* algorithms.

The confusion matrices represent the results comparing the true label for each test and the corresponding prediction made by a specific algorithm. Counting the number of misclassifications, it is possible to compute the classification accuracy. The Random forest classifier gives **95,8%** while the LDA approach result is **91,7%**. The scores confirm the capabilities of the array to recognize different mineral water brands using only half of the available electrodes and with a limited number of extracted features. The results have been produced by applying a **leave-one-out cross-validation method** considering **200s** of the voltage transitions in the test solutions: the model has been trained with 71 tests and applied to the remaining one to make a prediction. The operation has been repeated for all the 72 tests, and each time the prediction has been compared with the true label to fill in the confusion matrix. The Random forest classifier is part of the Ensemble learning algorithms' set, a complex formation of binary trees that gives a better accuracy with respect to a simpler linear discrimination (LDA). The most relevant results are reported in the following Table 6.1.

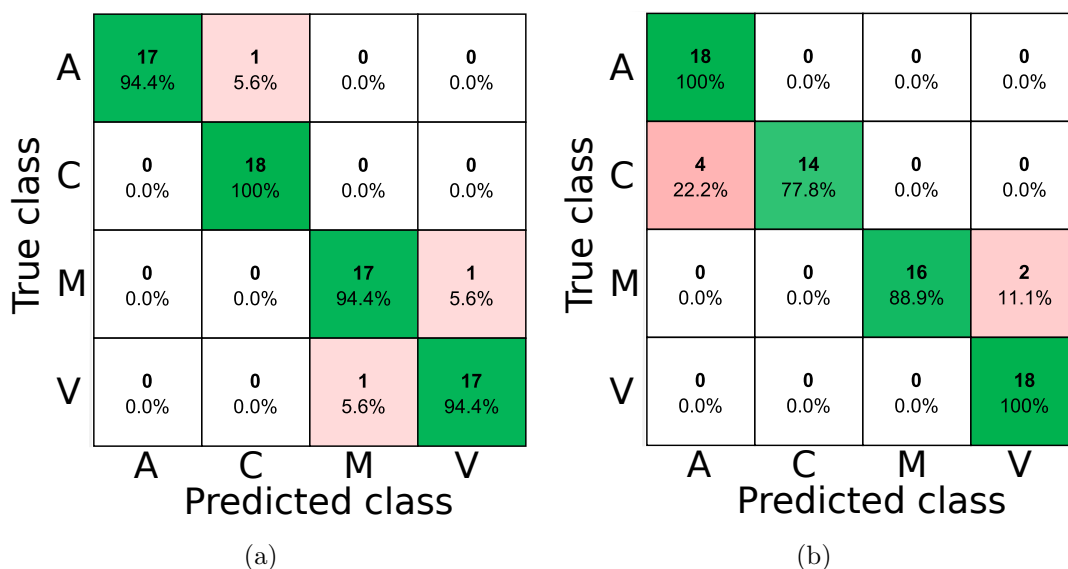


Figure 6.9. Confusion matrices obtained with Random forest (a) and LDA (b) classifiers for 72 water tests with cross-validation.

Features	LDA [%]	Random forest [%]	Other ensemble algorithms [%]
All (200s)	91,7	95,8	94,4
All (120s)	83,3	86,1	88,9
All (80s)	84,7	81,9	88,9
Only V_{12}	81,9	83,3	88,9
Only V_{23}	68,1	56,9	70,8
Only V_{34}	86,1	94,4	95,8

Table 6.1. Classification accuracies dependency on test time and voltage signals involved.

The classification results depend strongly on the time interval that has been set for all the tests. However, the overall performances for the liquids identification does not lose more than 10% when reducing the test time from 200s to 80s. Moreover, the classification scores go beyond 80% with all the algorithms, and approach 85% when considering 2 minutes of dipping in the test solution before putting the sensor array back in the reference. Thus, those results are an indication of the **rapid fingerprinting capabilities** of the electronic tongue that has been created. Machine learning approaches could also be exploited to guide the design specifications for a sensor array. Comparing the accuracies reported in Table 6.1, it is possible to derive some important information regarding the behaviour of the polymers deposited on the array. The features extracted from signal V_{23} produce worse results than the other two signals, with a significant drop of the corresponding classification accuracy. Thus, a further investigation would be needed to figure out the cause of the

low performances of the two polymeric films involved in that signal and, eventually, improve the electropolymerization to modify their properties. Nevertheless, it should be necessary to test the sensor array in other showcases involving complex liquids, in order to explore the variation of the cross-sensitive behaviour and the versatility of such *Electronic tongue* based on conductive polymers.

Chapter 7

Conclusions

The development of an *Electronic tongue* for liquids fingerprinting has proven to be successful. In the first chapters it has been shown the possibility to tune electrochemical properties and to create more stable polymeric coatings. The integration of those active materials on the same array of electrodes entails the creation of a cross-sensitive device: each polymer exhibits a certain sensitivity towards multiple ionic species depending on their charge and dimension. The corresponding potentiometric signal in a *complex* liquid is the result of a multi-interaction process. The exploitation of the differential voltages has been proposed to get rid of the reference electrode for the electrochemical measurement, enhancing the miniaturization and portability of the device. The mineral waters showcase confirms the potentiality of the fabricated sensor and its functionality. A crucial role has been played by the dimensional reduction for the application of the machine learning algorithms. Assisted features extraction from all the signals led to high classification accuracies, representing a reliable instrument for the reduction of the high-dimensionality time series data. The achievements of the present study poses the bases for the improvement of the device and its implementation, foreseeing a continuous development for multiple applications.

7.1 Future challenges

Following the results obtained in this work, some further investigations could be proposed:

- **Improve device reliability and reproducibility understanding polymers ageing and conditioning effects.** Indeed, soaking and conditioning of conductive polymers is one of the biggest issues to be addressed. So far, the lifetime for the device and its correct operation has been estimated to be of few days. Thus, there is currently a strong limitation in its possible commercialization. However, by adjusting the storing conditions and maintaining the

same doping level, it should be possible to minimize sensors drifting over time. Training of the same array after ageing and without electrochemical treatment of the polymers seems not to solve this major drawback;

- **Establish design rules for cross sensitive arrays.** It is expected that the sensitivity slopes for the differential measurements could be enhanced with certain combinations of deposition parameters of different conductive polymers. Understanding what are the best structural properties of those polymers is a main challenge;
- **Testing of additional polymer recipes to improve classification accuracy.** The recognition of the different water brands with the array presented in this work can be achieved without additional efforts. However, the versatility of the device would require the integration of other polymeric films so that the classification can be performed with a wider range of multi-components liquids;
- **Multivariate calibration to perform quantitative analysis.** The possibility to extract some accurate information related to the composition of the test solutions is a powerful way to enlarge the application fields for the electronic tongue. Since the device is based on cross-sensitive transducers, pattern recognition methods would need the assistance of additional mathematical procedures for the correct interpretation of the collected data to produce quantitative results;
- **New features exploration to validate fast liquids fingerprinting performances.** Extension of the domains of application and electrodes' functionalization with new active materials make more unpredictable the evolution of the potentiometric signal when the sensor is dipped in a test liquid. Hence, features extraction and machine learning algorithms should follow up on the evolution of the other building blocks of the *Electronic tongue*.

Bibliography

- [1] Y. Vlasov, A. Legin, A. Rudnitskaya, C. D. Natale, A. D'amico, "Nonspecific sensor arrays (electronic tongue) for chemical analysis of liquids: (IUPAC technical report)" in *Pure and Applied Chemistry, Vol. 77*, pp. 1965–1983, 2005.
- [2] A. Torapov, A. Toropova, L. Cappellini, E. Benfenati, E. D. Vlasov, "Odor threshold prediction by means of the Monte Carlo method" in *Ecotoxicol. Environ. Saf.*, pp. 390–394, 2016.
- [3] M. Podrazka, E. Bączyńska, "Electronic tongue-A tool for all tastes?" in *Biosensors, Vol.8*, pp. 1–24, 2017.
- [4] P. Ciosek, W. Wróblewski, "Sensor arrays for liquid sensing—Electronic tongue systems" in *Analyst, Vol.132*, pp. 963–978, 2007.
- [5] M. Huynh, W. Kutner, "Biosensors and Bioelectronics Molecularly imprinted polymers as recognition materials for electronic tongues" in *Biosens. Bioelectron.*, pp. 856–8646, 2015.
- [6] J. Seiter, M. DeGrandpre, "Redundant chemical sensors for calibration-impossible applications" in *Talanta*, pp. 99–106, 2001.
- [7] A. Legin, A. Rudnitskaya, Y. Vlasov, C. D. Natale, A. D'amico, "Features of the electronic tongue in comparison with the characteristics of the discrete ion-selective sensors" in *Sensors and Actuators, B: Chemical*, pp. 464–468, 1999.
- [8] A. Legin, A. Rudnitskaya, Y. Vlasov, "Cross-sensitivity evaluation of chemical sensors for electronic tongue: determination of heavy metal ions" in *Sensors and Actuators, B: Chemical 144*, pp. 532–537, 1997.
- [9] M. D. Valle, "Electronic tongues employing electrochemical sensors" in *Electroanalysis*, pp. 1539–1555, 2010.
- [10] D. Harvey, *Analytical Chemistry 2.0 : Electrochemical Methods* McGraw-Hill Education, 2016.
- [11] S. Sharath Shankar, "Development of neurotransmitter sensor using chemically modified carbon paste electrode by voltammetric investigations" in *Department of Industrial Chemistry, Kuvempu University*, pp. 1–43, 2012.
- [12] J. Rountree, D. McCarthy, S. Rountree, T. Eisenhart, L. Dempsey, in "A Practical Beginners Guide to Cyclic Voltammetry" 2017.
- [13] T.-H. Le, Y. Kim, H. Yoon, "Electrical and Electrochemical Properties of Conducting Polymers" in *Polymers*, pp. 1–10, 2017.

- [14] P. S. Sharma, A. Pietrzyk-Le, F. D'Souza, W. Kutner, "Electrochemically synthesized polymers in molecular imprinting for chemical sensing" in *Analytical and Bioanalytical Chemistry*, pp. 3177–3204, 2012.
- [15] M. M. Gvozdrenović, B. Z. Jugović, J. S. Stevanović, T. L. Trišović, B. N. Grgur, "Electrochemical Polymerization of Aniline" in *Electropolymerization edited by Ewa Schab-Balcerzak, Ch.4*, pp. 77–96, 2011.
- [16] M. H. Pournaghi-Azar, B. Habibi, "Electropolymerization of aniline in acid media on the bare and chemically pre-treated aluminum electrodes. A comparative characterization of the polyaniline deposited electrodes" in *Electrochimica Acta, Vol.4*, pp. 1593–1599, 1996.
- [17] S. Mu, J. Kan, "Evidence for the autocatalytic polymerization of aniline" in *Electrochimica Acta, Vol.52*, pp. 4222–4230, 2007.
- [18] B. O. S. Zhao, Y. Wu, "Electrochemical Preparation of Polyaniline Nanowires with the Used Electrolyte Solution Treated with the Extraction Process and Their Electrochemical Performance" in *Nanomaterials, Vol. 8*, 2018.
- [19] D. Ljerka, M. Zoran, K. Franjo, "The effect of supporting electrolyte on the electrochemical synthesis, morphology and conductivity of polyaniline." in *Polym.Sci Part A*, pp. 105–111, 1994.
- [20] G. Zotti, S. Cattarin, N. Comisso, "Cyclic potential sweep electropolymerization of aniline." in *Electroanal. Chem., 239*, pp. 387–396, 1988.
- [21] E. G. Garcia, M. Romero-romo, "Voltammetric Formation of Polyaniline on Gold and Platinum under Static and Forced Convection Conditions." in *ECS Transactions*, 2008.
- [22] L. Xing, Y. Kang, Y. Zhou, "Determination of sulfate in seawater by a novel all-solid-state sulfate sensor with H₂SO₄ doped polyaniline as sensitive membrane." in *International Journal of Electrochemical Science, Vol.12*, pp. 1506–1520, 2017.
- [23] K. Badea, V. Tsakovab, J. Schultzea, "Nucleation, growth and branching of polyaniline from microelectrode experiments." in *Electrochimica Acta, Vol. 37*, pp. 2255–2261, 1992.
- [24] W. L. Brooks, B. S. Sumerlin, "Synthesis and Applications of Boronic Acid-Containing Polymers: From Materials to Medicine." in *Chemical Reviews, Vol. 116*, pp. 1375–1397, 2016.
- [25] H. Çiftçi, U. Tamer, "Electrochemical determination of iodide by poly(3-aminophenylboronic acid) film electrode at moderately low pH ranges" in *Analytica Chimica Acta, Vol. 687*, pp. 137–140, 2011.
- [26] E. Shoji, M. Freund, "Potentiometric saccharide detection based on the pK_a changes of poly(aniline boronic acid)" in *Journal of the American Chemical Society, Vol. 124*, pp. 12 486–12 493, 2002.
- [27] P. N. Bartlett, J. H. J. Wang, "Electroactivity, stability and application in an enzyme switch at pH 7 of poly(aniline)–poly(styrenesulfonate) composite films" in *Journal of the Chemical Society, Faraday Transactions*, pp. 4137–4143, 1996.

- [28] H. R. Virdee, R. E. Hesier, “In Situ Resonance Raman Spectroscopic Investigation of a Polypyrrole Modified Gold Electrode” in *Croatica Chemica Acta*, Vol. 61, pp. 357–374, 1988.
- [29] N. R. Madhu, R. Awasthi, “Polypyrrole Composites: Electrochemical Synthesis, Characterizations and Applications” in *Electropolymerization edited by Ewa Schab-Balcerzak*, Ch. 7, pp. 131–158, 2011.
- [30] J. R. Reynolds, B. C. Thompson, T. A. Skotheim, *Conjugated Polymers: Properties, Processing, and Applications. Ed. 4* CRC Press. Taylor and Francis Group, 2019.
- [31] A. Kellenberger, D. Ambros, N. Plesu, “Scan rate dependent morphology of polyaniline films electrochemically deposited on nickel” in *International Journal of Electrochemical Science*, Vol. 9, pp. 6821–6833, 2014.
- [32] G. A. Snook, G. Z. Chen, “The measurement of specific capacitances of conducting polymers using the quartz crystal microbalance” in *Journal of Electroanalytical chemistry*, Vol. 612, pp. 140–146, 2008.
- [33] [Online]: <http://onlineresize.club/pictures-club.html>
- [34] [Online]: <https://www.keyence.com/ss/products/microscope/roughness/surface/sku-kurtosis.jsp>
- [35] R. Mažeikienė, G. Niaura, “In situ time-resolved Raman spectroelectrochemical study of aniline polymerization at platinum and gold electrodes” in *Chemija*, Vol. 29, pp. 81–88, 2018.
- [36] H. S. Abdullah, “Electrochemical polymerization and Raman study of polypyrrole and polyaniline thin films” in *International Journal of Physical Sciences*, Vol. 7, pp. 5468–5476, 2012.
- [37] [Online]: <https://www.elveflow.com/microfluidic-tutorials/microfluidic-reviews-and-tutorials/microfluidic-low-flow-liquid-flow-meter-a-review>
- [38] S. Wold, C. Albano, W. J. Dunn, U. Edlund, “Multivariate Data Analysis in Chemistry” in *Chemometrics, NATO ASI Series*, pp. 17–95, 1984.
- [39] A. Geron, *Hands-On Machine Learning With Scikit-Learn and Tensorflow: Concepts, Tools, and Techniques to Build Intelligent Systems* O’REILLY, 2017.
- [40] S. Theodoridis, S. Theodoridis, K. Koutroumbas, *Pattern Recognition, 4th Edition* Academic Press, 2008.